Expression and Characterization of P-type ATPases for Structural Studies

Dissertation

Zur Erlangung des Doktorgrades der Naturwissenschaften

vorgelegt beim Fachbereich Biochemie, Chemie und Pharmazieder
Johann Wolfgang Goethe Universität in Frankfurt am Main

von

Sivaram Chandra Chintalapati

aus Tenali, Indien

Frankfurt am Main 2007

Die Arbeit wurde in der Abteilung Structural Biology des Max-Planck-Instituts für Biophysik in Frankfurt am Main durchgeführt und vom Fachbereich Biochemie, Chemie und Pharmazie der JohannWolfgang Goethe Universität als Dissertation angenommen

Dekan:

1. Gutachter: Prof. Dr. Bernd Ludwig

2. Gutachter: Prof. Dr. Werner Kuehlbrandt

Datum der Disputation:

Diese Doktorarbeit wurde vom 28. Januar 2003 bis zum 15 Januar 2007 unter Leitung von Prof. Dr. Werner Kühlbrandt im Abteilung für Strukturbiologie am Max planck Institut für Biophysik in Frankfurt am Main durchgeführt.

Eidesstattliche Erklärung

Hiermit versichere ich, dass ich die vorliegende Arbeit selbständig angefertigt habe und keine weiteren Hilfsmitten und Quellen als die hier aufgeführten verwendet habe.

Sivaram Chandra Chintalapati
Frankfurt am Main, den 15 Januar 2007.

TABLE OF CONTENTS

Summary

Two types of proteins transport ions across the membrane – ion channels and ion pumps. Ion pumps transport ions against their electrochemical gradient by co-transporting another ion or a substrate molecule through a concentration gradient or by coupling this process to an energy source like ATP. Those that couple ATP hydrolysis to ion transport are called ion motive ATPases and can be classified as 'V', 'F' and 'P' types.

In this thesis, two sub-classes of P-type ATPases, P_{IIIA} and P_{IB} were studied. Attempts were made to over-express and crystallize the plant proton pump AHA2 (a P_{IIIA}-ATPase). Also, the two putative copper transporting ATPases, CtrA3 (CopB-like) and CtrA2 (CopA-like) from *Aquifex aeolicus* (both P_{IB} pumps) were over-expressed in *E. coli* and characterized.

P_{IIIA}-type pumps transport protons across the membrane and are found exclusively in plants and fungi, and probably some archaea. One of the most characterized proton pump biochemically is the *A. thaliana* proton pump AHA2. An 8Å projection map of this enzyme is already available (Jahn 2001). P_{IB}-ATPases, also called CPX type pumps transport heavy metal ions such as Cu^{+}, Cu^{2+}, Zn^{2+}, Pb^{2+}, Cd^{2+}, Co^{2+} across biological membranes and play an important role in homeostasis and biotolerance of these metals. CopA and CopB are two such proteins that transport copper across cell membrane found in many prokaryotes. CopB-like proteins are found almost exclusively in bacteria, with CPH sequence motif, while CopA-like proteins have CPC sequence motif, also found in eukaryotic copper transporters including human ATP7A and ATP7B. CopB extrudes Cu^{2+} across the membrane. CopA is activated by and transports Cu^{+} but the direction of transport is debated.

Attempts were made to over-express the plant proton pump AHA2 in yeast *Pichia pastoris*. However, the yeast expressed only a truncated protein, which

could not be used for further studies. It can be concluded that *P. pastoris* strain SMD1163 is not a good host for expression of AHA2.

Focus was then shifted to AHA2 that has been over-expressed and purified from *S. cerevisiae* strain RS72. Growth and purification protocols had to be changed from published methods because of laboratory constraints and this probably had an effect on the protein produced. The protein purified from *S. cerevisiae* could not be crystallized reproducibly for structural studies by electron microscopy.

CtrA3 was expressed in *E. coli* and purified using Ni^{2+}-NTA matrix. Like CopB of *A. fulgidus* (Mana Capelli 2003), it was active only in the presence of Cu^{2+} and to some extent in Ag^{+}. The protein was maximally active at 75°C, at pH 7 and in presence of cysteine. Lipids were essential for the activity of CtrA3. However, when the protein was purified in Cymal-6, CtrA3 could not hydrolyze ATP, even when lipids were added to the reaction mixture.

For reconstitution of CtrA3 into liposomes for 2D crystallization, several lipids were tested. To screen the lipids compatible for protein incorporation, CtrA3 was dialyzed with different lipids at a high lipid-to-protein ratio of 10:1 and centrifuged by sucrose density gradient. Protein incorporated in lipids localized with liposome fraction in the gradient. Most of the CtrA3 was incorporated into DPPC with no aggregation. This lipid was used for reconstitution of CtrA3 at low LPRs, and at an LPR of 0.3-0.5, the protein formed 2D crystals. A NaCl concentration of 50mM was necessary for the formation of crystals. However, salt removal by dialysis prior to harvesting was essential for obtaining well-ordered lattices of CtrA3. Addition of preservatives like trehalose and tannin or direct plunging in liquid ethane for cryo-microscopy destroyed the crystal lattice.

Similar to CtrA3, the gene responsible for expression of CtrA2 was amplified from genomic DNA of *A. aeolicus* and expressed in *E. coli* and purified

by Ni^{2+}-NTA. Functional characterization of CtrA2 was done by analyzing ATP hydrolysis activity of the enzyme. Similar to CopA of *A. fulgidus* (Mandal 2002), CtrA2 was activated in the presence of Ag^{+} and to some extent, Cu^{+}. It is possible that both the copper ATPases of *A. aeolicus* have different ion selectivity- CtrA3, specific for Cu^{2+} and CtrA2, specific for Cu^{+}. Maximal activity of CtrA2 was also at 75°C. Cysteine was essential for activity of CtrA2, but the protein was not dependent on addition of lipids for activation.

Reconstitution of CtrA2 was done similar to CtrA3 for screening of lipids for 2D crystallization. Of the lipids tested, DOPC reconstituted the protein best. However, screening at low LPRs did not yield any crystals.

Even though both CtrA3 and CtrA2 are similar heavy metal transporting P-type ATPases from the same organism and have 36% identity, they behaved completely different in their expression levels in *E. coli*, purification profiles, activity and reconstitution in lipids.

CHAPTER 1

INTRODUCTION

1.1 Proteins in biological membranes

The cell membrane acts as a barrier to the passage of most polar molecules and is critical for the existence of cell as it allows the maintenance inside the cell, of solute concentrations different from those in the extra-cellular fluid. However, cells do interact with their environment and have ways of transferring specific molecules across membranes in order to ingest essential nutrients, excrete metabolic waste products and regulate intra-cellular ion concentrations. Most of these functions are catalyzed and controlled by proteins embedded in the lipid bilayer.

The protein composition of any membrane is therefore an indication of its characteristic functional properties. Accordingly, the amounts and types of proteins in membrane are highly variable. For example, in myelin membranes that serve as electrical insulation for nerve cell axons, less than 25% of membrane mass is protein. By contrast, in mitochondrial and chloroplast membranes, 75% is protein. It is possible, from the sequence data, to identify α-helical membrane proteins. These proteins usually have blocks or segments of around 20-24 amino acids of which most are hydrophobic (for example, leucine, isoleucine and valine), through out the primary sequence. However, not all integral membrane proteins are α-helical. Outer membrane proteins of some gram-negative bacteria and some proteins of outer membranes of mitochondria and chloroplasts are of β-barrel type (Tamm et al. 2001).

A typical plasma membrane has approximately 50% of its mass accounted by proteins (Alberts 2002). These proteins perform a variety of functions in the membrane. Many proteins participate in transporting molecules between the aqueous compartments. Some serve as enzymes catalyzing vital processes. Some membrane proteins act as receptors, signal transducers that transmit stimuli received from outside to inside of the cell. Other membrane proteins act

as anchoring points for many of the cytoskeletal fibers, imparting shape and strength to the cells (Lodish 2003).

1.2 Transport of solutes across the cell membrane

Specialized transmembrane proteins perform the task of transporting molecules (solutes) across the membranes. The importance of membrane transport is indicated by the large number of genes in all organisms that code for transport proteins, which make up between 15 and 30% of membrane proteins in all the cells. These transporters have varying specificities with respect to the molecules they transport. Some proteins exchange ions with other ions or organic molecules (Alberts 2002).

1.3 Ion transporting proteins

The low dielectric constant of hydrocarbon chains of membrane lipids (ε= approximately 2) (Hanai 1965; Oki 1968) represents an energy barrier to ion movement of approximately 40kcal/mol. Thus, un-aided, only one in about 10^4 ions has enough energy to pass through bilayer. This energy difference is so large that the predominant ions in biological systems, Na^+, K^+, Ca^{2+} and others would never cross the membrane un-aided (Parsegian 1969; Begenisich 1994). Ion transporting proteins (ion pumps and ion channels) perform the task of transporting ions across the membranes. Even though pumps and channels share the fundamental property of transporting ions across the membrane, and the chemical principles of ion selectivity are likely to be similar, they fulfill very different functions. The pumps transport ions against their electrochemical gradient by coupling this process to an energy source or by co-transporting another ion or a substrate molecule through a concentration gradient. Ion channels are passive transporters, catalyzing the downhill movement of ions, often at very high ion conduction rates. However, they do differ architecturally, to

serve specific needs: channels to conduct ions rapidly and pumps to move ions against an electrochemical gradient (Gouaux and Mackinnon 2005).

1.4 Ion pumps and ATP hydrolysis

While some ion pumps couple the transport of one ion to the downhill transport of another substrate (compensating conductance), several pumps transport ions using the energy obtained by hydrolyzing ATP, thus creating a potential in the absence of any compensating conductance. The potential generating pumps are called uniport pumps i.e., they transfer charge in one direction (Parsegian 1969). The ATPases involved in ion translocation are present in a diverse variety of biological membranes. At least three different classes of ion-motive ATPases can be identified; 'V', 'F' and 'P' (Pedersen 1987).

Ion-motive ATPases of the 'V' type are defined as those associated with membrane-bound organelles other than mitochondria and the endoplasmic or sarcoplasmic reticulum; they are found in vacuoles, lysosomes, endosomes, clathrin coated vesicles, hormone storage granules, secretory granules and Golgi vesicles (Rudnick 1986).

ATPases of the 'F' category are defined as those of the F_oF_1 type found in bacteria, chloroplasts and mitochondria. These consist of water-soluble F_1 moiety involved in catalytic activity (ATP hydrolysis or synthesis) and as F_o moiety involved in H^+ translocation (Hatefi 1985).

ATPases of the 'P' type are those that have, in their sequence, a characteristic conserved sequence motif DKTGT, of which D is the reversibly phosphorylated aspartate (Inesi and Kirtley 1992). Another common feature of all the P-type ATPases is that they are inhibited by ortho-vanadate, which acts by reducing the apparent cooperativity between two or more substrate binding sites in these proteins (Dufour et al. 1980).

1.5 P-type ATPases

1.5.1 Introduction:

P-type ATPases are large, ubiquitous and varied family of membrane proteins that are involved in many transport processes in all living organisms. The main function of these pumps is to use ATP to maintain an ion gradient across the cell membrane. These proteins help in the uptake (e.g., the bacterial Kdp K^+ ATPase (Solioz et al. 1987)), efflux (e.g., the muscle sarcoplasmic reticulum Ca^+ATPase), or exchange (e.g., the animal cell Na^+/K^+ ATPase) of cations. To translocate these ions, the ATPases undergo large conformational changes (Jorgensen 1975). The ion pumping cycle involves several intermediate states and is based on Post-Albers cycle (Figure 1.1) for Na^+K^+-ATPase (Albers 1967; Post et al. 1972).

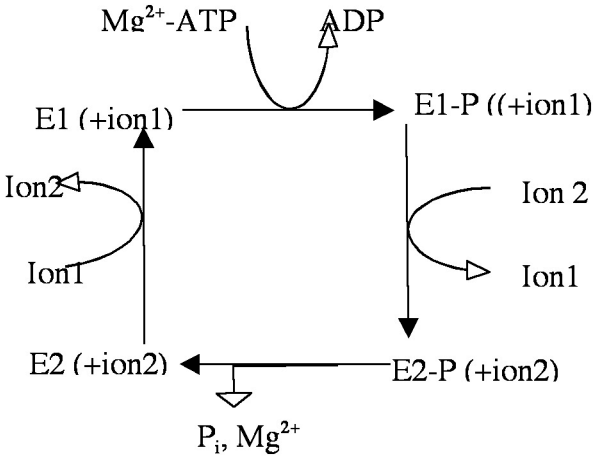

Figure 1.1: Schematic representation of ion translocation by P-type ATPases, based on Post-Albers scheme for Na^+/K^+-ATPase; ion1: ion translocated from inside to outside, ion2: ion translocated form outside to inside, E1/E2-P: phosphorylated state of the enzyme. Ion binding triggers phosphorylation of enzyme by Mg^{2+}-ATP.

1.5.2 Types of P-type ATPases:

Even though the basic structural outline and catalysis mechanism is similar, P-type ATPases are a diverse family of proteins and can be further classified.

Based on sequence homology and substrate specificities, the P-type ATPase family is divided into five branches, I to V (Figure-2). Within these branches, different sub-types or classes can be distinguished (Axelsen and Palmgren 1998; Palmgren and Axelsen 1998) (Okamura et al. 2003).

Type IA sub-group pumps are found in bacteria, with Kdp (K^+-pump) as prototype. Kdp protein sub-unit B (72kDa) is the smallest known P-type ATPase (Altendorf et al. 1998; Kuehlbrandt 2004). The A sub-unit binds the ion. It has been hypothesized that this complex is an ancestral P-type ATPase and in modern P-type ATPases, the ion binding and catalytic domain became fused (Axelsen and Palmgren 1998)

The substrates for the type IB P-type ATPases are soft-transition metal ions. The homeostasis of indispensable trace elements such as Cu^+ and Zn^+ is achieved by balancing the activity of these efflux pumps against metal uptake proteins (Rosen 2002). Unlike the IA type pumps, type IB ATPases work as single chain proteins. These, along with type IIA pumps (see below) appear to be most fundamental to life. They are found in every kingdom of the evolutionary tree (Okamura et al. 2003). Mutations in human copper efflux pumps cause rare but lethal, hereditary Menkes and Wilson diseases.

As evident from figure 1.2, type II ATPases are the most diverse of the P-type ATPases. Type IIA comprises the sarcoplasmic reticular (SR) Ca^+ATPase while the plant Ca^+ATPase belongs to type IIB. Type IIC ATPases include the Na^+/K^+ and gastric H^+/K^+-ATPases. They work as hetero-oligomers and the

catalytic α-subunit has all the characteristics of a typical P-type ATPase. Type IID pumps are the eukaryotic Na^+-ATPases.

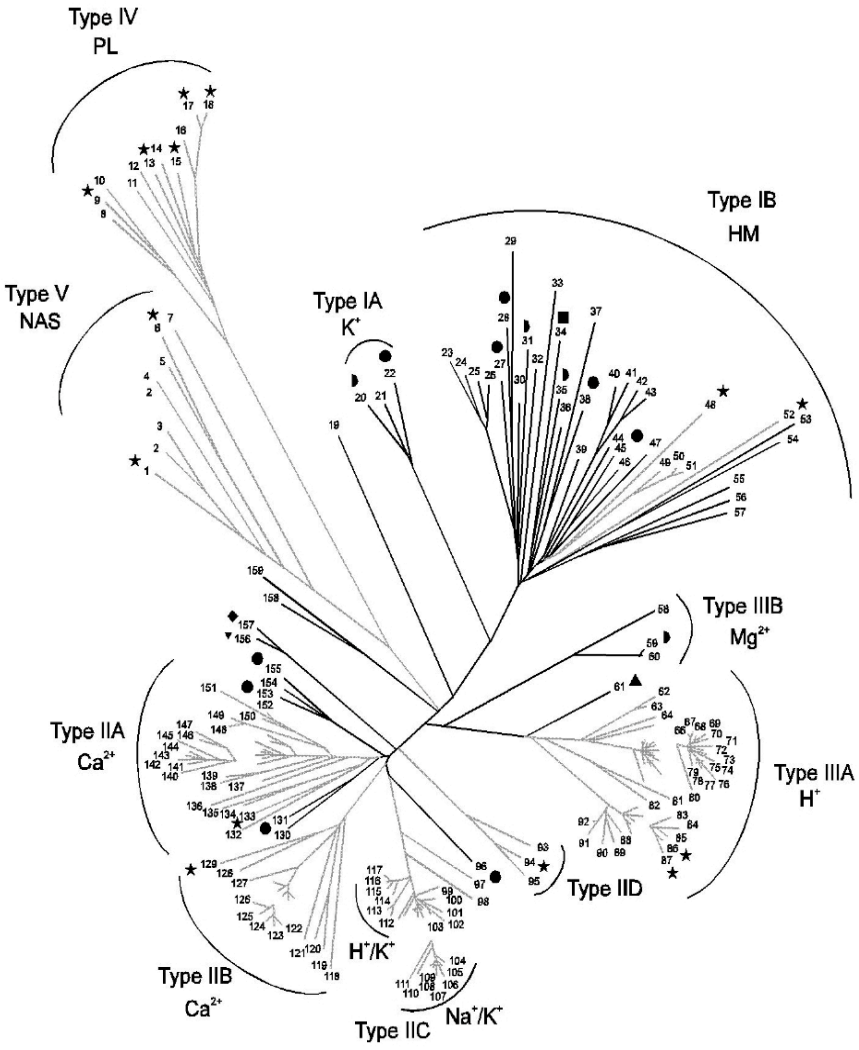

Figure 1.2: Phylogenetic tree of P-type ATPases. ◗: E.coli;■: Haemophilus influenzae;▲: Methanococcus jannaschii; ◆: Mycoplasma genitalium;▼: Mycoplasma pneumoniae;★: Saccharomyces cerevisiae;●: Synechocystis PCC6803; HM: Heavy Metals; NAS: No Assigned Specificity; PL: Phospholipids. The numbers correspond to the numbers used in (Axelsen and Palmgren 1998), Table-1. Figure adopted from (Axelsen and Palmgren 1998) and http://www.patbase.kvl.dk/tree.html.

After type II, type III ATPases are the most studied P-type pumps. Type IIIA ATPases are H^+-pumps that are found almost exclusively in plants and fungi (with the exception of putative H^+-pump of *M. jannaschii*). A small class of bacterial Mg^+-pumps, closely related to type IIIA pumps is grouped under type IIIB ATPases.

Type IV ATPases are found only in eukaryotes, where they are involved in lipid transport and maintenance of bilayer symmetry. These proteins probably act as 'lipid flippases' and translocate phospholipids from outer to inner leaflet of plasma membrane (Daleke 2003; Pomorski et al. 2003). However, very little is known about these proteins and considering the close structural homology of known P-type ATPases, it is still not clear how the binding site at the centre of a large transmembrane protein can adopt to translocate both ions and phospholipids.

The latest addition to the classification is the type-V ATPases found in eukaryotic genomes (Axelsen and Palmgren 1998). These proteins are probably also ion pumps even though their specificities and substrates are not yet identified.

1.5.3 Structural studies of P-type ATPases:

All P-type ATPases are multi-domain membrane proteins with molecular masses of 70-150kDa. From membrane topology predictions, they all have an even number of trans-membrane helices; the N and C-termini are on the cytoplasmic side of the membrane. The membrane domain consists of ion transport path. The cytoplasmic side of the protein is made up of three domains, A (actuator), P (phosphorylation) and N (nucleotide binding) (Toyoshima 2000).

1.5.3.1 Ca^{2+}ATPase:

Much of the structural information available on P-type ATPases is the result of studies on type II and III ATPases. A high-resolution structure of a type II pump, Ca^{2+}ATPase from sarcoplasmic reticulum of rabbit muscle, was solved at 2.6Å (Toyoshima 2000). The transmembrane domain consists of ten α-helices and two calcium ions were shown bound to the protein. From other members of the family, only images at a resolution of 8Å are available (Hebert 2000).

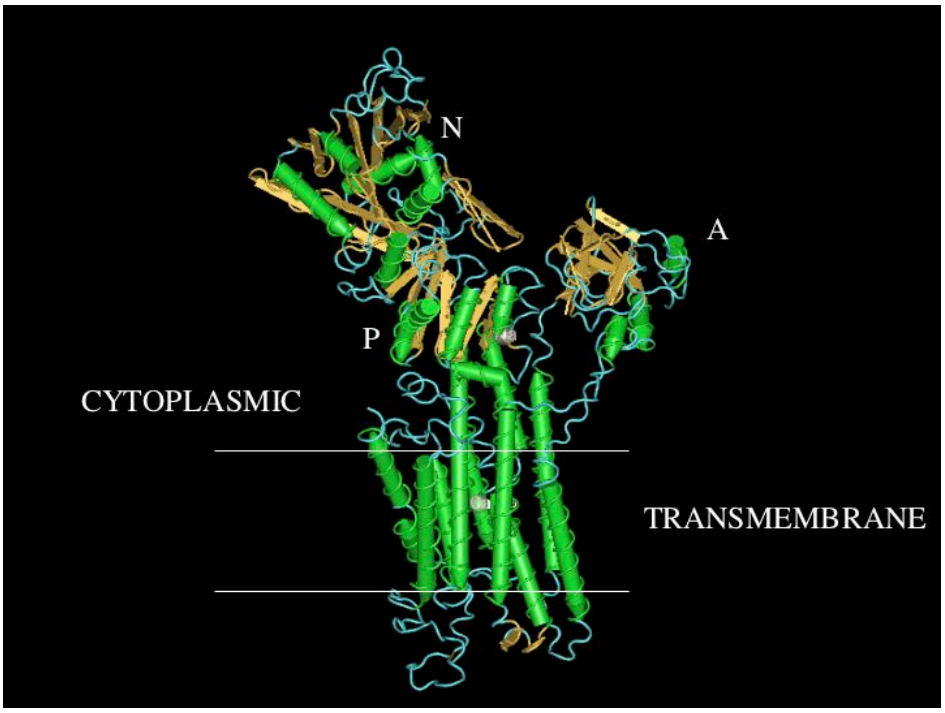

Figure 1.3: 3D structure of Ca^{2+} ATPase, showing position of transmembrane region, A, N and P domains. This is a screen image of 3D structure of ISU4 version of Ca^{2+}-ATPase submitted to PDB.

The cytoplasmic region consists of three well-separated domains: domain A might work as actuator or anchor for domain N, which binds nucleotides, and

domain P contains the Asp (351 in Ca^{2+} pump), the residue of phosphorylation (Figure 1.3).

Huge domain movements occur during catalysis, from E1 state of the enzyme to E2 state (Figure 1.4). The phosphorylation site is more than 25 Å away from the bound nucleotide meaning that domain closure must occur during ATP hydrolysis. Other data indicate that domain N is mobile in the presence of Ca^{2+} but fixed in its absence, and that domain N comes close to domain P in the phosphorylated states. The distance between the ATP-binding pocket and bound Ca^{2+} ions is ~80 Å. Flexible hinge regions make these large domain movements possible.

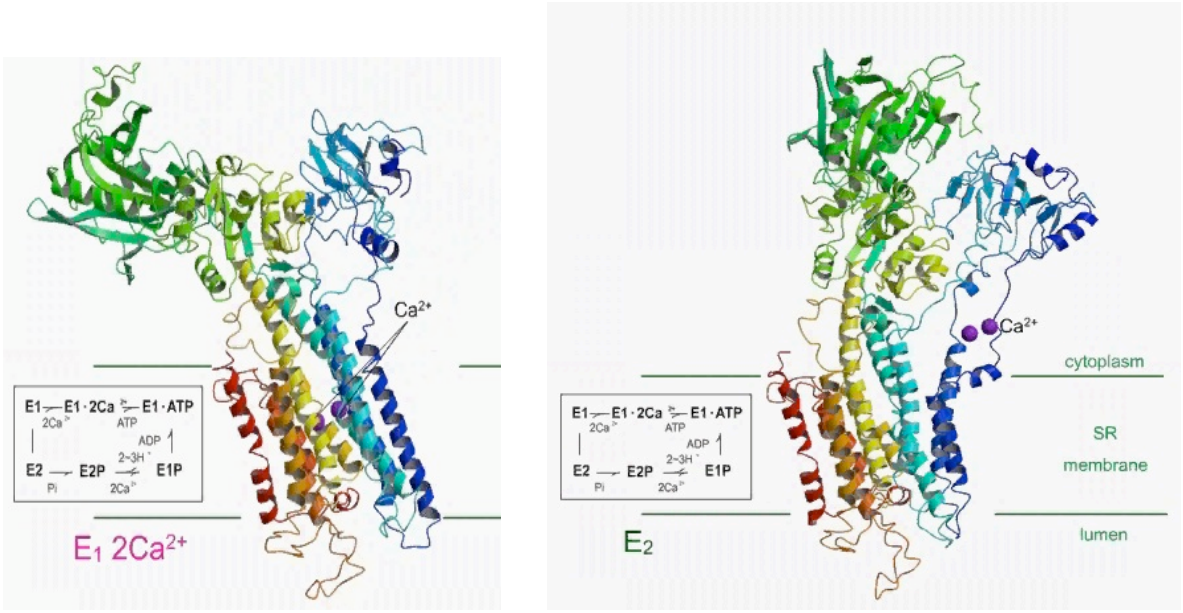

Figure 1.4: Two catalytic states of Ca^{2+} ATPase: Huge conformational differences between E1 (shown here bound to $2Ca^{2+}$ ions) and E2 states. The figure is a screen shot from supplementary movie from (Toyoshima et al. 2004)

1.5.3.2 Na^+, K^+ ATPase:

Na^+, K^+ ATPase is the largest protein complex known to date in P-type ATPase family. The minimal functional unit of this protein is a hetero-dimer of α- and β- subunits (Jorgensen and Andersen 1988). Electron microscopy image reconstruction of this protein at 9.5 Å is reported (Hebert et al. 2001). The 3D model of Na^+, K^+ ATPase fits nicely into the Ca^{2+}ATPase model. A major difference between the maps of Na^+, K^+ ATPase and Ca^{2+}ATPase is that the former pump adopts a more closed conformation.

1.5.3.3 Proton pump from *Neurospora crassa*:

Even though large single 3D crystals (400μm x 400μm x 150μm) of *Neurospora crassa* H^+-pump were obtained, they diffracted only to 0.4nm and the structure was not solved using these crystals (Scarborough 2000). An atomic homology model of this pump (a type III ATPase) was built based on the 2.6Å structure of Ca^{2+}ATPase (Kuehlbrandt 2002). To deliver ATP to phosphorylation site, the nucleotide-binding domain has to rotate by approximately 70°. Even though the sequence homology in the membrane domains was low between the Ca^{2+}ATPase and *Neurospora* proton pump, a perfect fit could be observed, especially in membrane helices M3, M4 and M5. This indicates that at least in the membrane regions, the structure of P-type ATPases is highly conserved. There were notable differences in the cytoplasmic regions, nevertheless.

1.5.3.4 The need to study more P-type ATPases:

In order to understand the mechanism of energy transfer through the membrane helices and differences in specificities of ion binding of these ATPases, diverse proteins from different subgroups of P-type ATPases need to be studied. High-resolution structures of more P–type ATPases need to be

solved for understanding fine details of ion transport across the membrane and its coupling to ATP hydrolysis.

For example, on comparison of membrane topology of a heavy metal ATPase (type IB P-type ATPase) and a non-heavy metal ATPase (Ca^{2+}ATPase), considerable differences in number and arrangements of transmembrane regions can be observed (Figure 1.5) (Bissig et al. 2001).

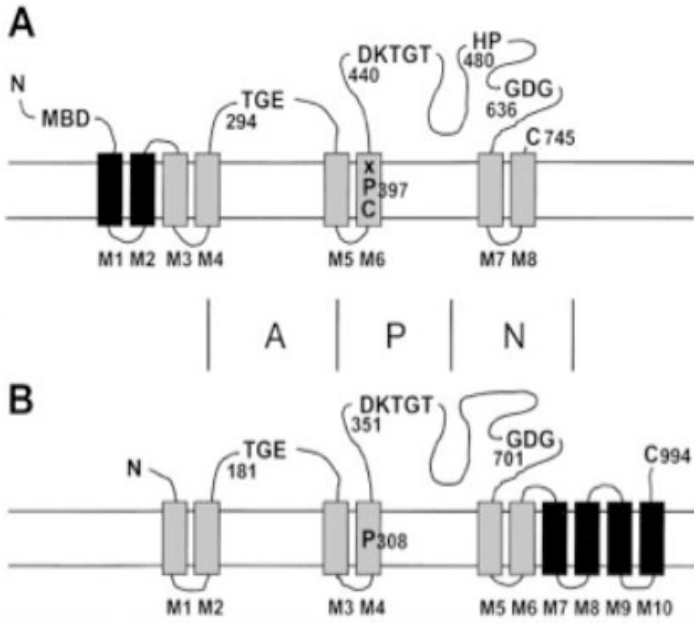

Figure 1.5: (A), *E. hirae* CopB membrane topology compared to Ca^{2+}ATPase of sarcoplasmic reticulum (B). Unique helices for one type of protein is indicated in black and common to both types are indicated in grey. (Figure adopted from Bissig et al. 2001)

These results suggest that even though all P-type ATPases appear to have similar structural features, there are many architectural differences that necessitate detailed study of more of these pumps for understanding the specificity and transport of ions of this class of molecules. In addition, to understand the specificity of these proteins for particular ions, more molecular biological, biochemical, biophysical and structural studies must be done.

1.6 The focus of current study

The current study is aimed at understanding more about P-type ATPases and to make available large quantities of these proteins for structural studies by electron microscopy and/ or X-ray crystallography. To achieve this goal, three P-type ATPases, a plant proton pump (AHA2 from *Arabidopsis thaliana*) and two putative copper transporters, CtrA2 and CtrA3 (from *Aquifex aeolicus*) that are similar to known P-type copper transporting pumps CopA and CopB, were studied. A brief review of literature, importance, and medical relevance of these proteins are presented below. The methods employed in general for studying these proteins are also discussed.

1.7 Plant plasma membrane proton transporting ATPases

The main function of plant plasma membrane proton pumps is to activate secondary transport by the proteins whose activity is dependent on proton motive force. In addition, when the intracellular pH drops to less than 7.0, the acidification of cytosol activates the H^+ pump to enhance extrusion of protons. Other essential functions of this protein, essential for normal plant growth, are salt tolerance and cellular expansion (Morsomme 2000). Probably, one of the most characterized plant H^+ pumps biochemically is the *Arabidopsis thaliana* protein, AHA2 (Palmgren 2001). Structural studies of the proton pumps, by homology modeling (Kuehlbrandt 2002) or by 3D maps of 2D crystals (Auer 1998) have shown considerable similarities with Ca^{2+}ATPase.

One striking feature of the proton pump is the carboxy-terminus region that acts as an auto-inhibitory domain (Portillo et al. 1989; Palmgren et al. 1991). It has been shown biochemically that the conserved residue Asp^{684} in the transmembrane segment M6 of AHA2 is very essential for proton translocation (Buch-Pederson 2003). Substitution of this aspartate with glutamate results in

very little proton pumping and mutation to any other amino acid results in no pumping of this enzyme.

1.8 Heavy metal transporting ATPases

Heavy metal transporting ATPases, also called CPX-ATPases or soft metal transporting P-type ATPases, belong to P_{1B}-ATPases family. About a hundred genes encoding P_{1B}-type of ATPases have been identified in archaea, bacteria and eukaryotes (Axelsen and Palmgren 1998). These enzymes transport metal ions such as Cu^{+}, Cu^{2+}, Ag^{+}, Zn^{2+}, Pb^{2+}, Cd^{2+} and Co^{2+} across biological membranes, thus playing important role in homeostasis and biotolerance of these metals (Vulpe and Packman 1995; Solioz and Vulpe 1996; Rensing et al. 1999). It is assumed that these proteins have a catalytic mechanism similar to that observed in well-characterized P_{II} type ATPases.

These enzymes appeared very early in the evolution of life and are expected to play critical roles for ion homeostasis in cell physiology (Okamura et al. 2003). The importance of these proteins in cells is evident from the fact that mutations of the two human Cu^{+}-ATPases, ATP7A and ATP7B, cause Menkes and Wilson diseases (Bull and Cox 1994). These proteins also play complex roles in plant micronutrient metal metabolism. Eight genes responsible for expression of P_{1B} type of ATPases are found in *Arabidopsis thaliana* genome (Williams et al. 2000).

1.9 Characteristic features of P_{IB}-ATPases

From hydropathy studies, it is proposed that P_{IB}-ATPases have 8 transmembrane regions. A striking feature of all P_{IB}-ATPases is that they have a metal binding motif in the transmembrane region of the helix (TM 6) that is immediately upstream from phosphorylation site (Arguello 2003). This motif has a conserved sequence of CPC, CPH, CPS, SPC or TPC. This motif is necessary

for protein function and most likely determines the ion to be transported. In Ca^{2+}ATPase, the residues corresponding to this motif are IPE, as part of the sequence val^{304}-Ala-Ala-Ile-Pro-Glu^{309} and are involved in ion transport (Toyoshima 2000). Mutations in this motif, for example, CPC to CPA yields a non-functional protein (Yoshimizu et al. 1998). Similar results were observed when CPH to SPH mutation was introduced in *E. hirae* CopB (Bissig et al. 2001). In addition to this motif, conserved regions were also observed in TM 7 and TM 8. In the center of TM 7, YN sequence is completely conserved. It is possible that these three TM regions co-ordinate together to form a metal binding pocket to facilitate transport of the ion.

Another conserved motif of interest in CPX type of ATPases is the HP (His-Pro) sequence located in large cytoplasmic loop, about 40 amino acids downstream of the phosphorylation site with the signature sequence Asp-Lys-Thr-Gly-Thr. By analogy to Ca^{2+}ATPase, this region would be located in N domain, but no recognizable sequence similarity could be observed between Copper ATPases and Ca^{2+}ATPase in this region. The HP motif is affected by the Wilson disease mutation H1069Q (Bissig et al. 2001).

Most P_{IB} type proteins also have at their N-terminus, 1-6 metal binding domains, either as CxxC motif or a Histidine rich sequence. It is possible that these domains have a regulatory rather than an essential role in catalytic mechanism, since some functional P_{IB}-ATPases lack this domain (Voskoboinik et al. 1999; Mitra and Sharma 2001). These proteins are divided into six subgroups (Table 1.1) depending on the conserved sequence in TM 6 and N terminal metal binding domain (N-MBD) (Arguello 2003; Arguello et al. 2003).

Table 1.1

Type	TM 6 conserved motif	N-MBD	No. of CxxC	Transported ion
IB-1	CPC	GMTCxxC	up to 6	Cu^{+}, Ag^{+}
IB-2	CPC	CxxC	up to 3	Zn^{2+}, Cd^{2+}, Pb^{2+}
IB-3	CPH	His rich	0	Cu^{2+}, Cu^{+}, Ag^{+}
IB-4	SPC	His rich (?)	0	Co^{2+}
IB-5	TCP $(x)_5P$	None	0	?
IB-6	CPS, APC, CPC	CxxC/ none	0-1	?

1.10 Copper transport by P_{IB}-ATPases

The human Wilson and Menkes disease proteins ATP7B/WND (P35670) and ATP7A/MNK (Q04656) are grouped as IB-1 subgroup. These proteins are responsible for transporting copper across the membrane. P-type ATPases for transporting copper have been identified in several prokaryotes (Francis and Thomas 1997; Bin Fan 2002; Arguello et al. 2003; Stoyanov 2003). On sequence comparison, these proteins belong either to IB-1 or IB-3 subgroup (i.e., they have either CPC or CPH conserved motifs). It is also interesting to note that CPH containing copper transporters are not found in eukaryotes (Arguello 2003). CopA and CopB proteins from *E. hirae* and *A. fulgidus* are very well characterized among prokaryotic copper transporters and give valuable insights into the functioning of these proteins.

1.10.1 CopA:

CopA (*E. coli, E. hirae, A. fulgidus*) belongs to P_{IB-1} subgroup of P-type ATPases. Proteins belonging to this subgroup are found in archaea, prokaryotes

and eukaryotes. CopA is characterized by the signature sequence CPC in TM6. Enzymatic studies show that this protein is activated by Ag^+ and Cu^+ and to a lesser extent by Cu^{2+}, but not by other divalent metal ions (Rensing et al. 2000; Wunderli-Ye and Solioz 2001; Mandal 2002). Transport assays on *E. coli* CopA (Rensing et al. 2000) suggest that this protein is responsible for efflux of copper from the cell. From sequence analysis, *E. coli* CopA also has two CxxC N-MBD motifs, while homologs from *A. fulgidus*, *E. hirae* have only one. Menkes disease protein has six CxxC motifs. Studies suggest that the six metal binding motifs of Menkes disease protein are involved in intra-cellular trafficking (Voskoboinik et al. 1999). Since this is not an issue with prokaryotes, this domain might be involved in sensing copper ion and binding them in the cytosol for transfer to translocation domain. Even though prokaryotic and eukaryotic proteins differ in the number of CxxC domains, the functional similarities of these proteins is striking (Voskoboinik et al. 1998; Rensing et al. 2000).

There is also some indirect evidence to suggest that CopA serves in copper uptake under copper limiting conditions. Disruption of *ctpA* gene of *Listeria monocytogenes* reduces growth of these cells in copper limiting media (Francis and Thomas 1997). It is also reported that ΔCopA strains of *E. hirae* grow poorly in media where copper is limited by complexation with copper chelators and also more resistant to Ag (I) than wild type strains (Odermatt et al. 1994). A heavy metal ATPase is also involved in supplying copper to the cells for photosynthesis (Tottey et al. 2001). If in fact CopA transports copper into the cells, this would mean that the direction of copper transport relative to ATP binding site would be opposite to that postulated for most copper ATPases and actually shown for CopB of *E. hirare* (Solioz and Odermatt 1995) and for human Menkes and Wilson ATPases (Voskoboinik et al. 1998; Voskoboinik et al. 2001). For this to be the case, these copper ATPases must act as Cu^+-H^+ ATPases, transporting H^+ out of the cell and Cu^+ into the cell. Many P-type ATPases studied do in fact transport ions simultaneously in both directions.

1.10.2 CopB:

CopB belongs to P_{IB-3} type of ATPases. Copper transporting ATPases with signature sequence CPH are placed under this subgroup. *E. hirae* CopB is the first IB-3 enzyme to be characterized (Odermatt et al. 1993). This protein is activated in the presence of Cu^{+} and Ag^{+} and it was shown that Cu^{+} is transported by this enzyme (Solioz and Odermatt 1995). However, studies on CopB from *A. fulgidus* (Mana Capelli 2003) suggest that this protein is activated more by Cu^{2+} than Cu^{+} and Ag^{+}. A main characteristic of CopB is that it does not posses the N-terminal CxxC binding motif. Instead, it features a histidine rich N-terminus, that most likely constitutes a metal binding domain and like in CopA, has a regulatory role.

Copper (and silver) transport was demonstrated in CopB. Wild type *E. hirae* can tolerate up to 8mM copper in the media and it was shown by genetic analysis that CopB is required for this resistance (Odermatt et al. 1993). The physiological role of CopB is to control cytoplasmic copper by extruding it from the cell. CopB has two putative metal binding regions. Imidazolium group of His in CPH motif in the membrane probably coordinates the metal during transport and determines enzyme specificity. His rich N-MBD might bind and translocate Cu^{2+}. This domain is not essential for enzyme function, but is required for enzyme activity. CopB truncated at the N-terminus does not show any change in metal selectivity. This truncated protein is functionally active, but with a lower turnover rate. It has been proposed that metal binding to His-N-MBD promotes its interaction with one or more of the cytoplasmic loops (Arguello et al. 2003; Mana Capelli 2003). Being a hard Lewis base, the imidazolium group of histidine preferably binds to Cu^{2+}, an intermediate Lewis acid (Pearson 1963). Similar protein in *Pseudomonas syringae*, psCopB is a component of plasmid encoded copper resistance system (Mellano and Cooksey 1988).

1.11 Copper homeostasis in cells

Copper is an essential metal ion for most organisms, required for enzymes such as cytochrome c oxidase (mitochondrial electron transport chain), superoxide dismutase (for protection against free radicals), tyrosinase (pigmentation), peptidylglycine alpha-amidating mono-oxygenase (neuropeptide and peptide hormone processing), and lysyl oxidase (collagen maturation). However, copper in excess is toxic to cells because of its ability to catalyze the generation of free radicals by the Fenton reaction (Lloyd and Phillips 1999; Urbanski and Beresewicz 2000) and binding ectopically to proteins to disturb their structure (Valko et al. 2005). It is for this reason that copper homeostasis has been very important for cells and every organism has elaborate means at its disposal to control uptake, distribution, de-toxification and elimination of copper (Balamurugan and Schaffner 2006).

Uptake of copper by yeast and mammalian cells is by high affinity membrane bound copper transporters, exemplified by copper transporter family of proteins (Valentine and Gralla 1997). Extra-cellular copper, usually Cu (II) is reduced by plasma membrane reductases to Cu (I), which is the substrate for these proteins (Petris 2004). In bacteria, energy dependent copper uptake by a specific copper transporter has not been directly demonstrated.

Since free copper causes oxidative damage, cells have evolved intra-cellular chaperones that bind copper with high affinity and deliver it to specific target proteins. Atx I is such a chaperone identified in yeast (Pufahl et al. 1997). A bacterial homolog of the Copper chaperon, CopZ has been identified in *E. hirae* (Cobine et al. 1999).

ATP-dependent copper transporters of the P-type ATPase family are responsible for de-toxification and elimination of excess copper from cells. In humans, this task is carried out by the Wilson disease protein and Menkes

disease protein (Suzuki and Gitlin 1999; Voskoboinik and Camakaris 2002). Excess copper in prokaryotic cells is pumped out by copper ATPases (Arguello et al. 2003; Stoyanov 2003).

1.12 Clinical importance of copper transporters

The importance of copper transport in cells can be realized from the diseases resulting from imbalance of copper homeostasis, Wilsons disease and Menkes disease (DiDonato and Sarkar 1997). Mutations in Wilsons disease protein, ATP7B/WND, caused by deletions, insertions and splicing errors, lead to slow copper accumulation in liver, kidney, brain, cornea and mammary gland (Harris 2003). Symptoms of this disease usually appear in the second decade of life and in an adult patient include liver disease, tremors, muscle rigidity, slurred speech, or personality changes such as depression. Diagnosis is not always straightforward, since the disease is associated with a large number of mutations and DNA testing of the patient or family members is not reliable. Copper-related tests could be applied to make the diagnosis or rule it out. Treatment involves drug therapy for life and a copper restricted diet.

Menkes disease is a systemic copper deficiency that affects the metabolism of major internal organs, particularly the central nervous system (Harris 2003). ATP7A is important for adequate copper supply to the brain, systemic absorption of copper in mucosal cells lining the intestine, and re-absorption in kidneys (Voskoboinik and Camakaris 2002). Mutations in ATP7A/MNK protein, caused by insertions/deletions, nonsense or missense mutations would lead, in majority of cases, in production of a truncated ATP7A protein (Tumer et al. 1997). Symptoms of this X-linked recessive disorder include stunted growth, skeletal defects and progressive degeneration of central nervous system (Voskoboinik and Camakaris 2002). Cellular copper retention is the basis of diagnosis of this disorder. Copper-histidine complex administration can, in

many cases delay, but never reverse the destructive course of disease (Christodoulou et al. 1998).

1.13 Membrane proteins for structural studies

One of the main bottlenecks in structural determination of membrane proteins is their availability. Crystallization trials typically require milligram amounts of pure protein. Only few membrane proteins can be isolated from natural sources in this quantity for structural studies. It is clear therefore that suitable over-expression systems for membrane proteins are needed. Since there is no one particular expression system that caters for the need of over-expression of membrane proteins, several systems need to be tested for the quantity and quality of proteins expressed (Bannwarth and Schulz 2003).

1.13.1 *E. coli* expression system:

This is by far the most popular and well-studied expression system. The main advantages of this system are:

a. Low cost,

b. Homogeneity of expressed protein (no post-translational modifications), and

c. Short generation times (~20min) and short delay in expression (Grisshammer and Tate 1995)

Optimization of expression is less tedious and quick with *E. coli* because of these reasons. All these characteristics render *E. coli* very appropriate to the constraints of structural biology. However, there are many factors that limit the use of *E. coli* as a universal over-expression system.

i. Over-expression may lead to inclusion body formation. Refolding of membrane proteins is thought to be complex and not well understood. But this is

not completely un-desirable, at least in the case of the β-barrel membrane proteins from bacterial outer membranes (Schulz 2000). Production of proteins in inclusion bodies can be quite helpful. Proteins are produced in very large quantities and purification can be easier as separation of inclusion bodies from rest of the cell itself is a purification step. *E. coli* outer membrane phosholipaseA (OmpLA) and porin OmpG have been successfully expressed, purified from inclusion bodies and crystallized (Blaauw et al. 1995; Dekker et al. 1995; Yildiz et al. 2006).

ii. The proteins expressed might be toxic to the bacteria. In this case, either the protein is not expressed or the cell dies soon. There have been attempts to overcome this problem by identifying and characterizing mutant hosts, for better expression yields and better membrane incorporation (Miroux and Walker 1996).

iii. The major hurdle of the *E. coli* expression system is to use it for the expression of eukaryotic membrane proteins. In a majority of cases, these proteins are either not expressed at all or misfolded. Since this system lacks the post-translational modification machinery, like glycosylation, it is possible that the expressed proteins (for example GPCRs) are functionally inactive (Sarramegna et al. 2003). However, this system has been successful for expressing potassium channels from plants (Uozumi 2001). Plant K^+ transporters could even functionally complement their counterparts in *E. coli*.

An alternate prokaryotic expression system is the gram-positive bacterium *Lactococcus lactis*. It has been used for successful homologous over-expression of mechanosensitive channels and transporters. Human KDEL receptor, hydrogenosomal ATP/ADP carrier, and yeast mitochondrial carriers were successfully expressed in this system (Kunji et al. 2005). Because this bacterium has mild proteolytic activity, there is less possibility of degradation of expressed membrane protein.

1.13.2 *Saccharomyces cerevisiae*:

S. cerevisiae is the first yeast employed for recombinant expression. This system is ideal for recombinant expression of eukaryotic proteins since it combines the ease of use of bacterial system with suitable environment for eukaryotic proteins. Like bacteria, yeast is simple to cultivate on inexpensive growth media. However, as eukaryotes, it provides an environment for post-translational processing resulting in a product that is identical or more similar to native (eukaryotic) protein. Foreign genes can be maintained in *S. cerevisiae* as plasmids in high copy number, but this requires selection marker for maintenance. Alternatively, low copy number gene integration is also possible (Sudbery 1996).

S. cerevisiae has been studied thoroughly and its genome was completely sequenced in 1996 (Goffeau et al. 1996). Approximately 95% of the genome has been systematically knocked out and many of the mutants are commercially available. A main advantage of this system is the comparatively small genome and ease of molecular and genetic manipulation (Ton and Rao 2004). Strong promoters have been identified and are employed for over-expression; these include PMA1, PDR5, GAL1, CUP1 and heat-shock promoters.

Many different eukaryotic (and archaeal) membrane proteins are successfully expressed in *S. cerevisiae*: K^+-channels (Anderson et al. 1994), calcium transporters (Ton and Rao 2004), plasma membrane proton pumps (Villalba JM 1992; Mahanty et al. 1994; Morsomme et al. 2002), GPCRs (Reilander and Weiss 1998), multidrug efflux pumps (Niimi et al. 2005), to name a few. In addition to expression, complementation assays and other functional analysis can be carried out with eukaryotic membrane proteins expressed in yeast (Bill 2001). Despite the advantages and successes, *S. cerevisiae* system is limited as an expression system. This is mainly because of the yields obtained are some times low for structural studies, possibly because of toxicity issues.

Also, partial glycosylation can be an issue. High cell densities cannot be achieved with this yeast and during fermentation, plasmids (especially Yeps) can be unstable (Etana Padan 2003).

1.13.3 *Pichia pastoris*:

The yeast *P. pastoris* is a very useful system for over-expression of eukaryotic proteins. This system has all the advantages of *S. cerevisiae*: ease of growth and genetic manipulation and presence of a eukaryotic protein synthesis pathway. In addition, very high cell densities can be reached in fermentation. The expression of any foreign gene in *P. pastoris* comprises three principal steps:

i. Insertion of gene into expression vector
ii. Linearization and introduction of the vector into *P. pastoris*
iii. Screening of transformed strains for expression of recombinant protein.

The screening process also involves identifying the strain expressing the highest quantity of protein, since different strains can exhibit different levels of protein expression.

The foreign gene is placed under regulation of *AOX* promoter that is tightly regulated and thus provides a reliable means of expression after induction (Macauley-Patrick et al. 2005). *AOX* is a very strong promoter and repressed by initial carbon source (glucose) ensuring that good cell growth is obtained before induction. Induction of transcription is by the addition of methanol. However, monitoring methanol levels in fermentation is not easy. It is also a fire hazard. Sometimes, a very strong promoter is actually un-desirable. There is evidence that for certain foreign genes, high levels of expression can overwhelm the post-translational machinery resulting in production of misfolded, un-processed or mislocalized proteins (Brierley 1998).

Alternatives to the *AOX* promoter also exist, though they are not very common. *GAP, FLD1, PEX8* and *YPT1* are well-characterized promoters for expression in *Pichia pastoris* (Cereghino and Cregg 2000). Protease-deficient strains SMD 1165 (*his4 prb1*), SMD1168 (*his4 pep4*) and SMD1163 (*his4 prb1 pep4*) have been shown to be effective in reducing degradation of some foreign proteins- human thrombomodulin and insulin like growth factor (White et al. 1995; Brierley 1998). Main disadvantages of this system are that this organism is not very well characterized; it is difficult to obtain a knockout mutant. Not much variation is possible if the recombinant protein is not expressed.

1.13.4 Other eukaryotic expression systems:

Yeast such as *Schizosaccharomyces pombe*, *Hansenula polymorpha* have also been used for heterologous expression of proteins. However, these systems need to be characterized further for their feasibility to express membrane proteins in correctly folded and functional forms.

Baculovirus/ insect expression system is an alternative to express fully functional eukaryotic membrane proteins. A large number of vectors and viral liniarized DNA for transient or stable expression are commercially available and are being developed. This system is most successfully employed for over-expression of GPCRs (Sarramegna et al. 2003). The general principle of this system is to place the gene of interest in a plasmid with sequences of high homology for bacculovirus genome under the control of a strong promoter (ex. polyhedrin). Co-transfection of plasmid and viral DNA into insect cells allows insertion of gene of interest into viral genome in vivo by homologous recombination. Main drawbacks of this system are long generation time of insect cells, excessive cost and low yield of final recombinant protein (Fraser 1992).

Integral membrane protein expression is not difficult in mammalian cells and has been used for decades in drug and biological discovery. The main

advantages of this system are that they present the environment closest to the native tissue of human or higher eukaryotic membrane protein and complex post-translational modifications are possible. Three different types of mammalian expression systems exist- internal ribosomal entry site (IRES) based, ecdysone inducible expression system and semiliki forest virus (SFV) expression system (Rhodes et al. 1998). Of these systems, only SFV expression system is capable of producing recombinant membrane proteins at levels needed for structural studies. However, it takes weeks and months to generate a stable cell-line and excessive costs involved in the process add to the limitations of this system for over-expressing membrane proteins.

Transient expression of eukaryotic membrane proteins has been reported in cos cells and *Xenopus* oocytes, though only for functional studies. The main limitation of these systems in addition to long doubling time of cells and excessive cost is that it is very difficult to scale up transient expression (Schertler 1992). Another eukaryotic expression system that expresses recombinant light harvesting complex-II for structural studies is transgenic tobacco (Flachmann 1999).

1.13.5 Cell-free expression systems:

Cell-free expression systems are also being developed to enable expression of membrane proteins, but these are in very early stages of development (Klammt et al. 2004; Koglin et al. 2006).

1.14 Methods to study membrane proteins

The function of a protein is defined by its structure. In order to understand how a protein works, it is important to understand its three-dimensional structure. Three different methods are at the disposal of biophysicists to determine the structure of proteins: X-ray crystallography, NMR spectroscopy and electron

microscopy. These techniques yield different and complementary information about the structure of proteins. It must be emphasized that the primary structure of proteins (sequence of amino acids) and important preliminary information on protein functioning is obtained by biochemical techniques.

Other biophysical methods provide important complementary information; spectrophotometric methods such as circular dichroism (CD) provide details on the helical content of proteins or asymmetric environment of aromatic residues. UV-visible absorbance spectrophotometry assists in identifying metal ions, aromatic groups or co-factors attached to proteins while fluorescence methods indicate local environment for tryptophan side chains. A detailed listing of all membrane protein structures available, with references is documented at

http://www.mpibp-frankfurt.mpg.de/michel/public/memprotstruct.html

Number of high-resolution protein structures deposited till July 04, 2006 by different techniques is summarized in Table 1.2:

Table 1.2:

Technique	Number of Structures in PDB	%
Total number of protein structures known	34376	100
X-ray	29509	85.84
NMR	4706	13.68
EM	88	0.25
Other*	73	0.21

Source: Protein Data Bank, **http://www.rcsb.org/pdb**

* Other methods include homology modeling, neutron diffraction, FTIR, etc.

Only X-ray crystallography and electron microscopy are introduced here. NMR, even though a valuable tool for structural analysis of proteins, has limited use for studying membrane proteins of size greater than 50kDa. It must be noted, however, that solid-state NMR is emerging as a new tool for studying membrane proteins. In principle, there is no upper limit in the size of molecule for studying by solid state NMR, as it does not rely on molecular motion like solution NMR.

1.14.1 3D crystallization and X-ray crystallography:

X-ray crystallography depends on directing a beam of x-rays on to a regular repeating array of many identical molecules, so that the x-rays are diffracted from it in a pattern from which the structure can be retrieved. Well-ordered crystals are a pre-requisite and are difficult to grow. The formation of crystals is dependent on different parameters, including pH, temperature, protein concentration, nature of solvent, precipitant, added ions and ligands, and detergent, in case of membrane proteins. To screen these parameters, it is imperative that large amount of pure and homogeneous protein sample is available. The amphipathic surface of membrane proteins present additional challenges for crystallization attempts and need to be addressed.

The first bottleneck in membrane protein crystallization is the availability of a sufficient amount of protein. At present, many of the membrane protein structures that have been solved are of proteins that occur in high abundance in natural environment. These include proteins of respiratory chain or photosynthetic membranes in eukaryotes or bacterial outer membrane proteins. However, recombinant DNA technology led to successful over-expression of many membrane proteins and is opening the door for more 3D structures (Hunte and Michel 2002).

Diffraction of crystals is the next hurdle in determining 3-dimensional structure of proteins. Controlling protein purity and homogeneity, and optimizing

crystallization conditions can improve the diffraction quality of crystals. Small changes in pH, salt and precipitant concentrations, additives, protein concentration, type and purity of detergent have profound effects on formation of crystals and quality of diffraction (Hunte 2003).

The presence of flexible detergent micelle might pose problems for crystallization, as any degree of flexibility in protein crystals is detrimental for data collection. Detergent plays an important role not only in screening crystallization conditions, but also in improving the crystals and diffraction quality (Kuo et al. 2003).

To decrease the flexibility of crystals and to increase hydrophilic protein-protein contact, antibodies or their fragments generated against an epitope have been used effectively (Hunte 2003). Recently, 3D structure of *E. coli* chloride channel (ClC) bound to antibody fragments was solved at 2Å (Dutzler et al. 2003).

The importance of lipids in crystallization is increasingly being realized. Recently, the structure of cytochrome b_6f was solved at 3Å after addition of lipids (lipid augmentation technique) (Zhang and Cramer 2004). Crystallization in lipids is also being explored as a technique. These include the cubic-phase method, vesicle fusion method and bicelle method (Caffrey 2003). However, these techniques are limited to rhodopsin or other colored proteins at this moment and need to be studied in detail for their feasibility in routine crystallizations. One reason for the limitation is that the crystals, especially micro-crystals of non-coloured proteins could go undetected.

1.14.2 Electron microscopy:

Electron microscopy methods provide insights into structure and function of membrane molecules and complexes. Structure determination of large

complexes, which are either too large or too flexible for X-ray crystallography, is accomplished through single-particle imaging by cryo-electron microscopy. In this method, macromolecules are trapped in random orientations and images from all possible orientations are combined and averaged to provide enhanced views. A homogeneous protein sample is a prerequisite for single-particle image processing. The advantage of this method is that it bypasses the need to crystallize the protein either in 3D or in 2D arrays (Unger 2001). The *E. coli* large ribosomal sub-unit structure has been determined at 7.5 Å using this method (Matadeen et al. 1999). Many other macromolecular complex structures solved by single-particle analysis have been published (Frank 2002). Main drawbacks of this method are (i) it cannot be applied to small macromolecules (lower limit is around 250kDa at present) and (ii) the resolution achieved is low (around 10 Å).

Another powerful technique to understand structural features of membrane proteins is to image 2D-crystals in electron microscope. 2D crystallization of membrane proteins can be achieved by decreasing the detergent concentration in a homogeneously distributed protein-lipid-detergent mixture. Detergent removal by dialysis is a commonly used technique for membrane protein reconstitution for two-dimensional crystallization. Here, purified protein is reconstituted in a controlled way into complex or defined lipid bilayers at low lipid to protein ratios.

Depending on protein-lipid-detergent interactions, many different varieties of 2D crystals can be observed. Some proteins form 2D crystals in vivo. Different parameters including pH, temperature, protein, detergent, lipid, additives can be varied to improve crystal quality (Mosser 2001). 2D crystals can be visualized under an electron microscope, imaged and processed. In electron crystallography, Fourier methods are used to average the signal of the ordered proteins. Main advantages of electron microscopy (Kuehlbrandt 2003) are-

a. 2D crystallization trials require less protein than 3D crystallization

b. Protein concentration of 1-2mg/ml is enough to set up 2D trials.

c. It is possible for proteins to form 2-dimensional well-ordered crystals in heterogeneous environment i.e., 2D crystallization is more forgiving in protein purity than 3D crystallization. However, the levels of impurities tolerated depend on the protein being studied.

d. 2D crystals are known to form in systems where different oligomeric forms exist in equilibrium (Collinson et al. 2001)

e. Since crystal formation is in a lipid environment rather than in detergent, the conditions may be considered close to physiological or native-like.

Different tools are available to remove detergent and reconstitute protein in lipid, but the method to use depends on the protein being studied and largely depends on the lipid-protein-detergent interactions. Resolutions in the range of 5-10Å can be routinely achieved by electron crystallography (Unger 2000). Recently, the 1.9Å resolution structure of junctional Aquaporin 0 was determined by electron crystallography of double-layered two-dimensional crystals (Gonen et al. 2005).

The importance of studying membrane proteins in a lipid environment is evident from the fact that the 3D map of EmrE, a bacterial multidrug transporter, differs significantly in lipid bilayer and in detergent (Ubarretxena-Belandia et al. 2003; Ma and Chang 2004). A classic example of the power of electron microscopy for studying structure-function relationships of membrane proteins is the observation of pH induced structural changes in NhaP, a bacterial sodium-proton antiporter (Vinothkumar et al. 2005). The shifting of a helix bundle relative to dimer core of the protein that occurred at pH 6 or above could perhaps be observed only with electron microscopy. It is thus wise to pursue both 3D and 2D crystallization, if possible, not only for complementary information, but also to validate results.

1.15 Aim of current study

1.15.1 Plant proton ATPase:

The plant proton pump, AHA2 has already been crystallized in this lab and a projection map at 8Å is available (Jahn 2001). One of the aims of current study was to improve the crystallization for a better resolution projection map. In addition, since the expression levels of this protein over-expressed in *S. cerevisiae* were limiting the structural studies, attempts were made to over-express this protein in the yeast *P. pastoris*. Expression and purification of this protein in *S. cerevisiae* were standardized and crystallization was attempted. Problems in expression of AHA2 in *P. pastoris* and 2D crystalliztion are presented.

1.15.2 *A. aeolicus* copper ATPases:

Aquifex aeolicus is an obligate chemolithoaurotroph that has growth-temperature maxima near 95°C and is among the most thermophilic bacteria known. The complete genome of this organism has been sequenced (Deckert 1998). Three genes coding for P-type ATPases (E1-E2 family) were identified in the genome. The gene AQ724 codes for a putative P_{II}-type ATPase. AQ1125 and AQ1445 code for putative copper-transporting enzymes, CtrA3 and CtrA2 that are similar by sequence homology to CopB and CopA respectively. These two copper transporters have been characterized in the following study. Both proteins were amplified from the genomic DNA of *A. aeolicus*, cloned and over-expressed in *E. coli*. The expression, purification, functional characterization and crystallization of these proteins is presented.

CHAPTER 2

MATERIALS AND METHODS

2.1 Materials

Purest grade chemicals were used for all experiments. Ni^{2+}-NTA superflow was from Qiagen and Sigma, DDM was from Glycon and other detergents were from Anatrace (Ohio, USA). Lipids for reconstitution and crystallization were purchased from Avanti Polar Lipids Inc. (USA). Restriction enzymes for molecular biology experiments were purchased from New England Biolabs, Thermo-stable DNA polymerase and T4-DNA ligase were purchased from Invitrogen. Synthetic oligos used as primers were purchased from MWG Biotech (Germany). Recipes of media used are listed in Appendix.

Sequencing of DNA for verification of clones was done by Sequencing laboratories Göttingen GmbH (Germany). Freeze-fracture of vesicles was done in-house, kindly by Dr. Winfred Hasse.

2.2 Basic molecular biological techniques

Basic techniques for handling of DNA and cells were followed as described in the manual 'Molecular Cloning, A Laboratory Manual' by Sambrook, Fritsch and Maniatis. Agarose gels for DNA analysis and extraction were always run in TAE (40mM Tris pH 8.6+ 0.114% acetic acid+ 2mM EDTA).

2.2.1 Strains of yeast used:

P. pastoris: SMD1163

S. cerevisiae: RS72

2.2.2 Strains of bacteria used:

E. coli:

Amplification and storage of plasmid: TOP10F', DH5α

Expression: BL21 (DE3), BL21 (DE3) RP CodonPlus, C43

2.3 PCR amplification and cloning

Primers for genes were designed from the sequences as recorded in genbank, with flanking sequences for recognition by specific restriction enzymes. The PCR mixture contained 50-100ng template, 100pmol of each of the forward and reverse primers, 200μM of each of dNTPs, and 1.5 units of ThermalAce polymerase (Invitrogen). Amplification cycle involved cycling the temperature 35 times between 95°C (denaturation), 52°C (annealing), and 74°C (elongation) in a thermocycler. Amplified genes were separated on 1% agarose gel and purified. Insert and vector DNA were digested with the respective restriction enzymes, ligated together with T4-DNA ligase and transformed into TOP10F' cells (Invitrogen) for amplification.

2.4 Transformation

2.4.1 *Saccharomyces cerevisiae*:

The procedure followed for transformation, growth and down-stream processing was followed as reported in (Jahn 2001) with minor modifications. *Saccharomyces cerevisiae* RS72 cells were grown in YPAG broth at 30°C (10ml per a transformation) to an Abs_{600nm} of 0.6-1.0. Cells were washed in 0.5 volumes of Solution-I (1M Sorbitol + 0.01M Bicine-NaOH pH8.35 + 3% Ethylene Glycol + 5% DMSO) and re-suspended in 0.02 volumes of same solution. Cells could be frozen at this step in 200μl aliquots till use, though the efficiency of

transformation decreases upon storage for long periods. 2mg/ml stock of Salmon Sperm DNA (single stranded DNA) was boiled just before use. 9μl of this solution and 1μl of plasmid pMP649 (1-10μg of DNA) was added to one aliquot of cells. 700μl of Solution-II (40% PEG1000 + 0.2% Bicine-NaOH pH 8.35) was added to the mixture, vortexed for 1minute and incubated at 30°C for 1hr. The mixture was centrifuged and cell pellet was re-suspended in 600μl of Solution-III (0.15M NaCl + 0.01M Bicine-NaOH pH 8.35). 200μl of this transformation mixture was spread per SGAH plate. Colonies could be seen after 3-4 days of incubation at 30°C.

2.4.2 *Pichia pastoris*:

Protocols for *Pichia pastoris* transformation, growth and down-stream processing were followed as described in Invitrogen manuals. The plasmid for transformation was linearized with the restriction enzyme PmeI. *Pichia pastoris* strain SMD1163 was grown overnight at 30°C in YPD medium. This culture was used as a seed to inoculate into fresh 100ml YPD medium and grown to an Abs_{600nm} of 1.3-1.5. Cells were harvested at 1500Xg for 10minutes at 4°C and washed twice in cold sterile water. They were then suspended in 2ml of cold sterile sorbitol (1M) and washed once. Cells were finally suspended in 100μl of the same solution. To 80μl of this suspension, approximately 10-20μg of plasmid in about 10μl volume was added and incubated on ice for 5minutes. The mixture was transferred to an ice-cold sterile electroporation cuvette (0.2cm) and a pulse of 1.5kV, 200Ω and 25μF was applied. 1ml of ice-cold sorbitol (1M) was added to the suspension and plated on 4 RDB plates. Colonies were collected after incubation at 30°C for 3 days and spread on YPD plates with different concentrations of G418 for selection.

2.4.3 *E. coli*:

2.4.3.1 Chemical transformation:

2.4.3.1.1 Preparation of Competent Cells:

An overnight culture of the desired *E. coli* strain was sub-cultured into 100ml fresh Luria-Bertani (LB) broth and gown at 37°C till the Abs_{600nm} reached 0.6. The cells were collected by centrifugation at 2500xg for 15 minutes at 4°C. The pellet was gently tapped to loosen and re-suspended in 30ml of cold, sterile $CaCl_2$ (100mM) and left on ice for 1hr. The suspension was centrifuged again at 1500xg for 15 minutes at 4°C to pellet the cells. The pellet was re-suspended in 8ml of cold sterile $CaCl_2$ (100mM) and 2ml of cold sterile 60% glycerol. Aliquots of 200μl were stored at -80°C till use.

2.4.3.1.2 Method:

Frozen competent cells were thawed on ice. The required amount of DNA was added to the vial (typically in nanogram amounts) and incubated on ice without mixing for 5-10 minutes. Cells were heat-shocked at 42°C for 90 seconds and immediately transferred to ice. 750μl of SOC medium was added to the vial and incubated with gentle shaking for 1hr at 37°C to allow revival of cells and expression of antibiotic resistance marker gene. Approximately 100μl of this suspension was plated on LB agar plate containing the antibiotic to select transformed cells.

2.4.3.2 Electroporation:

Electrocompetent *E. coli* cells for electroporation (Top10F') were purchased from Invitrogen. 45μl was used per transformation. Frozen cells were thawed on ice. The required amount of DNA was added to electrocompetent cells

and incubated on ice for 5minutes. The mixture was transferred to a fresh sterile electroporation cuvette (GenePulser® cuvette, BioRad Inc) and electroporated at 2000V, 300Ω and 25μF. Normally, pulses of 4.9msec time-span were achieved. SOC medium was added to the cell-suspension immediately and incubated at 37°C for 1hr to allow revival of cells and expression of antibiotic resistance marker gene. This suspension was plated on LB agar plates containing antibiotic(s) to select transformed cells.

2.5 Maintenance of stocks

2.5.1 Yeast strains:

2.5.1.1 Glycerol stocks:

Freshly transformed cells of yeast were grown overnight in 5ml of YPD (*Pichia pastoris*) or YPAG (*Saccharomyces cerevisiae*) with selection marker at 30°C. Cells were diluted to a final glycerol concentration of 20% and frozen at -80°C.

2.5.1.2 Agar plates:

2.5.1.2.1 *P. pastoris* strains:

Transformed *P. pastoris* strains selected from RDB plates were spread on YPD plates with G418 (0.5mg/ml) and grown at 30°C. The plates were transferred to 4°C and could be stored for up to 2-3 weeks.

2.5.1.2.2 *Saccharomyces cerevisiae*:

Since the genetically modified RS72 strain used was not very stable for long times after transformation, cells were freshly transformed from glycerol stock for growth and expression but never maintained on agar plates.

2.5.2 Bacterial strains:

2.5.2.1 Glycerol stocks:

Freshly transformed cells of bacteria were grown overnight in 5ml of LB broth with selection marker at 37°C. Cells were diluted to a final glycerol concentration of 20% and frozen at -80°C.

2.5.2.2 Agar plates:

Cells from a fresh transformation were spread evenly on LB agar plates with selection marker and grown overnight at 37°C. The plates could be stored at 4°C for approximately 2weeks. Alternatively, cells from glycerol stocks or old plates were sub-cultured by streaking on a fresh LB agar plate with selection marker, grown overnight at 37°C and stored at 4°C for two weeks.

2.6 Growth of cells for expression of proteins

2.6.1 *P. pastoris*:

Single colonies from YPD-G418 plates were inoculated in 10ml of MGY medium and grown to an Abs_{600nm} of 2-3. Cells were pelleted and re-suspended in MM medium and grown for 48-72 hrs (methanol was added to a final concentration of 0.5% every 24hrs to maintain induction). To test expression, a

sample of cells was harvested at regular intervals (in 1ml aliquots), lysed with equal amounts of glass-beads (0.25-0.5mm) and run on SDS-PAGE.

2.6.2 *S. cerevisiae*:

Freshly transformed cells from SGAH plates were scraped into 10ml SGAH broth and grown for 2days at 30°C. This broth was added to 100ml fresh SGAH medium and grown overnight at 30°C. Each 100ml of SGAH broth was added to 1L fresh YPD (change of carbon source from galactose to dextrose, for induction of expression) and grown for 16hrs. Cells were harvested at 1000xg for 15min at 4°C, washed once in ice-cold water and either used immediately or stored at -80°C.

2.6.3 *E. coli*:

2.6.3.1 When cells were not induced:

This method was employed to routinely grow cells and produce recombinant CtrA3 and CtrA2, unless otherwise mentioned. Single colonies of cells harboring the required plasmid were inoculated in 25ml of LB broth with antibiotic and grown overnight at 37°C (seed culture). 2L of fresh LB medium (with antibiotic) was inoculated with 500μl seed culture and grown further for 14hrs at 37°C on a shaking platform. The cells were harvested, washed once with TBS (20mM Tris-HCl pH 7.5+ 150mM NaCl) and either stored at -80°C or processed immediately, with similar results.

2.6.3.2 Induction:

2L of fresh LB broth with antibiotic was inoculated with seed culture as in section 2.6.3.1 above to an Abs_{600nm} of 0.1 and grown at 37°C shaking till the absorbance reached 0.6. Cells were then induced with 1mM isopropy-β-D-

Ithiogalactopyranoside (IPTG, for pET28A plasmids)/ 200ng/ml Anhydrotetracycline (AHT, for pASK-IBA plasmids) and grown further for 2-3 hrs. Cells were harvested, washed and stored at -80°C or processed immediately.

2.7 Preparation of microsomes from yeast cells

To the cell pellet from 1l tube, 7ml of homogenization buffer (HB: 200mM Tris pH7.5+ 40mM EDTA pH 8.0+ 40% glycerol+ 0.5mM DTT+ 0.09% ATP) was added and suspended to homogeneity. Cells were lysed by adding an equal volume of glass-beads (0.25-0.5mm) and vortexing vigorously, adding 2mM PMSF every 10minutes. KCl was added to a final concentration of 250mM to lysed cells to increase the ionic strength of the buffer and centrifuged at 1000xg for 15min at 4°C. The supernatant was carefully transferred to fresh tubes, PMSF added again and centrifuged at 100,000xg for 1hr at 4°C. The pellet containing membranes was re-suspended in minimum quantity of GTED20 (20% glycerol, 100mM Tris pH 7.5+ 1mM DTT+ 1mM EDTA pH8.0 in 100ml) and stored at -80°C till use.

2.8. Separation of plasma membrane and endoplasmic reticulum from total membranes of *S. cerevisiae*

Total membrane suspension of *S. cerevisiae* was applied on the top of a discontinuous sucrose gradient made of 4ml of 25% w/w sucrose and 35%w/w sucrose. The sample was centrifuged at 110,000xg (30,000rpm in Beckman SW40Ti rotor) for 16hrs at 4°C. The ER fraction was recovered from the 25/ 35 interface, while the pellet consisted of the plasma membrane fraction (Villalba 1992).

2.9 Preparation of membranes from *E. coli*

Harvested cell pellet was suspended to homogeneity in re-suspension buffer (TBS+ 10% glycerol+ 2mM EDTA) at a ratio of approximately 5ml per 1g of cells and filtered through nylon gauze (20μm mesh size). Cells were lysed by passing through a cell disrupter (Constant Systems) or by sonication (for small volumes). Unbroken cells and debris were removed by low-speed centrifugation (4500xg for 20minutes at 4°C). The supernatant was centrifuged at 100,000xg for 1hr and membranes thus pelleted were re-suspended in a minimal volume of re-suspension buffer and stored at -80°C till use.

2.10 Solubilization and purification of recombinant protein from yeast microsomes

Micrsosome suspension was added to solubilization buffer (50mM Mes pH 6.5, 20% glycerol, and DDM) so that the final membrane protein concentration was 3mg/ml and the detergent was three times that of protein (w/w). The suspension was left at 4°C for 30minutes with gentle mixing before centrifuging at 100,000xg for 1hr at 4°C. 1ml of Ni^{2+}NTA matrix was used for every 10mg of membrane protein. The supernatant from ultra-centrifugation was added to pre-equilibrated matrix and gently mixed at 4°C overnight. The suspension was transferred to a column; un-bound material drained off at low flow rate and the matrix was washed thrice with 20 volumes of wash buffer-I (50mM MES pH 6.5+ 10mM imidazole+ 500mM KCl+ 20% glycerol+ 0.15% DDM+ 0.5mM DTT+ 0.5mM EDTA+ 1mM PMSF). The matrix was then washed twice with the same buffer but containing 250mM KCl (wash buffer-II) and twice with the same buffer containing 50mM KCl (wash buffer-III). The bound protein was eluted by adding 1 volume of elution buffer (50mM Mes pH 6.5+ 500mM imidazole+ 50mM KCl+ 20% glycerol+ 0.075% DDM+ 0.5mM DTT+ 0.5mM EDTA+ 1mM PMSF) and

concentrated approximately 10 times with vivaspin concentrators (Vivascience Ltd.) containing polyethersulfone membrane.

2.11 Solubilization of *E. coli* membranes

When screening for optimal solubilization, membranes containing the required protein were treated with different detergents (Table 2.1) at varying w/w

Table 2.1

Detergent	Ratio (w/w) to membrane protein
n-dodecyl-β-D-maltoside (DDM)	3
Cyclohexyl-n-hexyl-β-D-Maltoside (Cymal 6)	5
n-octyl-β-D-glucopyranoside (OG)	5
Lauryldimethylamineoxide (LDAO)	5
N-nonanoyl-N-methylglucamin (MEGA-9)	5
$C_{12}E_9$	5
Triton X-100	5

ratios to total membrane protein. The mixture of membranes and detergent was diluted to a final concentration of 3mg/ml membrane protein and incubated for 1hr at 4°C with gentle mixing. Un-solubilized membranes were removed by ultra-centrifugation at 100,000xg for 45 minutes at 4°C. The supernatant was immediately processed for purification.

2.12 Purification by affinity chromatography

Ni^{2+}NTA matrix was equilibrated with 10 column volumes of equilibration buffer (typically 20mM Tris pH7.5, 250mM NaCl and 0.015% DDM) and then loaded with solubilized membranes. The loaded column was washed thoroughly

(10-20 column volumes) with washing buffer (typically 20mM Tris pH7.5, 250mM NaCl, 10mM imidazole and 0.015% DDM). Bound protein was eluted with 500mM imidazole and 50mM NaCl. High salt concentration was necessary during washing to remove most non-specifically bound proteins. After elution, imidazole was removed from peak protein fraction by buffer-exchange in an ultra-filtration vial, and concentrated to approximately 10mg/ml.

2.13 Gel filtration

Analytical gel filtration was carried out with Superdex 200, Superose 6 or Superose 12 (Amersham/Pharmacia) to check homogeneity of protein sample from affinity chromatography.

2.14 Hydrophobic interaction chromatography (HIC)

3 ml of Phenyl Sepharose (Amersham) was packed in a column and equilibrated in buffer-A (50mM Mes/KOH pH 6.5, 50% saturated $(NH_4)_2SO_4$, 20% glycerol, 0.075% DDM, 1mM EDTA, 1mM DTT). The protein (AHA2 purified from Ni^{2+}-NTA) was mixed with equal volume of saturated $(NH_4)_2SO_4$ and loaded on to this column. The column was washed with 10 column volumes of buffer-A and bound protein was eluted with 5ml of different concentrations of ammonium sulfate in buffer-A (40%, 35%, 30%, 20%, 10%). The fractions containing protein were pooled and dialyzed overnight to get rid of ammonium sulfate.

2.15 Protein estimation

Protein was estimated by the Coomassie G250 dye binding method (Sedmak 1968). 500μl of sample was mixed with 500μl of Bradford Reagent (Sigma), incubated at room temperature for 5minutes and absorbance was measured at 595nm. Bovine Serum Albumin (BSA) in the range of 1-10μg was used as a standard for comparison.

2.16 Polyacrylamide gel electrophoresis

2.16.1 SDS-PAGE:

Stock Solutions:

40% Acrylamide: (Bio-rad)
1.5M Tris HCl pH 8.8
Stacking Buffer 2X: 180mM Tris HCl pH 6.8, 0.2% SDS
10% SDS
10% APS (prepared fresh)
Running Buffer: 25mM Tris, 192mM Glycine, 0.1% SDS

Components	Resolving Gel (for 12gels)	Stacking Gel (1gel)
40% Acrylamide	25ml	0.187ml
1.5M Tris HCl pH 8.8	25ml	-
10% SDS	1ml	-
10% APS	200μl	25μl
Stacking gel (2X)	-	1.25ml
TEMED	150μl	5μl
Water to a final volume of	100ml	2.5ml

10% resolving gels were prepared using a multiple gel-casting unit from Hoefer and stored at 4°C. Just before use, 4% stacking gel was prepared and overlaid on the resolving gel. For sample preparation, the protein sample at desired concentration was mixed with equal volume of sample buffer (60mM Tris pH6.8, 1.5% SDS, 10% glycerol, 0.005% BPB). Samples were not boiled before loading on the gel. The gel was run at a constant voltage of 300V under a water jacket to prevent heating.

2.16.2 Staining of gels:

2.16.2.1 Coomassie staining:

Coomassie Brilliant blue R250 was dissolved in 45% methanol and 10% acetic acid. Gels were stained for 30 minutes and then de-stained with 40% methanol and 7.5% acetic acid.

2.16.2.2 Silver staining:

Gels were incubated in fixative solution (50% Methanol+ 12% Acetic acid) for about 1hr (or overnight) and washed thrice for 10minutes in 50% ethanol. They were then put in pre-treat solution (10mg $Na_2S_2O_3.5H_2O$ in 50ml water) for 1 minute, washed with water and incubated in 0.2% silver nitrate for 15 minutes. Gels were then washed in water again and developer solution (3g Na_2CO_3 in 50ml of water and 100µl formaldehyde) was added. As soon as the bands developed to required intensity, the gels were washed thoroughly in water and transferred to fixative.

2.16.3 Western blot analysis of proteins:

Proteins on the gels were transferred (transfer buffer: 25mM Tris, 192mM glycine) on to PVDF membrane using a semi-dry transfer apparatus (Bio-Rad). Transfer was confirmed by staining in Ponceau solution (Sigma). Membranes were then washed in TBS and blocked with 5% milk in TBS for 30min-overnight to avoid non-specific binding of other proteins. Primary antibody (typically anti-His, raised in mouse, Sigma, unless otherwise mentioned) solution (antibody in TBS+ 1% BSA+ 0.05% NaN_3) at a dilution of 1:500 or 1:1000 was added to membranes and incubated for 1hr at room temperature or overnight at 4°C. The membranes were then washed in TBS with 0.05% Tween20 (TBS-T) and incubated in alkaline phosphatase tagged secondary antibody solution (typically

anti-mouse AP conjugate, Sigma) at a dilution of 1:2000 for 1hr at room temperature. After washing in TBS-T again, each membrane was incubated in 10ml of developer solution (100mM Tris pH9.5+ 100mM NaCl+ 5mM $MgCl_2$+ 0.32mg/ml Nitro Blue Tetrazolium+ 0.16mg/ml 5-Brom-4-Chlor-3-indolyl phosphate-p-toluidin) till bands showed up.

2.17 Preparation of total lipids of *Aquifex aeolicus*

Cells of *Aquifex aeolicus* were purchased from Lehrstuhl für Mikrobiologie, University of Regensburg, Germany. 20g of cells were suspended in 100ml of re-suspension buffer (TBS+10% glycerol+2mM EDTA) and filtered through nylon gauze (20μm mesh size). Cells were lysed by passing through a cell disrupter (Constant Systems). Unbroken cells and debris were removed by low-speed centrifugation (4000xg, 20 minutes, 4°C). The supernatant was centrifuged at 100,000xg for 1hr and membranes thus pelleted were re-suspended in a minimal volume of re-suspension buffer. The membranes were then suspended in a chloroform methanol mixture (3:1) and kept at –20 °C overnight to allow denaturing and precipitation of proteins. The lower organic phase was evaporated in a rotation film evaporator and the lipid film was re-suspended and washed twice in chloroform. Water was removed by adding Sephadex powder (Pharmacia) and by filtering. Solvent was evaporated and dry lipids were solubilized in chloroform and stored at -20°C in aliquots of 1ml.

2.18 Preparation of lipid vesicles for activity assays and TLC

Lipids in Chloroform were dried under nitrogen and resuspended in water at a concentration of approximately 25 mg/ml. The suspension was sonicated for approximately 30 minutes (with intermittent breaks) on ice, under nitrogen for the formation of multilamellar vesicles. Then, the suspension was aliquoted and stored at -20°C.

2.19 Solubilization of lipids

Lipids were obtained from Avanti Lipids as stocks in chloroform, dried under nitrogen or argon and re-suspended in 5% OG solution to a final concentration of 10mg/ml. The stocks of solubilized lipids were stored at –20°C under nitrogen.

2.20 Thin layer chromatography

Chloroform: Methanol: Water (65:25:4) was added to a TLC chamber and equilibrated for 10minutes. Samples were loaded near the bottom of a TLC plate coated with SilicaG25 and placed in the chamber so that the loaded samples were above the solvent mixture. When the solvent front reached the top of the plate, it was removed from chamber, allowed to dry for a couple of minutes and sprayed with staining solution (Sulfuric Acid: Ethanol: Water 1:1:1). It was then shifted to 150°C to develop the spots (approximately 1minute).

2.21 Reconstitution of proteins in lipid vesicles

Proteins were incubated at a lipid to protein ratio (LPR) of 10 in different detergent solubilized lipids for 2hrs (100μl). The mixtures were dialyzed at 30°C for 1 week against a buffer without detergent. A step-gradient of sucrose was prepared in 11 X 34 mm polycarbonate ultra-centrifuge tubes (Beckman) by carefully dispensing 500μl each of 40%, 30%, 20% and 10% sucrose from bottom to top. Each sample of dialyzed mixture was then layered on this gradient and centrifuged at 125,000xg (44,000 rpm in Beckman TLS55 rotor) for 150minutes at 4°C. 500μl aliquots of centrifuged suspension from each tube were collected carefully in microfuge tubes, and protein precipitated by adding Tri-Chloro Acetic Acid (TCA) to a final concentration of 10%. Samples were let to stand on ice for 30 minutes and washed once with acetone. The pellets were

suspended in SDS sample buffer and run on SDS-PAGE and transferred on to a PVDF membrane for Western analysis.

2.22 2D Crystallization

2.22.1 Dialysis:

Protein was mixed at the desired LPR with detergent-solubilized lipid, incubated at room temperature or on ice for 2hrs before being transferred to dialysis bags for crystallization. Temperature, buffer composition and time period for dialysis were varied, depending on the protein, lipids and detergents. As an alternative to dialysis bags, dialysis buttons, purchased from Cambridge Repetition Engineers Ltd., were used.

2.22.2 Biobeads:

Biobeads were purchased from Bio-Rad. They were washed once in methanol and then in water. Protein and lipid in detergent were mixed as for dialysis. Known amount (in numbers, generally 10-12) of washed biobeads was added with tweezers to the microfuge tube containing protein-lipid mixture to remove detergent. The mixture was stirred throughout the procedure to maintain homogeneity. Temperature and amount of biobeads were varied in different experiments.

2.22.3 Electron microscopy:

2.22.3.1 Negative staining:

1μl of dialyzed sample was placed on a glow-discharged carbon coated copper grid (400 mesh size). The sample was allowed to adsorb for a minute. The grid was stained with 1% uranyl acetate and screened in a FEI Technai G^2

Spirit microscope equipped with a LaB6 filament and operating at 120KV. Images were recorded in low dose mode typically at a magnification of 42,000 either on film or a CCD camera.

2.22.3.2 Cryo-electron microscopy:

Specimens for cryoEM were prepared by back injection method (Kühlbrandt and Wang 1991). A fresh piece of carbon was floated on embedding medium of choice and the grid was coated with carbon from one side. Sample was applied to the side of the grid that carried the embedding medium and was gently mixed several times to ensure the adherence of the membranes onto the carbon. The grid was blotted on a filter paper for 10 seconds and air dried for 5 seconds before plunging into liquid nitrogen. Alternatively, it was directly plunged in liquid ethane without any embedding medium. Grids were observed in FEI Technai G^2 Spirit microscope operating at 120kV with a cryo-holder, or in the JEOL 3000 SFF electron microscope with an accelerating voltage of 300kV and specimen temperature of 4K.

2.22.3.3 Image collection:

Images recorded on Kodak SO-163 electron emulsion film were developed for 12 min in full strength Kodak D19 developer. The quality of negatives was evaluated by optical diffraction and those exhibiting strong reflections were selected for further processing.

2.22.3.4 Image processing:

Selected image areas of 4000x4000 pixels were digitized with a pixel size of 7 mm on a Zeiss SCAI scanner. Images were processed using the MRC image processing programs to correct lattice distortions and contrast transfer function (Crowther et al. 1996). Typically 3-4 cycles of unbending were carried

out for each lattice. The program ALLSPACE was used to determine the phase residuals (Valpuesta et al. 1994).

2.23 3D Crystallization

2.23.1 Robotic (sitting drop method):

100μl of commercial protein crystallization screens (Hampton Research, Jena Bioscience or Nextal Biotechnologies) were pipetted into 96 well crystallization plates. The plates were transferred to a pipetting robot (Cartesian Technologies) for dispensing protein and crystallization buffer (100nl+100nl, 200+200nl, 300nl+300nl or 400nl+400nl) into crystallization wells. Plates were sealed and incubated at 19°C and observed periodically.

2.23.2 Manual (hanging drop method):

1ml of crystallization buffer was either pipetted into or prepared directly in each of the 24 wells of crystallization trays (Hampton Research). 1μl of purified protein was mixed with 1μl of crystallization buffer on siliconized cover slip and placed inverted on the wells and sealed with vacuum grease (the trays purchased were with the sealant applied). The trays were incubated at 19°C and observed periodically.

2.24 ATP hydrolysis assay

Enzyme activity assay was performed as per (Hennessey and Scarborough 1988) with modification of ingredients required for copper ATPase activity (Mana Capelli 2003). Released inorganic phosphate (Pi) was determined as described by (Stanton 1968). The assay method was as follows.

In 100μl of reaction mixture, 10μg of protein was mixed with 40mM Tris-HCl pH7.5, 20mM cysteine, 400mM NaCl, 20mM ammonium sulfate, 50μg soya PC and 100μM $AgNO_3$/ $CuSO_4$ (depending on the protein tested: $AgNO_3$ for CtrA2 and $CuSO_4$. 5mM ATP-$MgSO_4$ was added to this mixture to start the reaction and incubated at 75°C for 10min. The reaction was stopped by addition of 100μl 10% SDS. The volume was made up to 860μl with water. 100μl of acid-molybdate reagent (2.5% ammonium molybdate in 5N $H2SO_4$) and 40μl of aminonaphtholsulfonic acid reagent (0.25% 1,2,4-aminonaphtholsulfonic acid in sulfite-bisulfite buffer) were added to the reaction mixture, let to stand at room temperature for 20 min and absorbance was measured at 815nm in a spectrophotometer. As a standard, 0.5-5μl of 4.39% potassium dihydrogen phosphate (1μl=10μg Pi) in 860μl of water was used. The salt, metal ion, protein concentration, lipids, temperature and pH were independently varied in different experiments as indicated in results.

The maximum activity of the enzymes was determined as μM of Pi released on ATP hydrolysis by an mg of protein in one minute. To calculate the amount of Pi released, the Abs_{815}nm of the enzymatic reaction was compared to a standard curve of potassium dihydrogen phosphate (1-20μg Pi) assuming that 1μg Pi=32.2nM.

CHAPTER 3

RESULTS

3.1 *Pichia pastoris* as an expression system for production of AHA2:

3.1.1 Cloning of AHA2 plasmid in *P. pastoris*:

The AHA2 gene with a C-terminus $MRGSH_6$ tag was amplified using plasmid pMP1296 as a template. Primers were designed by adding restriction sites for enzymes SnaB I and Not I, for cloning into an expression vector. After amplification by PCR, the DNA was purified and digested with these restriction enzymes. Typically 10μg of amplified DNA was recovered from each PCR reaction. 1 μg of the 2.8kbp fragment was then ligated with pPIC3.5K or pPIC9K (digested with the same enzymes) and transformed into *E. coli* TOP10F' for amplification of plasmid. The sequence of plasmid was verified and found to match the sequence of AHA2- $MRGSH_6$. Approximately 15μg of plasmid was digested with restriction enzyme PmeI to linearize. The liniarized plasmid was transformed into *P. pastoris* strain SMD1163 by electroporation for integration into genomic DNA. The clone hereafter will be called 9K-AHA2 or 35K-AHA2 depending upon whether the carrier vector is pPIC9K or pPIC3.5K and to differentiate between this expression product and AHA2 expressed in *S. cerevisiae*.

3.1.2 Expression analysis of 9K-AHA2 and 35K-AHA2:

From each transformation, 20 colonies were selected for expression analysis. 1ml aliquots of induced *P. pastoris* cells were harvested at 12, 24, 48, 72 hrs to check expression. Cells were either directly lysed with equal volume of glass beads and lysate mixed with SDS-PAGE sample buffer; or non-lysed cell debris removed by low-speed centrifugation, membranes prepared by centrifugation at 100,000xg and pellet suspended in SDS-PAGE sample buffer, for analysis. In all cases, care was taken that (approximately) equal amount of protein was loaded on the gel. Protein was transferred on PVDF membrane and probed with different kinds of antibodies (Table 3.1). Only monoclonal antibodies

against H^+-ATPase could recognize the expression product and standard AHA2 (Figure 3.1), while Anti-RGS antibodies could recognize the standard AHA2 (over-expressed in *S. cerevisiae*) only.

Table 3.1:

Primary Antibody	Company from where purchased/procured	Signal with 9K-AHA2/35K-AHA2	Signal with AHA2
Anti-His	Novagen	No	No
Anti-Penta His	Qiagen	No	No
Anti-RGS	Qiagen	No	Yes
Monoclonal anti-H^+-ATPase (46E5B11 hybridoma clone)	Dr. Michalke Wolfgang's laboratory, University Freiburg	Yes	Yes

All primary antibodies were used at a concentration of 1:500.

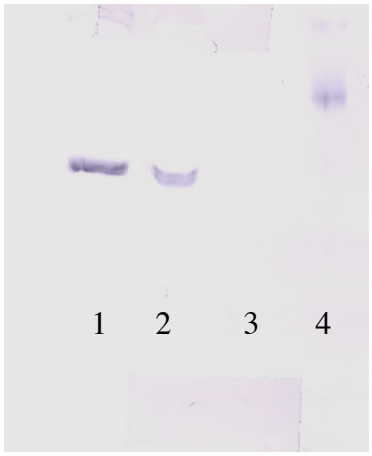

Figure 3.1: Expression Analysis: Western blot of 9K-AHA2, 35K-AHA2 and AHA2. Lane-1: TCA precipitated membranes of 35K-AHA2; lane-2: membranes of 35K-AHA2; lane-3: membranes of 9K-AHA2; lane-4: purified AHA2 over-expressed in *S. cerevisiae* (produced in this laboratory). 300μg of total membrane protein was loaded in lane-1, 100μg in lanes 2 and 3, and 200ng in lane-4.

As shown in Figure-3.1, no protein expression was observed when pPIC9K vector was used. Recombinant protein expression could be seen when pPIC3.5K was used, as visualized by western blot. However, this protein was not of the correct size. The possibility of fully expressed protein getting truncated by proteolytic action was ruled out because:

a. double protease deficient strain SMD 1163 was used.

b. addition of a wide variety of protease inhibitors- PMSF, AEBSF, benzamidine, trypsin inhibitor, pepstatin, EDTA at all stages of purification did not have any effect.

It is possible that the truncation of the protein was occurring at the transcriptional or translational level.

3.2 Over-expression of AHA2 in *S. cerevisiae*:

3.2.1 Expression and purification:

Expression of AHA2 in *S. cerevisiae* yielded approximately 0.15-0.2mg (as measured by Bradford's protein estimation method) of purified AHA2 (by Ni^{2+}-NTA) per liter of culture. The expressed protein was solubilized in DDM and purified on a Ni^{2+}NTA column as described in Materials and Methods. Amount of washing had an affect on purity of AHA2. When the column was washed with a total of 40 column volumes before elution, the protein was more pure, getting rid of more contaminants (lane 5 of Figure 3.2). Washing with 10 column volumes resulted in a less pure protein (lane 10 of Figure 3.2).

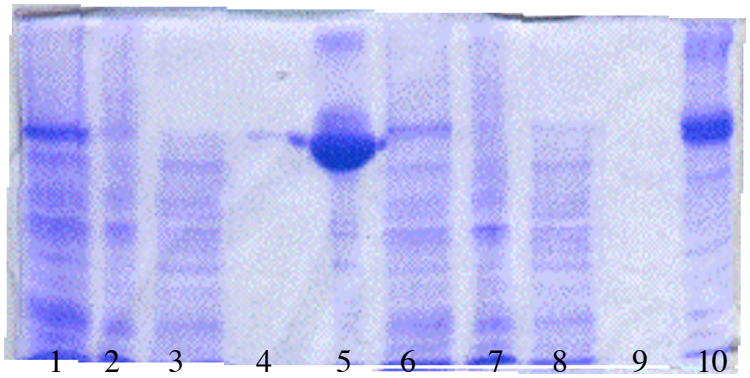

Figure 3.2: AHA2 Purification: Ni^{2+}-NTA purification of AHA2 with 40 column volumes wash (lane 1-5), compared to 10 column volumes of washing (lane-6-10). Lane 1,6: Solubilized membranes; 2,7: flow through from the column after binding; 3,4: washing of the matrix amounting to a total of 40 column volumes; 8, 9: washing of the matrix amounting to a total of 10 column volumes; 5, 10: purified AHA2. The gel was stained with comassie brilliant blue R250.

3.2.2 Hydrophobic interaction chromatography:

Hydrophobic interaction chromatography (HIC) was part of the purification process that led to 2D crystals of AHA2 (Jahn 2001) and is likely an important step for crystallization of AHA2. The authors used PorosPE20 matrix for this step. This matrix is no longer available, so, attempts were made to purify the protein by using phenyl sepharose matrix. PE20 has phenyl ether ligand substrate and phenyl sepharose matrix has phenyl group.

AHA2 purified from Ni^{2+}-NTA was mixed with saturated ammonium sulfate solution and loaded on the phenyl sepharose column. The column was then washed with a step-gradient of ammonium sulfate (40%-0%). AHA2 was eluted with 20% ammonium sulfate. However, the yield was very low (~25μg per 500μg loaded).

3.2.3 Separation of plasma membrane and endoplasmic reticulum fractions of *S. cerevisiae* membranes:

Total membranes from *S. cerevisiae* expressing AHA2 were layered on a sucrose gradient made up of 25% (w/w) and 35% (w/w) sucrose. The interface between 25% and 35% sucrose is expected to be rich in endoplasmic reticulum fraction and the pellet, rich in plasma membrane (Villalba 1992).

AHA2 was purified from these three fractions (total membranes, ER and plasma membranes) by Ni^{2+}-NTA and run on superose-6 gel filtration column. As evident from the Figure 3.3, the elution fraction from total membranes (in black) does not look monodispersed. This represents different populations of AHA2 present in this fraction. However, much of the AHA2 was found in the ER fraction (shown in blue) and as a homogenous population.

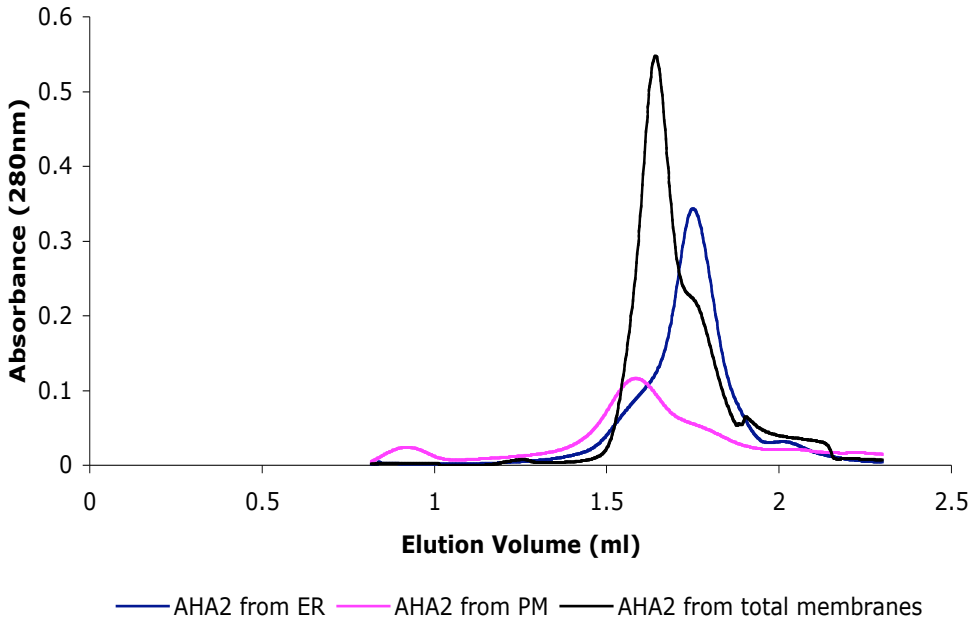

Figure 3.3: Gel filtration of AHA2 purified from ER, PM and total membranes, by superose-6 (Amersham Biosciences).

3.2.4 Electron Microscopy:

Protein was mixed with egg PC at different LPRs, from 3.0 to 0.1. The samples were incubated at room temperature for 2hrs before adding biobeads or starting dialysis. Dialysis period was varied from 7-14 days. Biobeads were added one at a time every 1hr (a total of 10-15 beads per 50μl protein-lipid-detergent mixture). 1μl of the sample was placed on a carbon-coated, glow-discharged grid, stained with 1% uranyl acetate and observed in Philips CM12 microscope at 120kV. The crystallization by biobeads was very irreproducible, with vesicles of different sizes. Dialysis did not result in any crystalline order.

Most of the time, when biobeads were used for removing detergent, vesicles of different sizes were observed (Figure 3.4 A), where a small fraction of protein showed signs of close packing (Figure 3.4 B); the rest of the protein was aggregated. Changing the time of detergent removal by adding more or less biobeads per hour did not improve the reconstitution or packing.

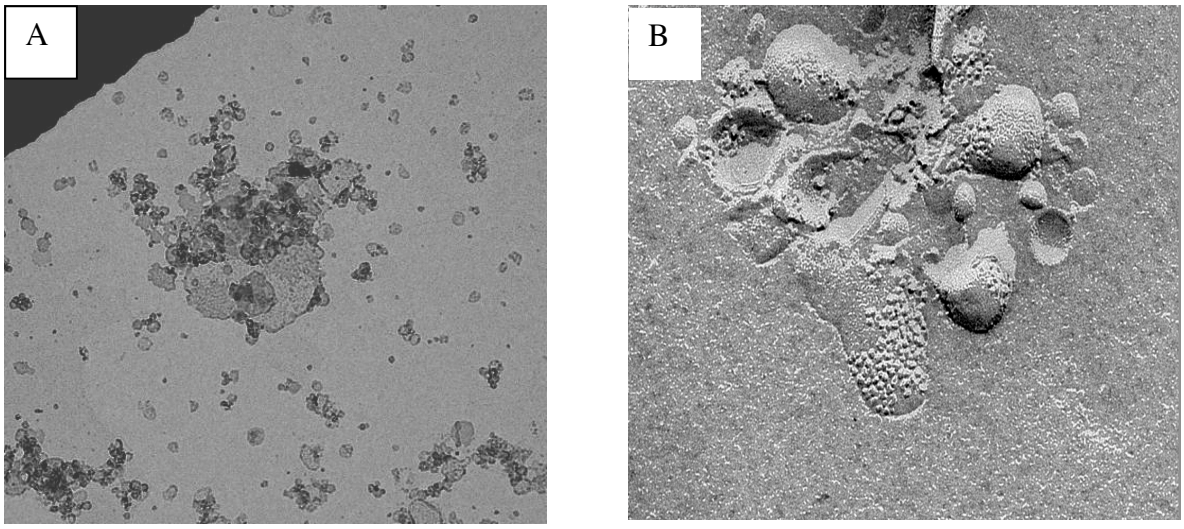

Figure 3.4: Morphology of vesicles seen when AHA2 was reconstituted in egg PC at an LPR of 0.4 and detergent removed by adding biobeads. (A) The vesicles observed after staining in 1% uranyl acetate, in Philips CM12 EM at a magnification of 1100X. (B) Freeze fracture analysis of the same sample.

When dialysis was employed for removal of the detergent, only small vesicles were observed in the microscope (Figure 3.5 A). On freeze fracture analysis of this preparation, no incorporation of protein was seen (Figure 3.5 B).

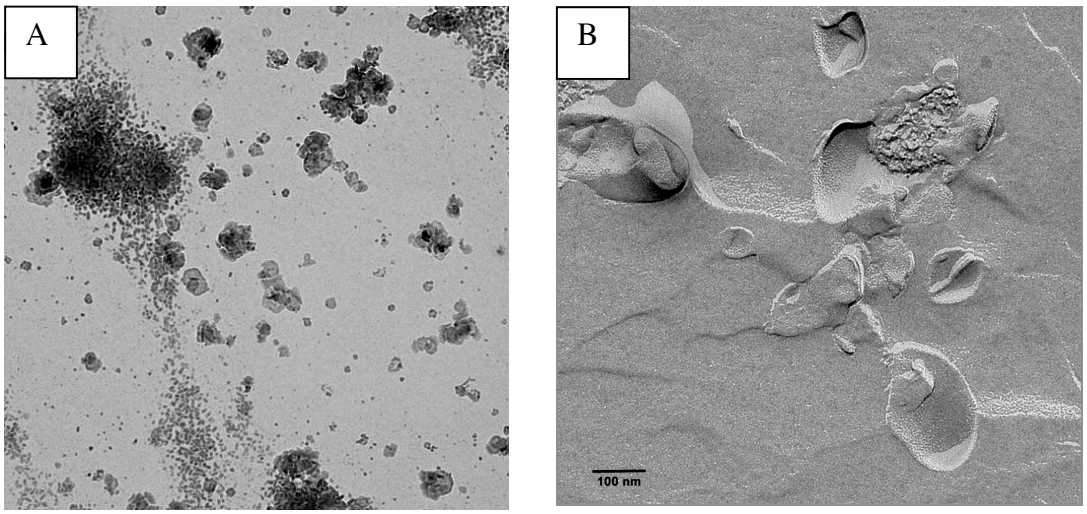

Figure 3.5: Morphology of vesicles seen when AHA2 was reconstituted with egg PC at an LPR of 0.4 and the detergent removed by dialysis. (A) The vesicles observed after staining in 1% uranyl acetate, in Philips CM12 EM at a magnification of 1100X. (B) Freeze fracture analysis of the same sample

3.3 Cloning of copper ATPases from *A. aeolicus* in *E. coli*:

The genes coding for the two P-type copper ATPases, ctrA3 (AQ1125) and ctrA2 (AQ1445) were amplified from *A. aeolicus* genomic DNA by PCR. The 5' and 3' end of the genes were used to design the primers, and restriction sites for enzymes BamHI/ NdeI/ NceI at 5' end of ORF and XhoI at 3' end (with or without termination codon), were added, for incorporation into commercially available pET28A or pASK-IBA plasmids. The different restriction enzyme sites were designed to add specific tags at N-terminus of the protein and C-terminus (Figure 3.6). The end products (clones and proteins) were named hereafter as in the figure for clarity in discussion. For example, 'ctrA3' has a His and T7 tag at N-terminus and His tag at C-termiuns, 'ctrA3-NcX' has no tag at N-terminus and a His tag at C-terminus.

The amplified DNA was purified after running on a 1% agarose gel and digested with respective restriction enzymes. The DNA was then ligated with pre-digested vectors. A ligation method with temperature cycle as illustrated below was used, for improving efficiency.

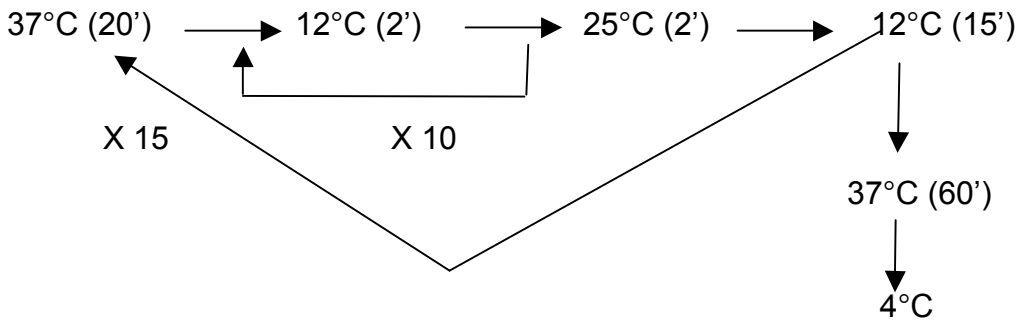

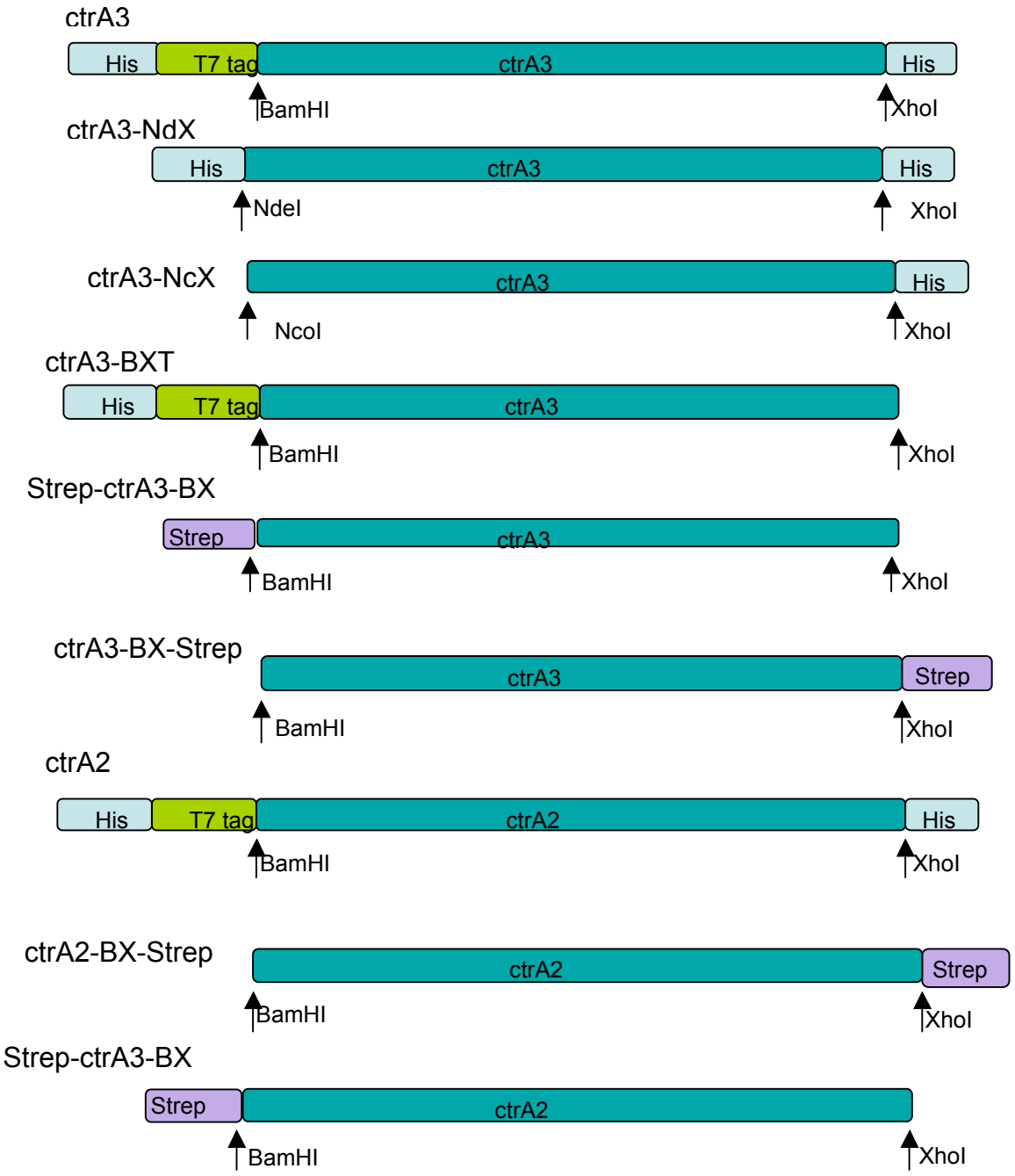

Figure 3.6: Clones of ctrA3 and ctrA2 with respective tags. All clones made with His and/ or T7 tags were in pET28A; those with 5' end strep tag in pASK-IBA7, and those with 3' end strep tag were in pASK-IBA3 (see Appendix for vector maps).

3.4 CtrA3

3.4.1 Expression of CtrA3:

Expression of CtrA3 was attempted with different clones (Figure 3.6) in various *E. coli* hosts. Expression was not observed at all in those clones where no tag was present at the 5' end of the gene (ctrA3-NcX and ctrA3-BX-Strep), without or with induction.

Expression of Strep-CtrA3-BX was very low, even after induction with AHT. Induction of the cells at different growth phases as monitored by Abs_{600}nm did not result in improvement of expression. Some expression was seen with ctrA3-NdX, with an N-terminal His tag (and a C-terminal His tag), but the best expression was observed with ctrA3 (N-terminal His and T7 tags, C-terminal His tag). Good, but not best expression levels were also obtained when C-terminal His tag was removed from this clone (ctrA3-BXT). For all further experiments, ctrA3 was used, unless mentioned otherwise.

Among different hosts tried for expression, *E. coli* strain RP CodonPlus (Stratagene) gave the best possible expression levels, even without any induction of cells. Expression in *E. coli* strains BL21 (DE3) and C43 resulted in very low expression. However, the expression improved after induction with IPTG in these cases, even though this expression was still less than that observed in RP CodonPlus strain. Expression analysis in different strains and plasmids tested is summarized in Table 3.2.

CtrA3 was routinely expressed in RP CodonPlus strain by growing the cells over-night at 37°C, without any induction by IPTG.

Table 3.2

Vector	Tag	Strain	Expression	
			CtrA2 (Aq1445)	CtrA3 (Aq1125)
PASK-IBA3	C-term Strep tag	BL21 (DE3)	-- (UI/I)	-- (UI/I)
		C43	-- (UI/I)	-- (UI/I)
		RP CodonPlus	-- (UI/I)	-- (UI/I)
PASK-IBA7	N-term Strep tag	RP CodonPlus	+ (I)	+ (I)
PET28A	N-term His tag, T7 tag, C-term His tag	RP CodonPlus	++ (UI/I)	+++ (UI/I)
		C43	++ (UI/I)	++ (UI/I)

3.4.2 Solubilization and purification:

Several detergents were tested for solubilization of CtrA3 from membranes (Table 2.1). Different detergent-protein ratios were chosen depending on the CMC of the detergent. DDM, Cymal 6 and OG could solubilize CtrA3 from *E. coli* membranes. LDAO, Mega-9 and $C_{12}E_9$ could partially solubilize, while Triton X-100 could not solubilize CtrA3 at all. Solubilized membranes were loaded on Ni^{2+}NTA column and bound protein was eluted with 500mM imidazole. CtrA3 thus purified showed a single band on SDS-PAGE and is more than 95% pure (Figure 3.7). Routinely, 1.2-1.5mg pure protein could be recovered after Ni^{2+}NTA per liter of overnight grown culture.

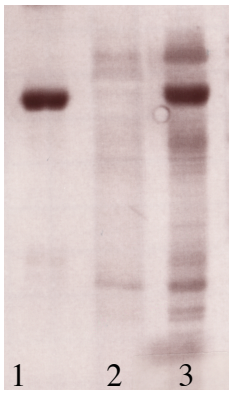

Figure 3.7: Purification profile of CtrA3. 10% SDS-PAGE profile of CtrA3 purification shows that the protein is more than 95% pure after Ni^{2+}NTA (lane-1). Lane-2 is the wash and lane-3 shows the solubilized membranes loaded on the column.

3.4.3 Gel filtration:

The homogeneity of purified protein was analyzed by gel filtration. CtrA3 purified from DDM was very homogenous (Figure 3.8 A), as judged from a sharp single peak elution from Superose-6 gel filtration column. The protein solubilized in and purified from Cymal-6 was not very homogenous (Figure 3.8 B) and elutes as at least two different populations.

CtrA3 purified from OG was very heterogenous (Figure 3.8 C). It is possible that in OG, the protein occurs in different oligomeric states. Also, the protein was less stable at room temperature, 4°C or -20°C when purified from OG and precipitates within 24hrs after purification.

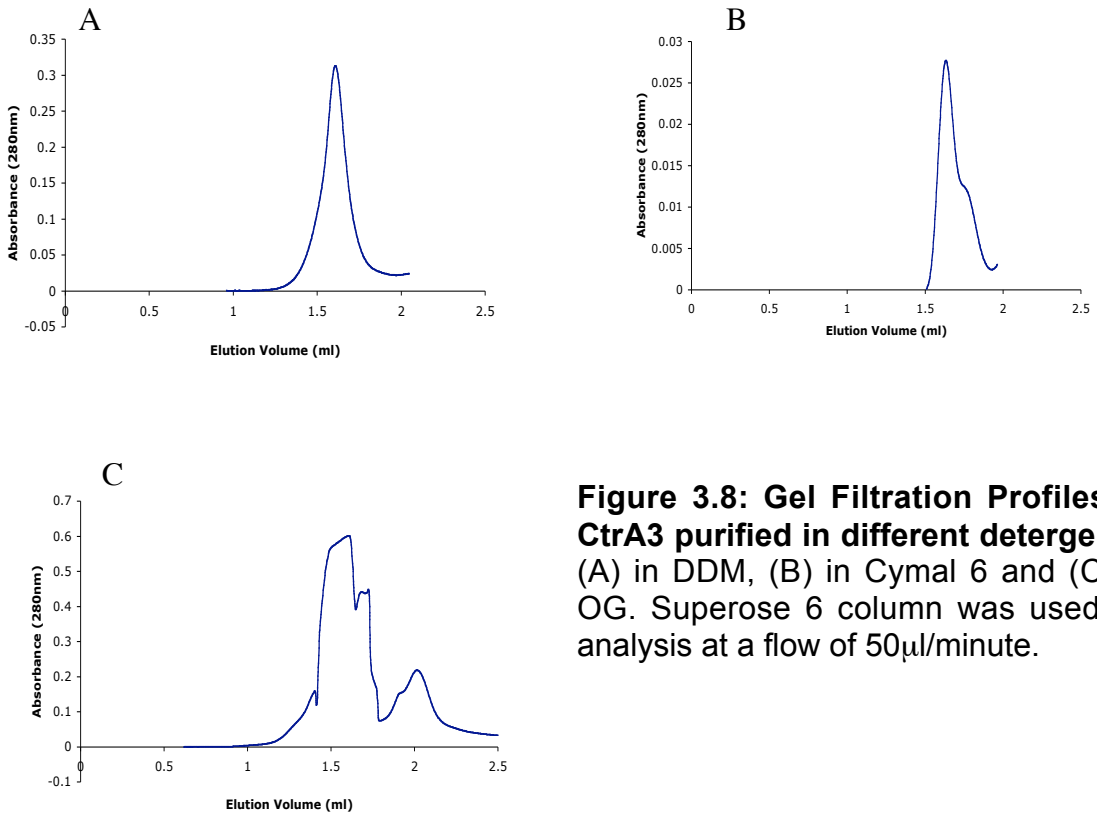

Figure 3.8: Gel Filtration Profiles of CtrA3 purified in different detergents: (A) in DDM, (B) in Cymal 6 and (C) in OG. Superose 6 column was used for analysis at a flow of 50μl/minute.

3.4.4 Activity assays:

3.4.4.1 Activity in presence of different metal ions:

As expected from their homology to other members of IB-3 subgroup of P-type ATPases (Mana Capelli 2003), the ATPase activity of CtrA3 could be stimulated by the Cu^{2+} ions. Ag^{+} also activated the protein, though only to about 40% of maximal activity. Addition of any other ion did not activate the enzyme (Figure-3.9) and the activity of this protein in the presence of Ni^{2+}, Zn^{2+}, Mg^{2+}, and Co^{2+} was only slightly above background. However, when DTT was added to reaction mixture along with $CuSO_4$ to reduce the copper ion and mimic the presence of Cu^{+}, the activity of CtrA3 decreased to 50% of the maximum value. Only minimum hydrolysis of ATP was observed when there was no ion present in the reaction mixture.

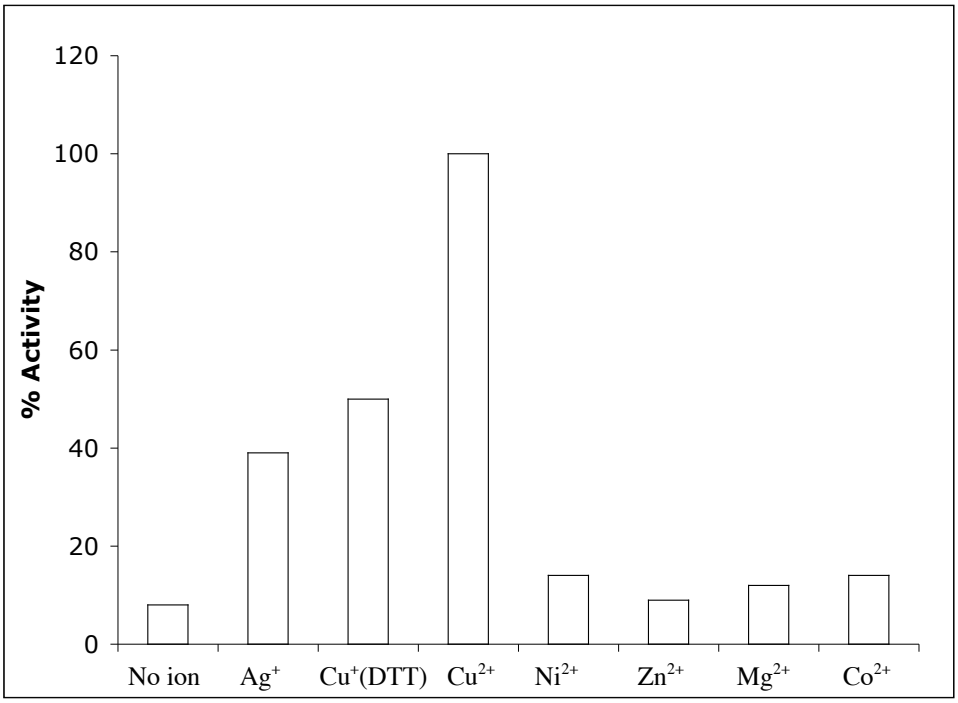

Figure 3.9: Activity of CtrA3 in the presence of different metal ions. Ag^{+} ($AgNO_3$), Cu^{2+} ($CuSO_4$), Ni^{2+} ($NiCl_2$), Zn^{2+} ($ZnCl_2$), Mg^{2+} ($MgSO_4$), and Co^{2+} ($CoCl_2$) were used at 100μM concentration. For Cu^{+}, 2mM DTT was added to $CuSO_4$ solution All other ingredients were as mentioned in Materials and Methods.

3.4.4.2 Activity at different temperatures:

Considering the fact that *A. aeolicus* is a hyperthermophilic bacterium that grows at 70°C to 90°C, ATP hydrolysis activity of CtrA3 was investigated at different temperatures in the range of 4°C to 90°C. Samples with all ingredients except ATP were incubated at respective temperatures for 15 minutes before starting the reaction by adding 5mM ATP. $CuSO_4$ at 100μM was used to activate the enzyme. CtrA3 starts to hydrolyze ATP at around 50°C. The protein was almost inactive at temperatures below 50°C. The activity of CtrA3 reached a maximum at 75°C and the protein retained 50% of this activity at 90°C (Figure 3.10).

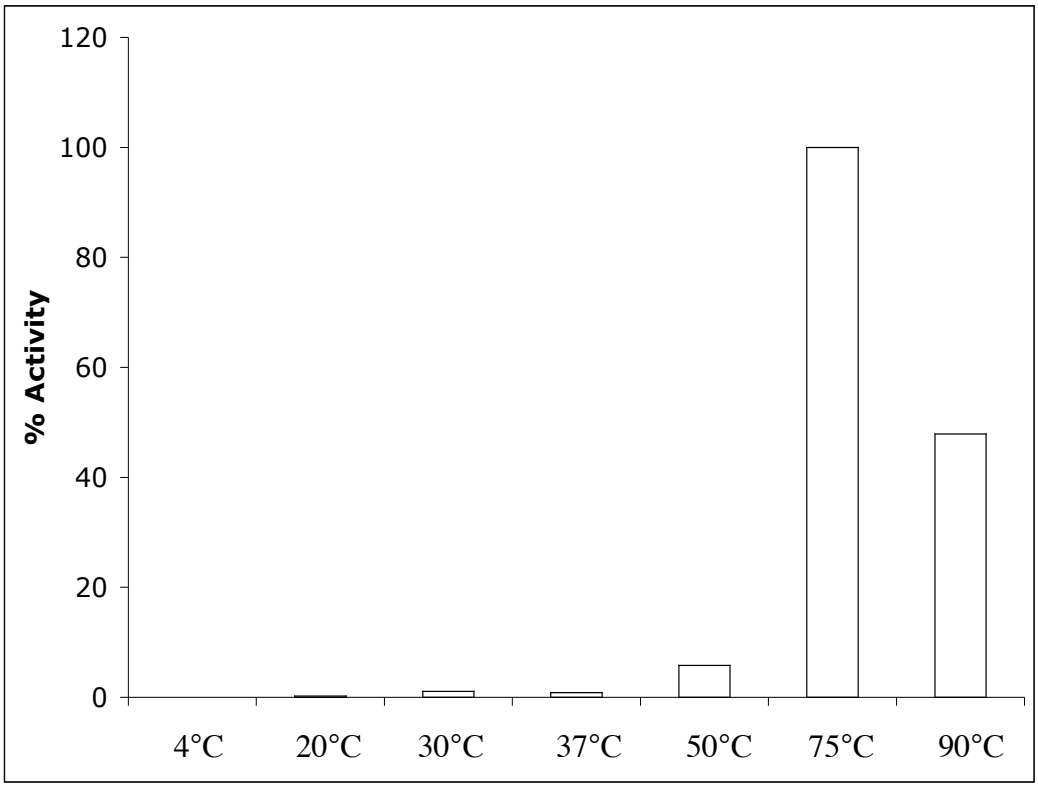

Figure 3.10: ATP hydrolysis activity of CtrA3 at different temperatures. All ingredients were as mentioned in Materials and Methods; the reaction vials were incubated at 4°C, 20°C, 30°C, 37°C, 50°C, 75°C and 90°C for 15 minutes for equilibration at that temperature and the reaction was started by adding 5mM ATP. 100μM of $CuSO_4$ was used to activate the enzyme.

3.4.4.3 Activity at different pH:

CtrA3 showed a typical bell shaped curve when tested for activity at different pH. The protein and other ingredients of the reaction as mentioned in Materials and Methods were incubated in buffers of different pH at 75°C before the starting the reaction with 5mM ATP. The protein is maximally activated at pH 7.0. The protein was completely inactive at pH 4.0 and below, but could retain 70% of its activity at pH 9.0 (Figure 3.11).

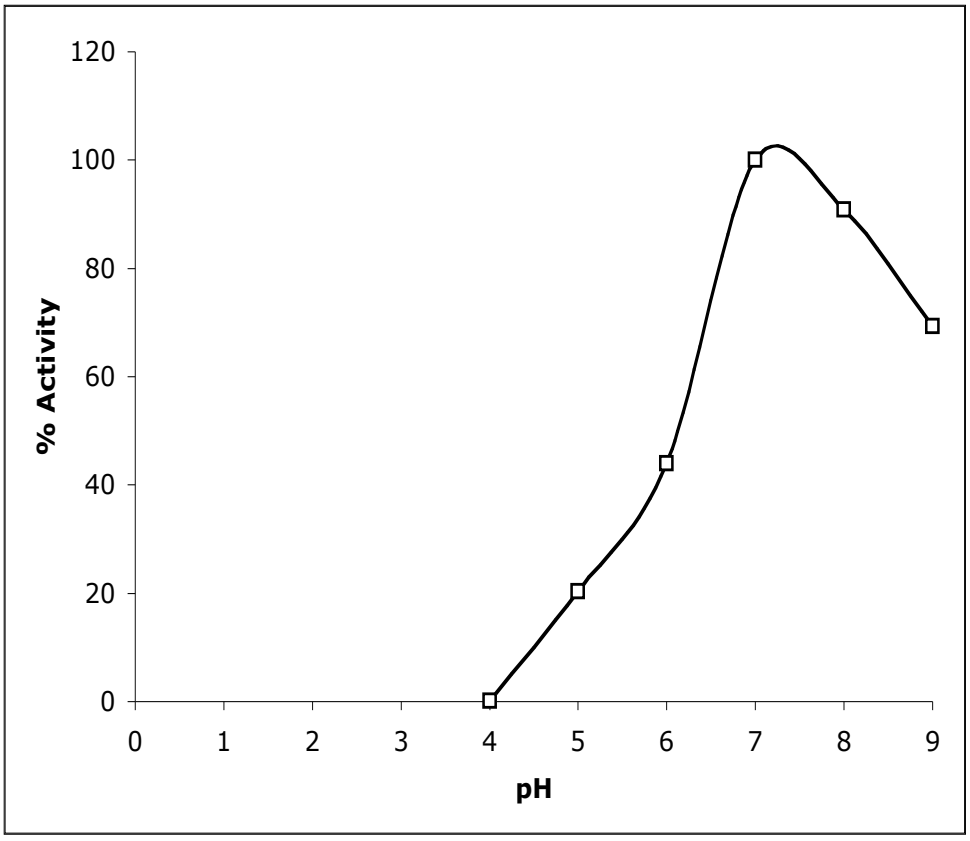

Figure 3.11: ATP hydrolysis activity of CtrA3 at different pH. The reaction mixture contained 100μM $CuSO_4$. All other ingredients were as mentioned in Materials and Methods. For different pH, the following buffers were used at 100mM: Na-Acetate (pH 4.0), K-Acetate (pH 5.0), MES (pH 6.0), MOPS (pH 7.0), Tris-HCl (pH 8.0) and Tris-HCl (pH 9.0).

3.4.4.4 Activity in the presence and absence of lipids:

To test the lipid dependence of CtrA3, different lipids suspended in water were added to the reaction mixture containing protein at an LPR of 5:1 (w/w) and let to stand for 15 minutes at 75°C before starting the reaction with 5mM ATP as described in Materials and Methods. Lipids were necessary for the activity of CtrA3 (Figure 3.12). The enzymatic activity of CtrA3 decreased to 20% when lipids were absent in the reaction mixture. However, different lipids tested did not have any effect on the activity of the enzyme. CtrA3 was active in the presence of *A. aeolicus* total lipid extract, even though the activity was not 100%. The protein was also found to be active in the presence of DPPC, where 2D crystals were obtained (see later, Section 3.4.6).

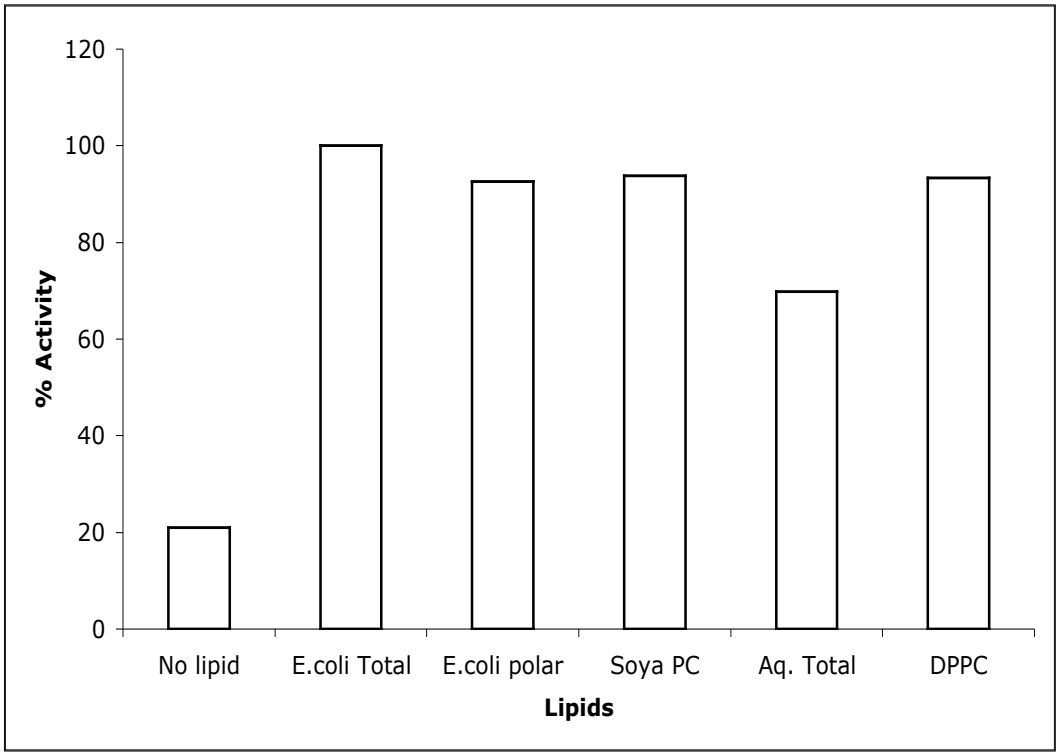

Figure 3.12: Activity of CtrA3 in the presence of different lipids. Lipids used were *E. coli* total lipid extract, E. coli polar lipids, soya PC, *Aquifex aeolicus* total lipids and DPPC, at the ratio of 5:1 (w/w) of protein in the reaction mixture. 100μM $CuSO_4$ was used to activate the enzyme. All other ingredients and conditions were as described in Materials and Methods.

The activity of CtrA3 was also heavily dependent on the purification protocol. CtrA3 was only active when it was purified in DDM. The activity of this protein was lost when purified in Cymal-6; only 15% of maximal activity could be detected irrespective of whether lipids were present or absent in the activity assay (Figure 3.13).

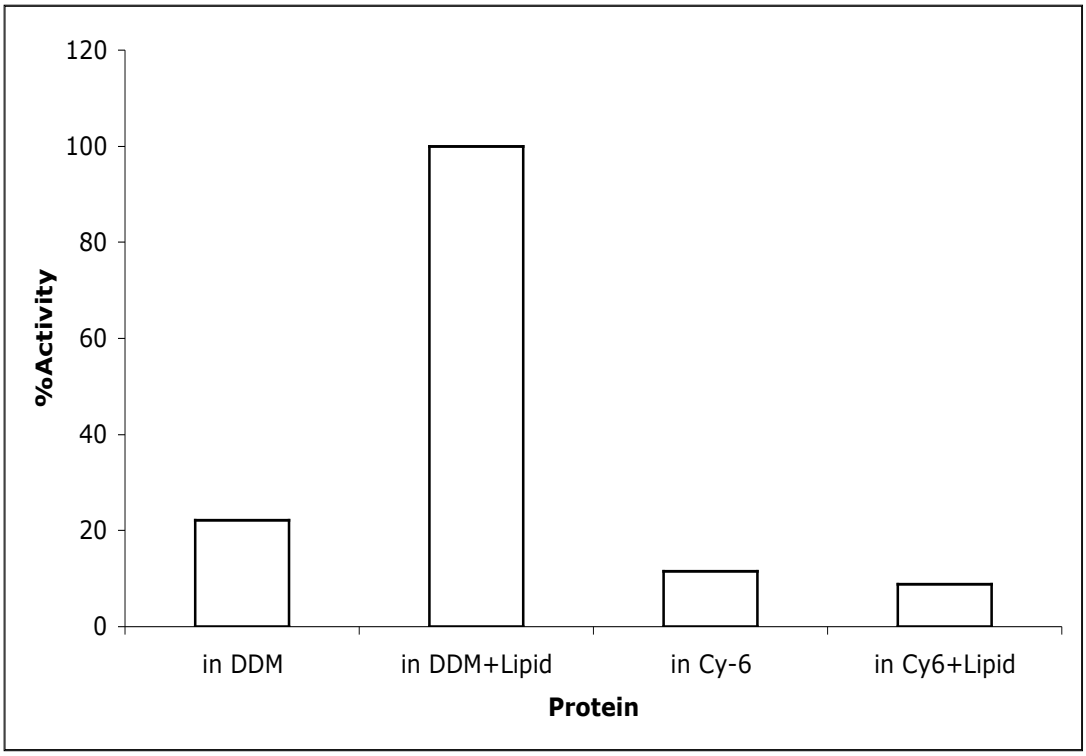

Figure 3.13: Activity of CtrA3 in the presence and absence of lipids and in different detergents. Lipid used was soya PC, 50μg per reaction mixture. 100μM $CuSO_4$ was used to activate the enzyme. All other ingredients and conditions were as described in Materials and Methods.

3.4.4.5 Saturation of Activity:

CtrA3 reached maximal activity of 2μM of Pi released/ mg of protein/ min in 5mM ATP (Figure 3.14). The maximum activity was calculated as described in

Materials and Methods. The enzyme reached saturation at this point and further increasing the ATP concentration has no effect on enzyme activity. Considering that K_M (Michaelis Menten Constant) of an enzyme is the substrate concentration where the enzyme has half maximal activity, from Figure 3.14, it is clear that CtrA3 has a K_M of approximately 1.1mM for ATP. The maximal activity of CtrA3 was reached in 10 minutes of start of the reaction (Figure 3.15).

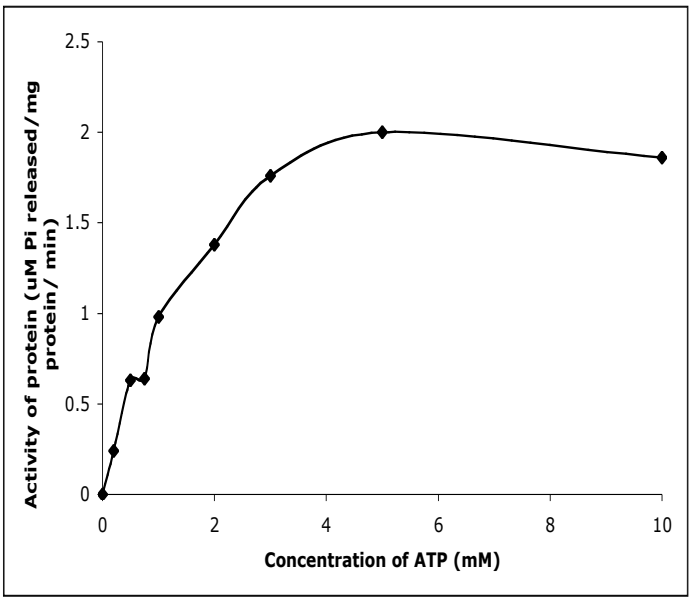

Figure 3.14 CtrA3 activity at different ATP concentrations: After mixing all the ingredients as described in Materials and Methods, the reaction was started by addition of different concentrations of ATP to reaction mixture, and stopped after 10 minutes.

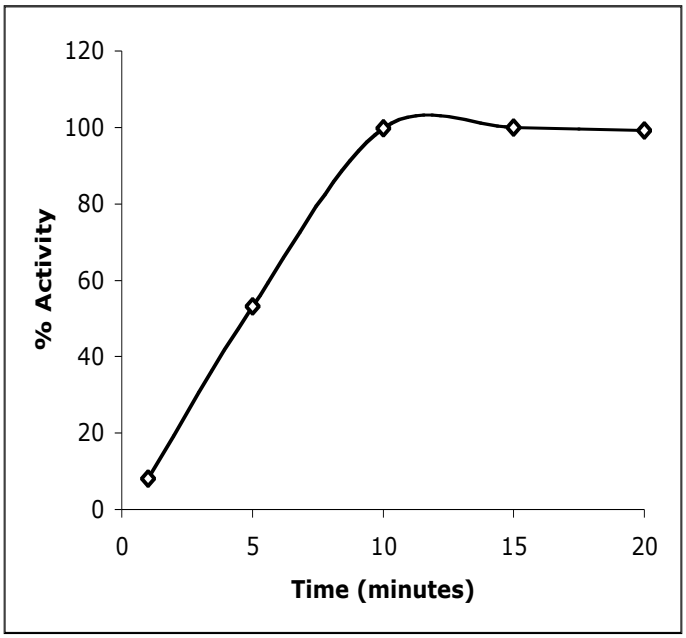

Figure 3.15 Saturation time of CtrA3 Activity: All ingredients as described in Materials and Methods were added and incubated for different time periods, before stopping the reaction with 10% SDS.

3.4.4.6 Cysteine dependence of CtrA3:

CtrA3 showed a strong dependence on cysteine for activity. Without any cysteine in the reaction mix, the protein showed only 20% of its maximal activity. 100% activity was achieved in 15mM cysteine. The activity decreased sharply on further increase of cysteine concentration (Figure 3.16).

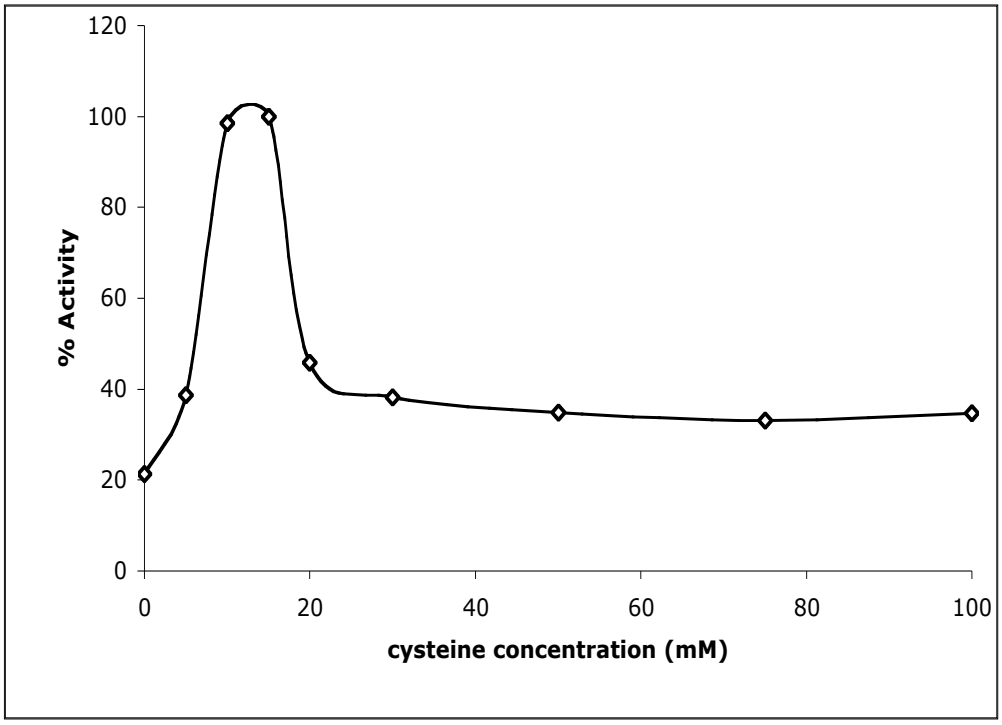

Figure 3.16 Effect of cysteine on activity of CtrA3: Different concentrations of cysteine were added to the reaction buffer. $CuSO_4$ at a final concentration of 100μM was added to the reaction mixture. All other ingredients and procedures were as described in Materials and Methods.

3.4.4.7 Effect of NaCl on activity of CtrA3:

Though CtrA3 was active in the absence of NaCl (approximately 40% of maximal activity), the activity increased linearly with the increase of NaCl concentration, up to 1000mM. Increasing the salt concentration further had no big effect on activity; CtrA3 retained approximately 80% of its maximum activity at 2.5 M salt (Figure 3.17).

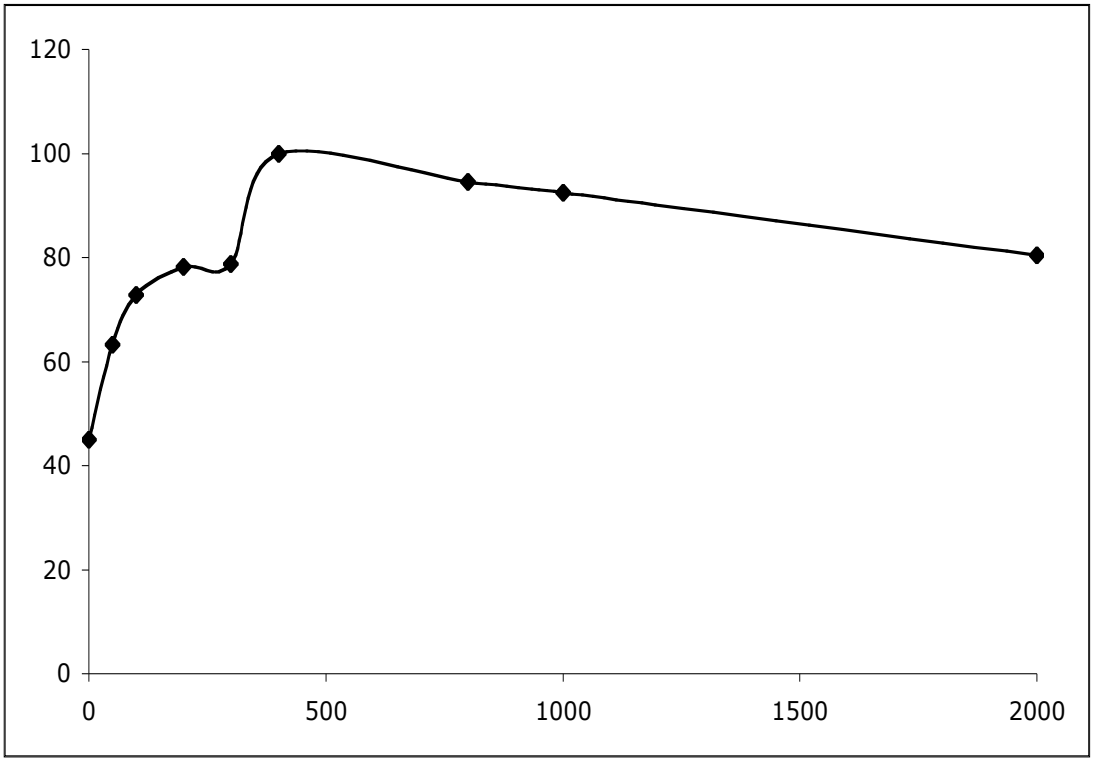

Figure 3.17 NaCl dependence of CtrA3: All ingredients except NaCl were as described in Materials and Methods. $CuSO_4$ was added at a final concentration of 100μM to activate CtrA3.

3.4.5 Analysis of *A. aeolicus* lipids:

Extracted lipids of *A. aeolicus* were run on TLC plates (Figure 3.18). Standard lipids PS, PE and PG and E. coli total lipids were also run for comparison. Mostly two bands were detected; the upper band has the same mobility like PE and the lower band has similar mobility as PS. E. coli PE and PG were detected as expected. The SDS-PAGE analysis of A. aelocius shows that the lipid extract has some protein contamination (Figure 3.19). At least one of the proteins detected has similar mobility like C-ring of F_0F_1ATPase used as standard.

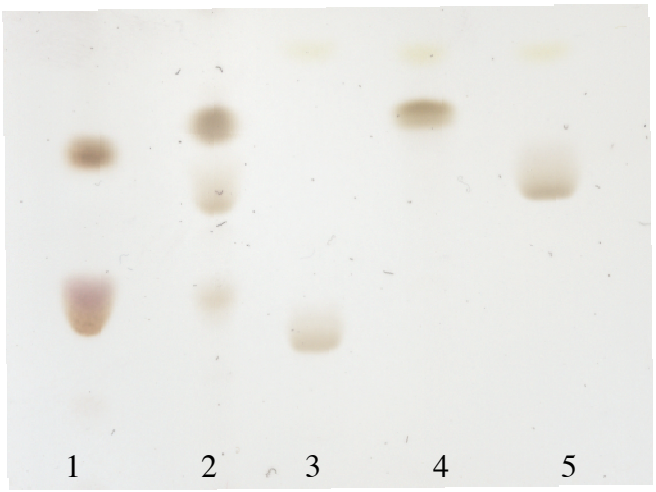

Figure 3.18 TLC analysis of *A. aeolicus* lipids. Lane 1: 5μl of 10mg/ml total lipid extract of *A. aeolicus*; lane 2: 5μl of 10mg/ml total lipid extract of *E. coli* total lipids; lane 3: 25μg of DPPS; lane 4: 40μg of DPPE; lane 5: 30μg of DPPG. All lipids were prepared and TLC run as described in Materials and Methods.

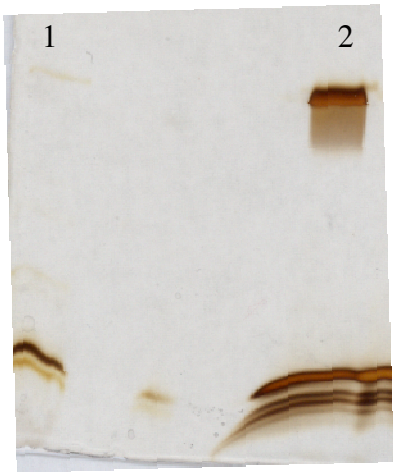

Figure 3.19 SDS-PAGE analysis of *A. aeolicus* lipids. Lane 1: 2μl of *A. aeolicus* total lipid extract (10mg/ml lipid); lane 2: 2μg of standard C-ring of *I. tartaricus* (kindly gifted by Dr. Thomas Meier, MPI for Biophysics, Frankfurt, for comparison). The gel was silver stained as described in Materials and Methods.

3.4.6 Reconstitution of CtrA3 in lipids:

Different lipids were tried for reconstitution of CtrA3, for 2D crystallization. After dialysis for a week and ultracentrifugation on a step-gradient of sucrose, the fractions were carefully collected from the top and labeled 1-5, 1 being the top most fraction and 5, pellet. All fractions were run on an SDS-PAGE and analyzed by Western blotting.

Since high LPRs were used and lipid vesicles have low density and float on sucrose-cushion, incorporation of protein into vesicles would result in protein localizing with lipids near the top of sucrose-gradient. As detergent was removed during dialysis, un-incorporated protein would aggregate and form a pellet during ultra-centrifugation.

CtrA3 reconstituted best in DPPC (Figure 3.20). Almost all the protein incorporated into vesicles and was seen in fractions 1 and 2, meaning that it was incorporated into lipids. Protein was not detected in pellet fraction (5) indicating that there was no aggregation.

E. coli polar lipids and PLPC were the worst candidates with most of CtrA3 not reconstituting in lipid and aggregating (in fraction 5). In case of *E. coli* polar lipids, degradation of protein was also observed. Even though CtrA3 reconstitution in DMPC was good, much of the protein was also detected in the pellet fraction (fraction 5). Reconstitution in *A. aeolicus* lipids was similar; even though the protein was reconstituted into the lipids (Fraction 2), some degradation in the reconstitution fraction and aggregation (Fraction 5) was observed.

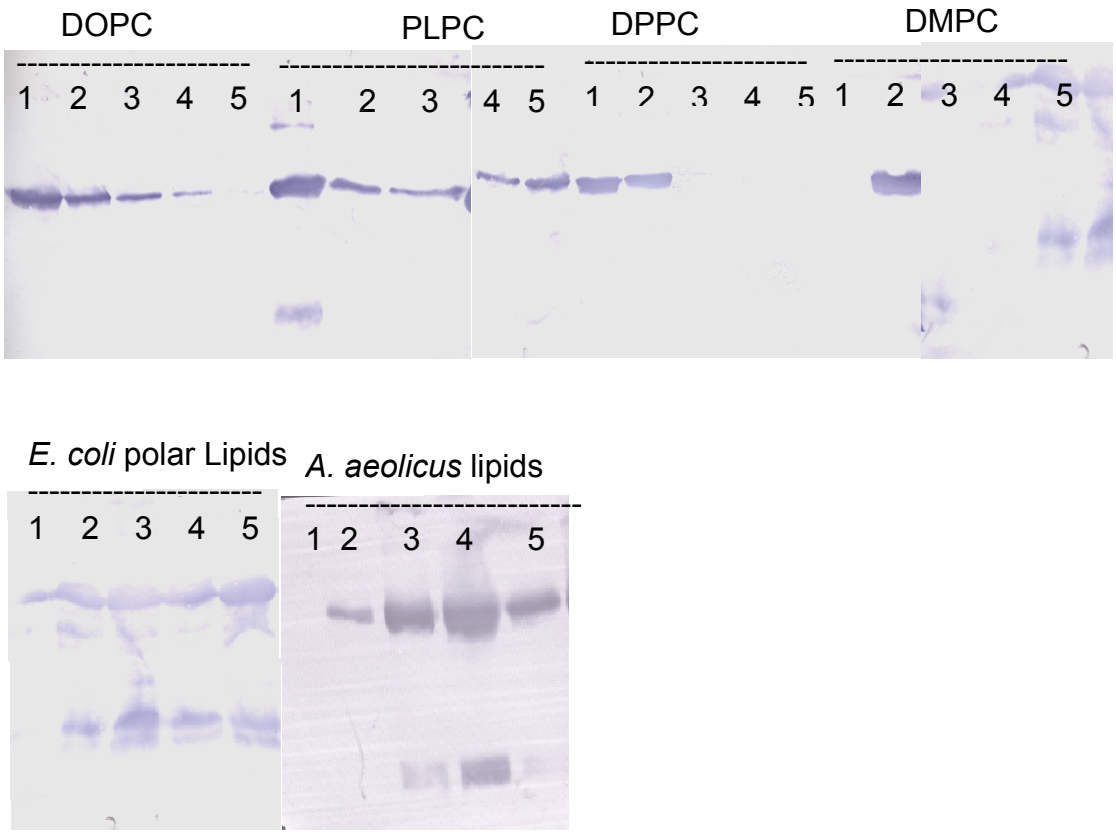

Figure 3.20 Reconstitution of CtrA3 in different lipids: The fractions of sucrose density gradient after ultracentrifugation were run on SDS-PAGE for western blot and probed by Anti-His antibody (1:1000). 1 is the top most fraction of gradient, while 5 is bottom most (pellet after centrifugation).

3.4.7 2D Crystallization and uranyl acetate staining:

Vesicles were observed when CtrA3 purified in DDM was dialyzed with DPPC at a lipid-to-protein ratio of 1.0 or less (Figure 3.21). The vesicles were approximately 1μm in diameter.

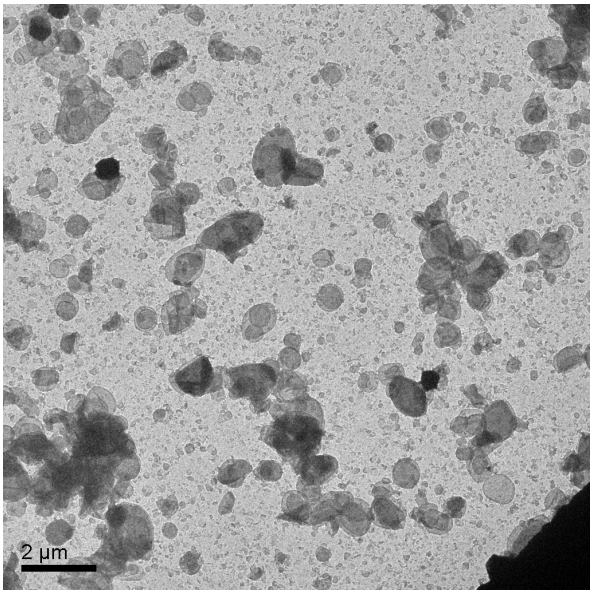

Figure 3.21 Morphology of membranes seen when CtrA3 was reconstituted in DPPC: The vesicles were observed after staining in 1% uranyl acetate, in FEI Technai G^2 EM, at a magnification of 1100X.

Ordered 2D arrays, in the shape of vesicles measuring 1μm-2μm across formed when CtrA3 was mixed with DPPC at an LPR of 0.3-0.5 and dialyzed for two weeks at 30°C. A NaCl concentration of 50mM in dialysis buffer was essential for 2D crystals to form. The order was patchy when NaCl was retained in the dialysis mixture. Salt removal by dialysis against salt-free buffer approximately 48hrs prior to harvesting was essential for obtaining well-ordered lattices of CtrA3 (Figure 3.22). Glycerol had a deleterious effect on reconstitution; large clumps and aggregates were observed all over the grid when glycerol was present in the dialysis buffers. Also, CtrA3 purified in Cymal-6 did not crystallize at conditions where CtrA3 purified in DDM crystallized. In fact, the incorporation of protein into liposomes was also not good when the protein was in Cymal-6. It was also observed that the microscope grids were dirty with a lot of aggregation of protein and clumps of vesicles when dialysis buttons were used as an alternative to dialysis bags.

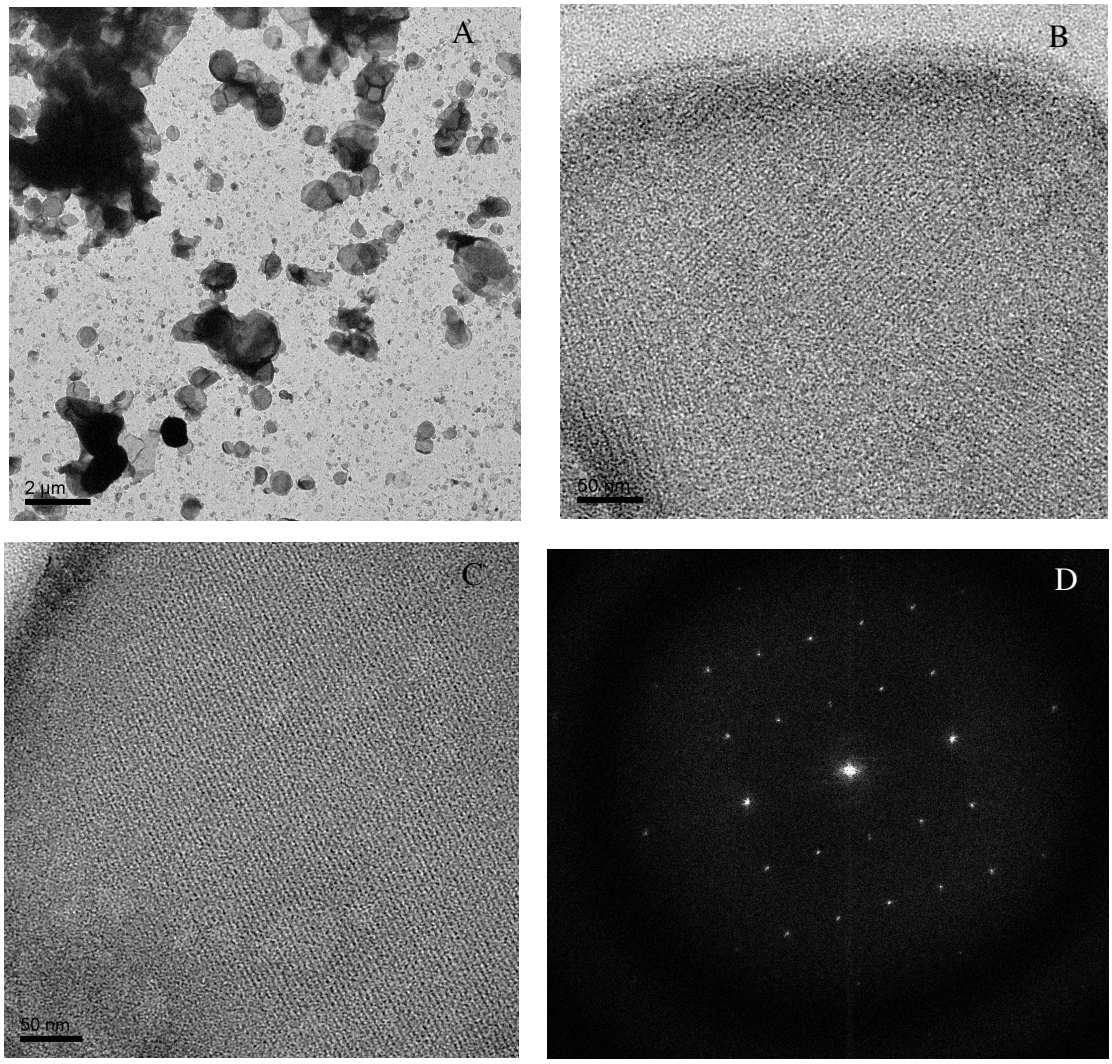

Figure 3.22 Effect of NaCl on crystal formation: (A) The vesicles formed when NaCl was retained in dialysis mixture, at an LPR of 0.5. The 2-D order was patchy (B) when compared to the sample where NaCl was removed completely 48hrs prior to recovery (C). (D) is the Fourier transform of (C), showing diffraction spots. The images were of 1% uranyl acetate stained grid taken at a magnification of 42,000X magnification in FEI Technai G^2 EM.

3.4.8 Cryo-microscopy and image processing:

4.5% Trehalose and 1% Tannic Acid, pH 6.7 were tested for embedding and preserving crystals of CtrA3 in DPPC. Attempts were also made to directly plunge the sample in liquid ethane or liquid nitrogen. For drying the grid before

plunging, both manual drying and plunging, and Vitrobot were tried. Lot of ice was found all over the grid when directly plunged without a cryo-preservative, and no order was seen in the vesicles when tannin was used as a preservative. Diffraction spots could be seen in the images where the sample had been embedded in trehalose, but only to the first order. Very rarely, diffraction spots to second or third order could be seen (Figure 3.23).

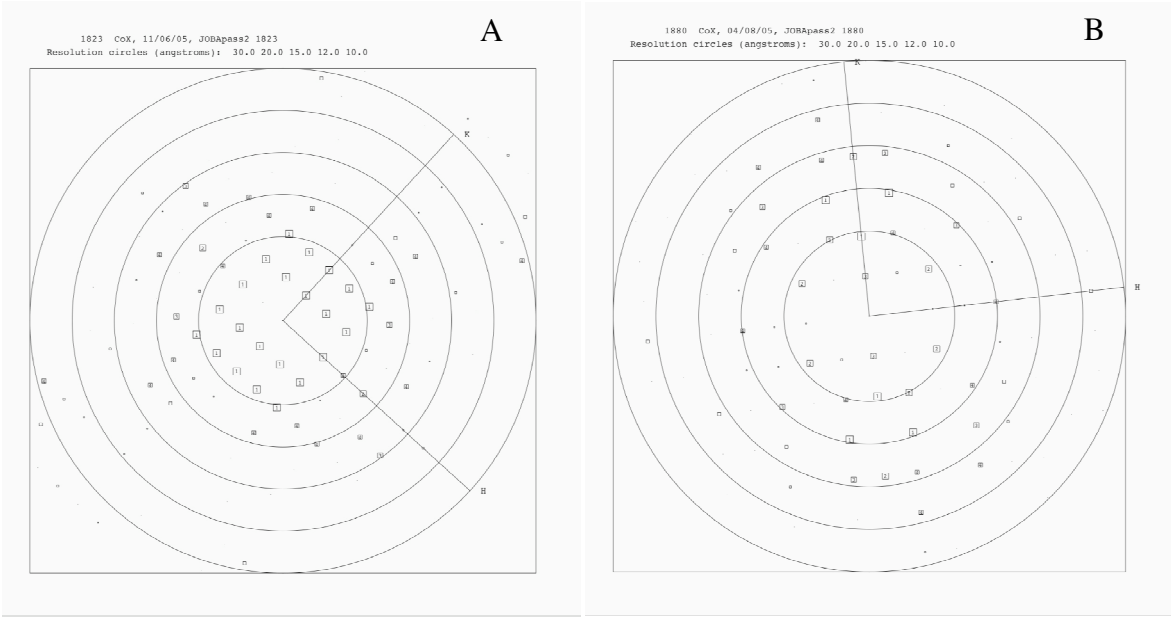

Figure 3.23 Calculated Fourier Transform from a single image of uranyl acetate stained sample taken in FEI Technai G^2 EM, at a magnification of 42,000X (A), and trehalose embedded sample taken in JEOL 3000SFF EM at a magnification of 52,000X (B). The circles represent 30Å, 20Å, 15Å, 12Å and 10Å resolution.

3.4.9 3D Crystallization:

Several hundred crystallization conditions were set up using both robotic and manual pipetting, either sitting-drop or hanging-drop, respectively. The

protein at a final concentration of 7-10mg/ml was used for setting up the drops. Some promising conditions (Figure 3.24) are tabulated here (Table 3.3).

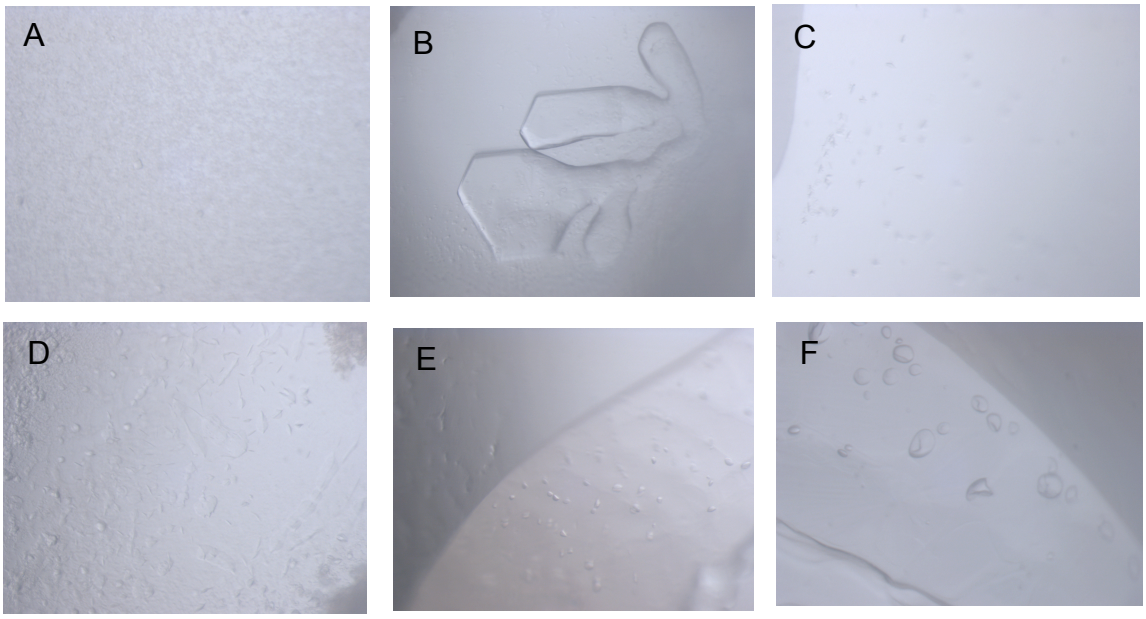

Figure 3.24 Preliminary 3D crystallization of CtrA3: The conditions corresponding to each figure are tabulated in Table 3.3.

Table 3.3

Label	Condition	Remarks
A	1.4M Na Citrate, 0.1M Na-Hepes 7.5	
B	0.6M $MgSO_4$, 0.1M Na-Hepes 7.5, 4%PEG400	
C	0.1M Tris 8.5, 2.0M Ammonium Phosphate	Spherulites
D	0.1M Na-Hepes 7.5, 30%PEG400	Micro needle shaped crystals
E	0.1M Lithium Sulfate, 0.1M Na_3-citrate 5.6, 12% PEG4000	
F	0.1M $MgCl_2$, 0.1M ADA 6.5, 12% PEG6000	Irregular shapes

3.5 CtrA2

3.5.1 Expression of CtrA2:

Different constructs were tried for expression of CtrA2 (Figure 3.6) in *E. coli*. Like CtrA3, CtrA2 could only be expressed with a tag at 5' end of the gene. RP-codon plus strain (Stratagene) expressed the protein better than C43. The expression was leaky, needing no induction by IPTG. The cells could be grown overnight at 37°C and harvested for processing. The expression levels were lower than that observed for CtrA3 and induction did not improve the expression. Approximately 0.75-1mg of CtrA2 could be purified from 1L of overnight grown cells. For all experiments, ctrA2 clone was used.

3.5.2 Sloubilization and purification:

CtrA2 could be solubilized in OG, Cymal-6 or DDM. The later two detergents could solubilize the protein completely from membranes, while OG could only solubilize it partially. Mega-9 could not solubilize the protein at all.

The protein in OG was not at all stable and precipitated soon after purification. CtrA2 could be purified in DDM (Figure 3.25), but needs glycerol to be stable for at least one week at either 4°C or -20°C. The protein was purified in Cymal-6 after solubilization either with the same detergent or DDM. CtrA2 thus purified was stable for more than a month at -20°C. Purification was essentially single step, using Ni^{2+}NTA.

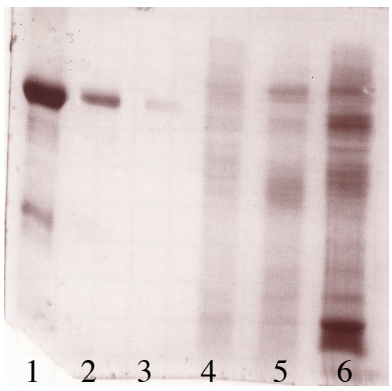

Figure 3.25 Purification profile of CtrA2: Ni^{2+}NTA elution profile; Lanes 1-3: Purified CtrA2 in different amounts (7μg, 4.5μg, 2.2μg loaded); lane-4: wash; lane-5: Flow-through; lane-6: solubilized membranes.

3.5.3 Gel filtration:

The homogeneity of CtrA2 purified in detergent was analyzed by gel filtration. Ni^{2+}-NTA purified CtrA2 was passed through pre-equilibrated Superdex 200 column (Amersham Biosciences). The protein purified in DDM (in the presence of 10% glycerol) showed some heterogeneity, as the eluted peak was not monodispersed (Figure 3.26 A). It is possible that the protein has at least two different oligomeric states in solution. When the protein was purified in Cymal-6, similar pattern was observed; only the second peak was equal in ratio to the first peak (Figure 3.26 B).

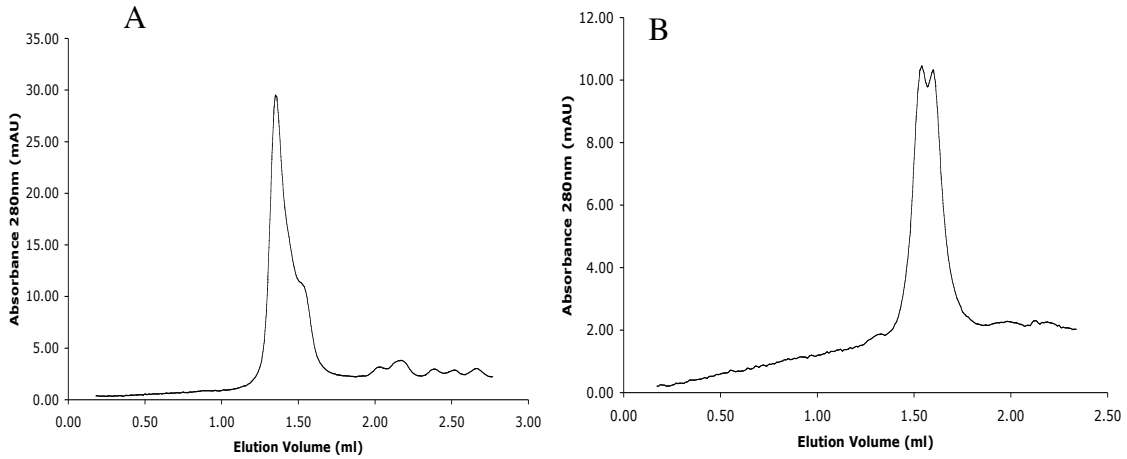

Figure 3.26 Gel Filtration Profiles of (A) CtrA2 purified in DDM and (B) in Cymal-6. Superdex-200 pre-packed column was used to run the samples in Amersham-Ettan system.

3.5.4 Activity assays

3.5.4.1 Activity in presence of different metal ions:

The activity of CtrA2 was stimulated by both Ag^{+} and Cu^{+}, but not by Cu^{2+}. Ag^{+} was twice as effective as Cu^{+} in its activation of the enzyme (Figure 3.27).

The activity of CtrA2 in the presence of other metal ions, Mg^{2+}, Zn^{2+}, Co^{2+} and Ni^{2+} was only slightly above background. No ATP hydrolysis activity of the enzyme was detected in the absence of any ions. For mimicking Cu^{+} environment, 2mM DTT was added to the reaction mixture containing $CuSO_4$.

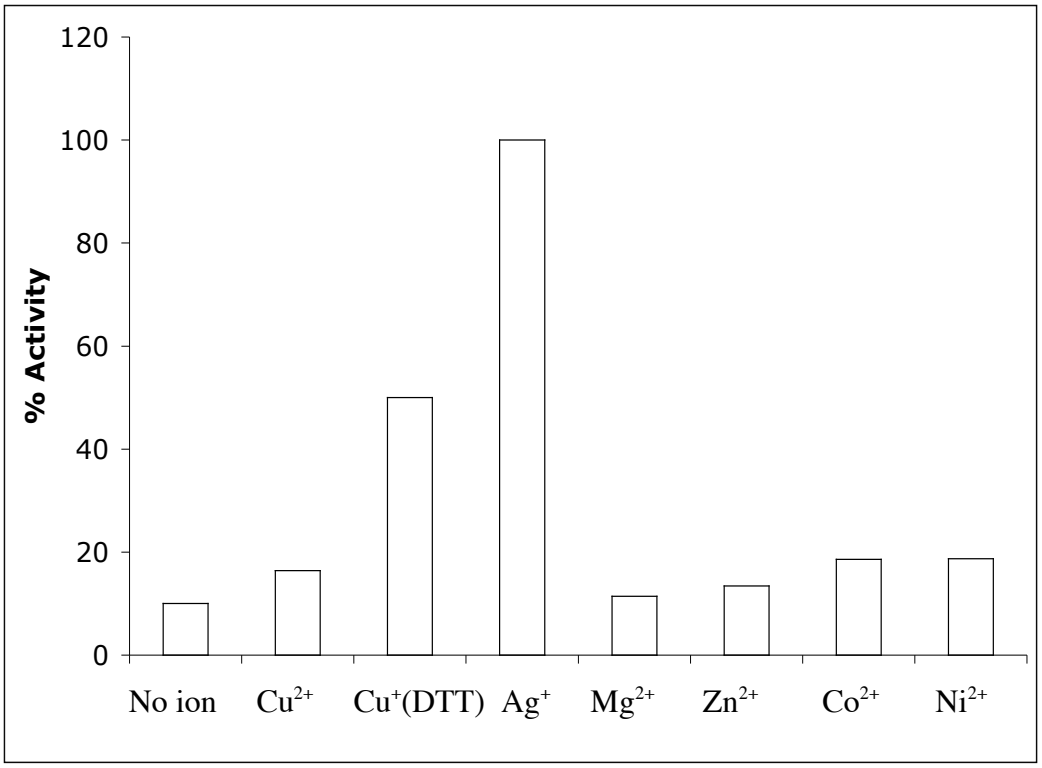

Figure 3.27 Activity of CtrA2 in the presence of different metal ions: Cu^{2+} ($CuSO_4$), Ag^{+} ($AgNO_3$), Mg^{2+} ($MgSO_4$), Zn^{2+} ($ZnCl_2$), Co^{2+} ($CoCl_2$), $Ni2^{+}$ ($NiCl_2$) were used at 100μM concentration. For Cu^{+}, 2mM DTT was added to $CuSO_4$ solution. All other ingredients were as mentioned in Materials and Methods.

3.5.4.2 Activity at different temperatures:

ATP hydrolysis activity of CtrA2 was tested at different temperatures, ranging from 4°C to 95°C, considering the fact that *A. aeolicus* is a hyperthermophilic bacterium growing at 70°C-90°C. Samples with all ingredients

except ATP were incubated at respective temperatures for 15minutes before starting the reaction by adding 5mM ATP. $AgNO_3$ at a concentration of 100μM was used to activate the enzyme. The activity of CtrA2 reached a maximum at 75°C and decreased to 70% of this value at 95°C. The protein remained significantly active at 50°C and activity, however low, was detected even at 30°C (Figure 3.28).

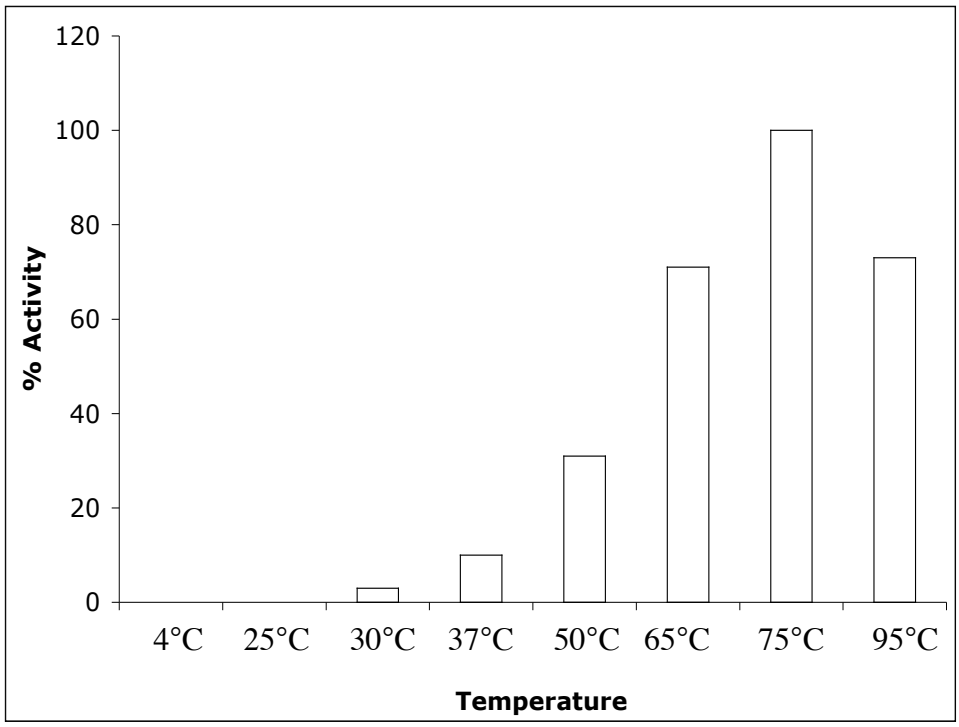

Figure 3.28 Activity of CtrA2 at different temperatures: All ingredients were as mentioned in Materials and Methods; the reaction vials were incubated at 4°C, 25°C, 30°C, 37°C, 50°C, 65°C, 75°C and 95°C for 15 minutes for equilibration at that temperature before starting the reaction with 5mM ATP. $AgNO_3$ at a final concentration of 100μM was added to reaction mixture to activate CtrA2.

3.5.4.3 pH dependence of CtrA2:

CtrA2 showed a broad bell shaped curve when tested for ATP hydrolysis activity at different pH. The protein and other ingredients of the reaction as mentioned in Materials and Methods were incubated in buffers of different pH at 75°C, before starting the reaction with 5mM ATP.

The maximal activity of the protein was observed at pH 7.0-7.5 (Figure 3.29). There was a sharp decrease in activity of CtrA2 from pH 6.0 to pH 5.0. The protein was not active at or below pH 4, but retained approximately 60% of its activity at pH 9.0.

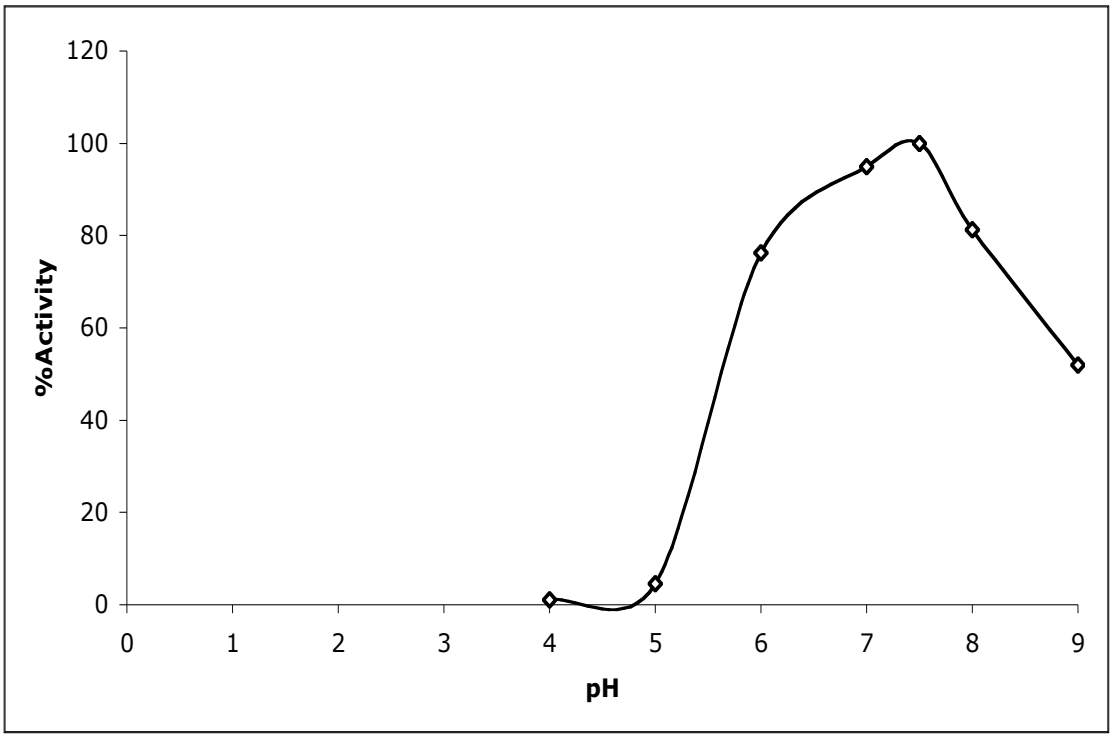

Figure 3.29 ATP hydrolysis of CtrA2 at different pH: The reaction mixture contained 100μM $AgNO_3$. All other ingredients, except buffer, were as described in Materials and Methods. The buffers used were Na-Acetate (pH 4.0), K-Acetate (pH 5.0), MES (pH 6.0), MOPS (pH 7.0), Tris-HCl (pH 8.0) and Tris-HCl (pH 9.0).

3.5.4.4 Necessity of lipids for activity of CtrA2:

Lipid dependence of CtrA2 was tested by adding different lipids suspended in water to the reaction mixture at an LPR of 5:1 (w/w). The mixtures were let to stand at 75°C for 15 minutes before starting the reaction with 5mM ATP as described in Materials and Methods. Additional lipids in the reaction mixture were not necessary for the ATP hydrolysis activity of CtrA2. Also, the activity of protein was independent of the lipid added. The protein showed almost equal activity in the presence of all the lipids tested: soya PC, *E. coli* total lipid extract, *E. coli* polar lipid extract or *Aquifex aeolicus* total lipids (Figure 3.30).

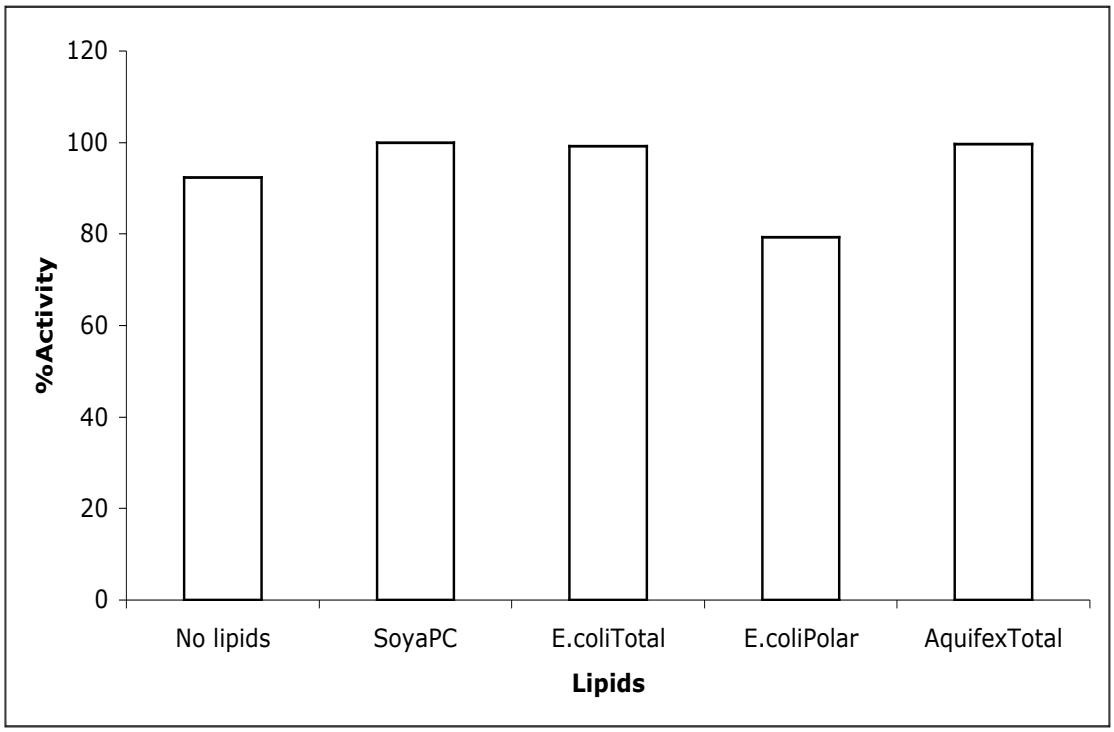

Figure 3.30 Effect of different lipids on activity of CtrA2: Lipids used were: soya PC, *E. coli* total lipid extract, *E. coli* polar lipid extract and *Aquifex aeolicus* total lipid extract, at the ration of 5:1 (w/w) of protein in reaction mixture.

3.5.4.5 Effect of salt concentration on activity of CtrA2:

CtrA2 reached 80% of its maximal activity with out the addition of NaCl. The maximal activity of the protein was in the presence of 400mM NaCl. However the activity of CtrA2 decreased on further increase in salt concentration (Figure 3.31).

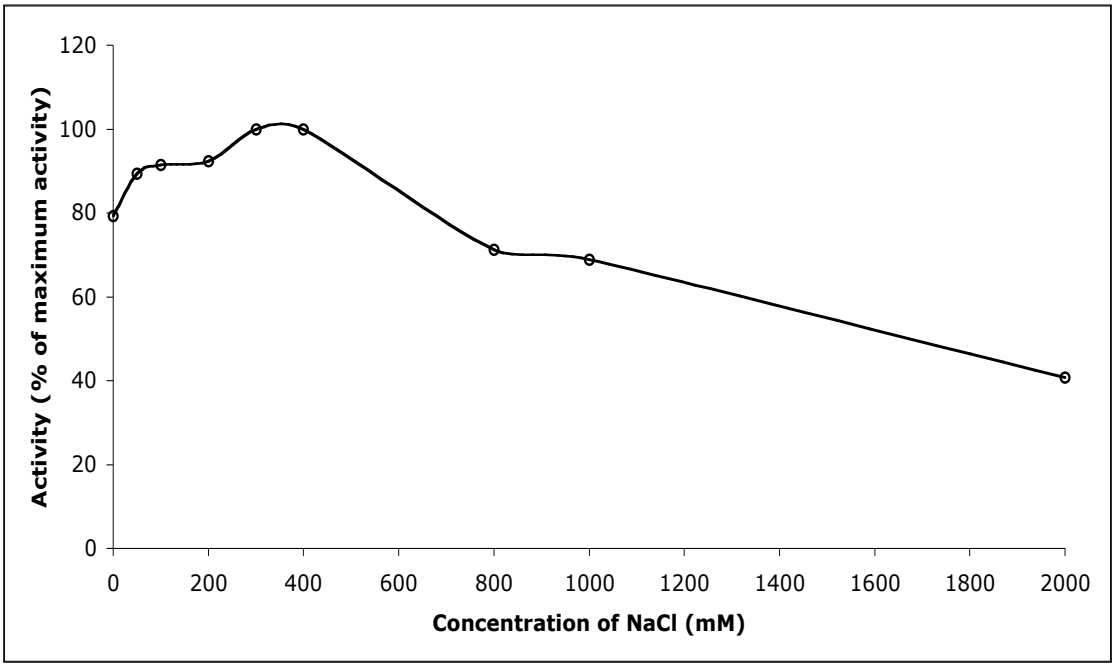

Figure 3.31 Salt dependence of CtrA2: All ingredients except NaCl were added as described in Materials and Methods. $AgNO_3$ at a concentration of 100μM was added to activate the protein.

3.5.4.6 Effect of cysteine on the activity of CtrA2:

Since dependence of copper pumps on thiols for activity is known (Mitra and Sharma 2001; Mandal et al. 2002), the effect of cysteine on CtrA2 was tested. Cysteine was essential for the activity of CtrA2 in vitro. In the absence of cysteine in the reaction mixture, the activity of CtrA2 was only 20% of its maximal

value. The maximal activity was observed in 20mM cysteine and increasing the concentration further till 100mM did not have any effect on the activity of CtrA2 (Figure 3.32).

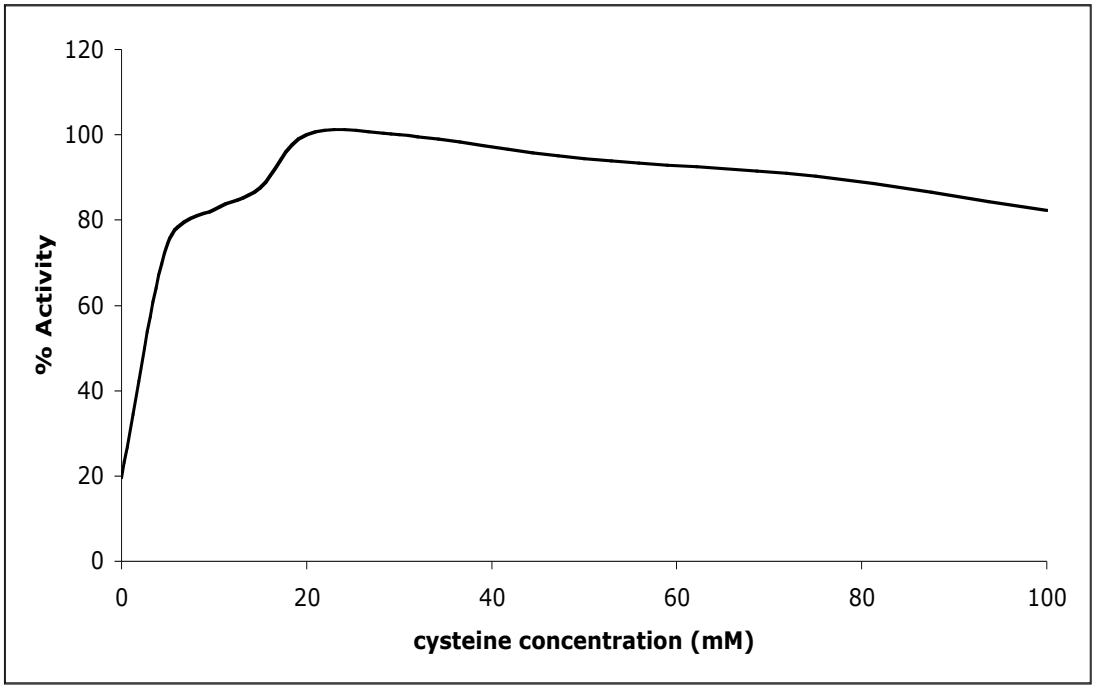

Figure 3.32 Cysteine dependence of CtrA2 activity: The protein was activated by adding 100μM $AgNO_3$. All ingredients except cysteine and the procedure were as described in Materials and Methods.

3.5.4.7 Saturation of activity:

CtrA2 reached its maximum activity of 1.2 μM of Pi released/ mg protein/ min in 5mM ATP. The enzyme reached a saturation point at this time and any further increase in ATP concentration did not have any effect (Figure 3.33). The K_M of the enzyme (substrate concentration where the enzyme has half maximal activity) for ATP is 1.6mM. The activity of the enzyme was calculated as described in Materials and Methods.

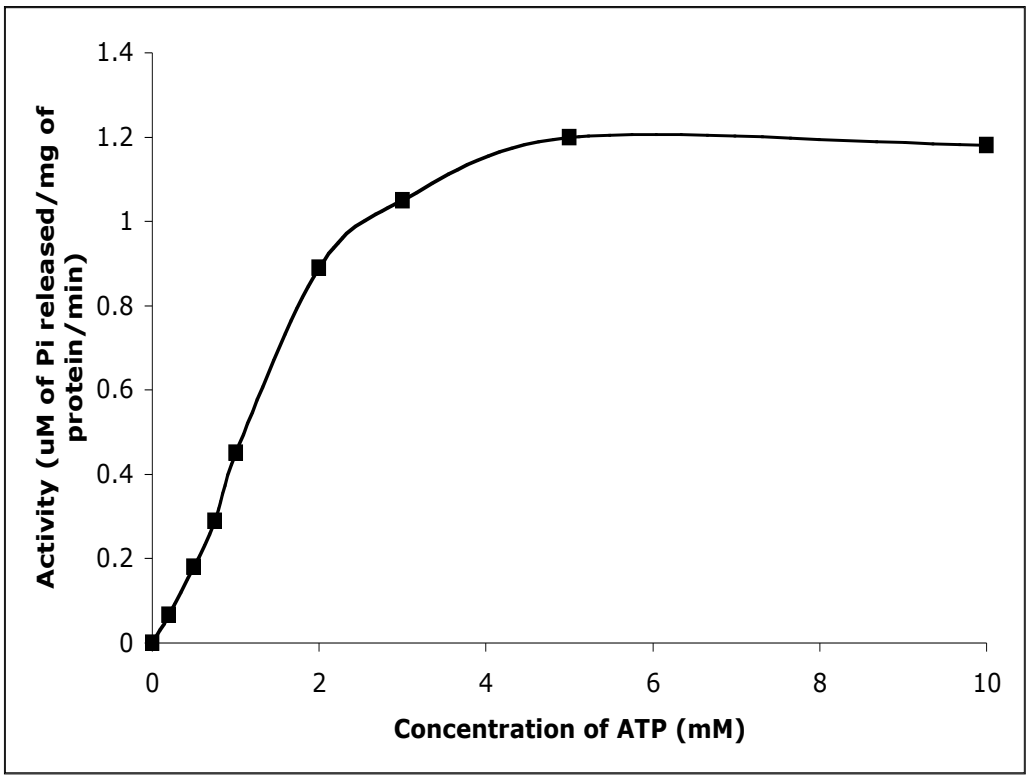

Figure 3.33 CtrA2 activity at different ATP concentrations: After mixing all the ingredients as described in Materials and Methods, the reaction was started by addition of different concentrations of ATP to the reaction mixture and the reaction was stopped after 10 min.

3.5.5 Reconstitution of CtrA2 in lipids

Reconstitution of CtrA2 was attempted in five different lipids, for crystallization (Figure 3.34). The strategy for identification of the best lipids was identical to that used for CtrA3 (See Chapter 3.4.6). Of these lipids, DOPC was the best. Most of the protein localized towards the top of the gradient (Fraction 1) where usually lipid localizes, indicating reconstitution. Also, no protein was seen in the pellet fraction of the sucrose-gradient (Fraction 5), meaning that there was

also no aggregation of the protein. Aggregation and degradation of protein was observed when DPPC, *E. coli* polar lipids and *A. aeolicus* lipids were used. PLPC was the worst candidate with much of the protein seen in the pellet fraction of the gradient.

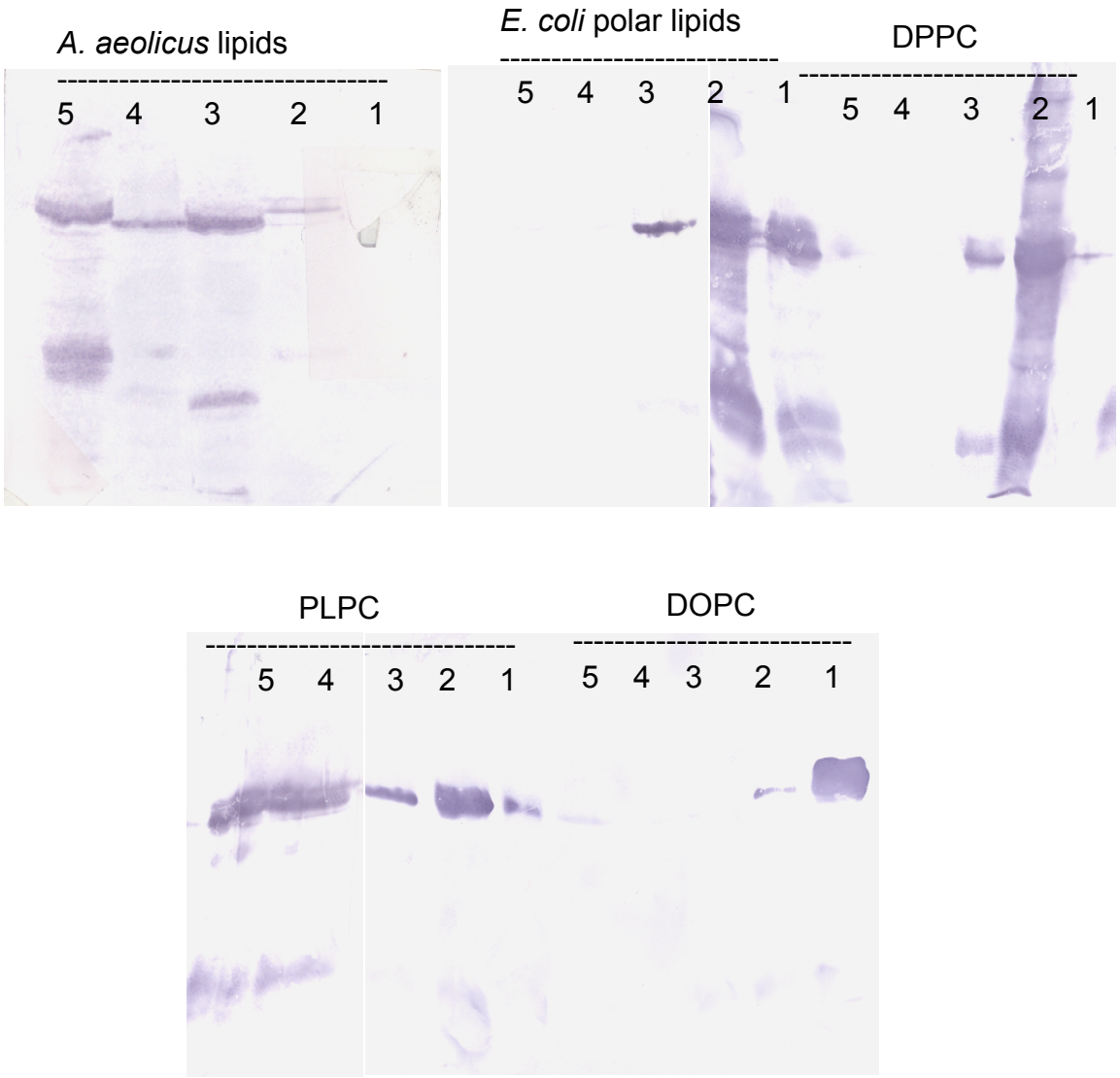

Figure 3.34 Reconstitution of CtrA2 in different lipids: Numbers 1-5 indicate the fractions from top to bottom of the sucrose gradient run on SDS-PAGE and probed with Anti-His antibodies (1:1000).

3.5.6 Screening for 2D and 3D crystals:

Small vesicles were observed when CtrA2 purified in DDM in presence of glycerol was mixed with *E. coli* polar lipids at an LPR of 1.0 but there was no order. Protein was aggregated at lower LPRs and did not incorporate into lipids. Tubes were observed at an LPR of 1.0 when protein was purified in Cymal-6 and reconstituted into DMPC (Figure 3.35). No ordered lattices were observed in these tubes. Lowering of LPR up to 0.3 did not induce the ordering of protein. No specific leads were evident from preliminary 3D crystallization screens.

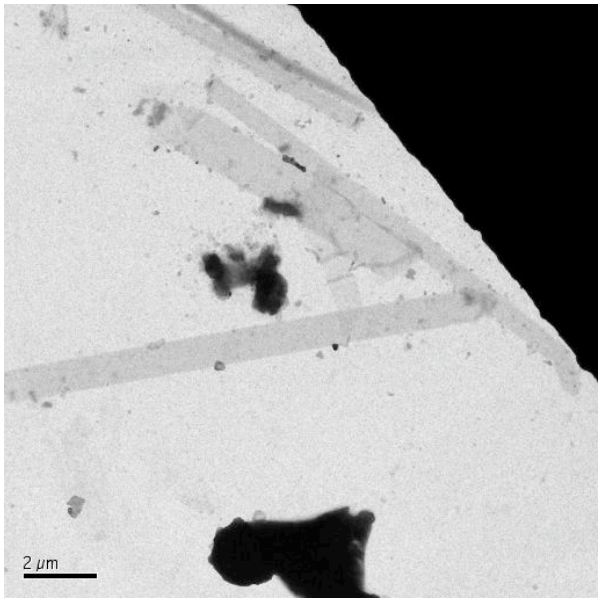

Figure 3.35 Tubes observed with CtrA2 reconstituted with DMPC: The image was recorded on CCD on a Technai G^2 electron microscope operating at 120kV, at a magnification of 1100X.

CHAPTER 4

DISCUSSION

4.1 Plant H^+-ATPase AHA2

4.1.1 Expression of AHA2 in *Pichia pastoris*:

For 2D and 3D crystallization, a high amount of protein, often in milligram quantities is required. In addition to this, batch-to-batch variation of membrane protein expression and purification must be avoided for reproducible results. For this reason, it is desirable to identify an expression system where large amounts of protein can be expressed and purified as a single batch. *Pichia pastoris* has been used for over-expression and characterization of many membrane proteins with varying degrees of success (Labarre et al. 2006; Licata et al. 2006; Lundstrom et al. 2006; Yang et al. 2006; Macauley-Patrick et al. 2005; Cai and Gros 2003; Parcej and Eckhardt-Strelau 2003). Expression of AHA2 was attempted in this because yields of AHA2 in *S. cerevisiae* only amounting to approximately 0.15mg per liter of culture were obtained (Results, 3.2.1).

AHA2 could not be expressed in *P. pastoris* under the conditions tested. It has been observed in other yeasts that proton ATPase is necessary and rate limiting for growth. For example, *S. cerevisiae* cells with reduced PMA1 expression have severely impaired growth rates (Vallejo and Serrano 1989). Similarly, when expression of PMA1 was increased using a multi-copy plasmid, cells showed signs of toxicity (Eraso et al. 1987). From these experiments, it was evident that balanced expression of H^+-ATPase is critical for the functional state of the cell. *P. pastoris*, as an organism is not as well studied as *S. cerevisiae* and mutants having controlled expression of proton pump are not readily available. Recombinant expression of proton pump was attempted with *P. pastoris* strain SMD1163. Only truncated protein was expressed (Figure 3.1). This could be because of partial transcription or translation of H^+-ATPase. Also, His antibodies failed to detect the tag that was present at the C-terminus of protein (Table 3.1), indicating that the protein was never expressed fully.

In comparison, AHA2 could be functionally expressed and purified from *S. cerevisiae* because a mutant strain RS72 (Cid et al. 1987) was used, where PMA1, the yeast proton pump was put under the control of a galactose promoter and AHA2 was introduced into the cells under a PMA1 promoter. When carbon source in the medium was shifted from galactose to glucose, the expression of PMA1 was suspended and AHA2 was expressed, which functionally complemented the yeast pump.

4.1.2 2D crystallization of AHA2:

2D crystals were earlier obtained from AHA2 expressed in *S. cerevisiae* that diffracted to 8Å (Jahn 2001). Biobeads were added to the crystallization solution containing 1mg/ ml purified protein (in DDM) together with detergent solubilized egg PC. After stirring for 3hrs at 22°C, the turbid supernatant contained well-ordered crystalline vesicles. However, attempts to reproduce this and improve the quality of crystals failed.

Protein purification varies from batch to batch, mainly in the lipids that the protein carries with it (Depalo et al 2004; Sebastian Richers, personal communication). In addition to variation in batches, other reasons could be speculated for failure of reproducibility. The published protocol had to be modified for the current study. I cultured the cells in 5l shake-flasks in contrast to 50 and 100-liter fermenters as reported. Hydrophobic interaction chromatography could not be carried out by Poros QE20 matrix because of lack of availability of the matrix (the production is abandoned). Attempts to use an alternative HIC column resulted in decrease of final yield (see Section 3.2.2). These two changes mean that the protein produced was in different conditions and carried different lipids with it. The total membrane fraction of yeast cells expressing AHA2 was not homogeneous (see Section 3.2.3) as this contained the protein that was incorporated into plasma membrane and also the part that was stuck in ER (Villalba JM 1992). However, this heterogeneity did not have any effect on

crystallization; the protein used by Jahn et al in their publication was from total microsomes. Using biobeads for 2D-crystallization, though rapid, was a very irreproducible way of removing detergent. This is mainly because of varying sizes of biobeads, and un-predictability of speed and amount of detergent removed in a specific time. All these factors play a very important role in the formation of 2D crystal arrays. Use of dialysis bags for removal of detergent was not successful as the dynamics of removal were very different from that of biobeads and it is possible that the total crystallization protocol including the lipid-protein ratio, detergent solubilizing the protein and lipid, temperature and buffer conditions need to be re-established for optimum incorporation of protein into lipid vesicles.

4.2 Copper ATPases from *Aquifex aeolicus*

4.2.1 The proteins:

An excess of heavy metal ions in the cell is toxic. On the other hand, a low minimal of certain transition metal ions, in particular Mn, Fe, Co, Ni, Cu, Zn, and in some cases Mo, is essential for the proper function of many enzymes. Membrane proteins that transport these ions in or out of the cell and thus maintain and control their cellular levels are essential for survival. P-type ATPases play a fundamental role in maintaining homeostasis and biotolerance of these metals in diverse organisms such as bacteria, archaea and eukaryotes (Axelsen and Palmgren 1998; Vulpe and Packman 1995; Solioz and Vulpe 1996; Rensing et al. 1999). An interesting feature of the heavy metal ATPases is their specificity for different metal ions even though their sequences are similar. The copper transporting P-type ATPases in particular are medically relevant since they are linked to Menkes and Wilson disease, which are caused by mutations in the human Cu-ATPase genes (Harris 2003). The presence of two distinct copper transporting ATPases in the same membrane and their different specificity for mono- or divalent ions led to speculations about their roles in copper homeostasis (Arguello et al. 2003; Stoyanov 2003). Both biochemical and

structural studies are required to understand more about these proteins. In this study, I produced and characterized CtrA2 and CtrA3, two new copper transporting P-type ATPases from the hyperthermophilic bacterium *Aquifex aeolicus.*

4.2.2 Expression of CtrA3 and CtrA2 from *Aquifex aeolicus* in *E. coli*:

The presence of a tag at N-terminus of the gene had a dramatic effect on the expression of CtrA3 and CtrA2. Expression of CtrA3 and CtrA2 was not possible without adding a tag at 5' end of the gene. The levels of expression were dependent on the length of the tag; a small His tag at the N-terminus resulted in low levels of expression while addition of a longer T-7 tag resulted in higher expression of protein. This could be because of some hairpin structures at this end in RNA when no tag was present, which prevents initiation of translation. However, it is very difficult to give a definitive answer for this behavior since many different factors play a role in protein expression by host cells. More intriguing is, when both T-7 and His tags were added at 5' end of the gene, the expression was leaky and induction was not necessary. It is not uncommon that pET recombinant expression system (Novagen) produces recombinant proteins without any induction. *E. coli* recombinant expression systems that utilize the *lac* operon control elements to modulate gene expression, including the pET system (Novagen), are known to produce leaky or uninduced expression (Dubendorff and Studier 1991; Kelley et al. 1995; Grossman et al. 1998). This is because the *lac* UV5 promoter, that drives the expression of T7 RNA polymerase allows basal level transcription in uninduced cells (Dubendorff and Studier 1991).

From the codon usage analysis of ctrA2 and ctrA3 genes, it was evident that most of the arginines (96% and 90% for ctrA2 and ctrA3 respectively) and prolines (29% and 55% for ctrA2 and ctrA3 respectively) are encoded by rare codons of *E. coli* (Table 4.1). Hence it is not surprising that the best expression levels were achieved in the RP CodonPlus strain of *E. coli* (Stratagene). These

cells, derived from BL21 (DE3), are designed to enable efficient high-level expression of proteins that contain codons rarely used in *E. coli*. They contain, in a chloromphenicol-resistant plasmid, extra copies of the *argU* and *proL* genes encoding rare tRNAs that recognize the arginine codons AGA and AGG, in addition to the proline codon CCC. It is likely that availability of these rare codon-carrying tRNAs in host cells improved expression levels significantly. The protein expressed was also correctly localized to the cell membrane, as detected by Western blotting. The expression of CtrA3 was higher than that of CtrA2. Approximately 1.2-1.5mg pure CtrA3 could be recovered from 1l of overnight grown (transformed) *E. coli* cell culture. The yield of CtrA2 was a little less, at approximately 0.75 -1mg/l of culture. The bacteria could survive with this high expression of CtrA3 probably because the protein was not active at 37°C (Figure 3.10). Even CtrA2 was only very mildly active at this temperature, where the bacteria were grown for expression (Figure 3.28), but this mild activity might be the reason why CtrA2 expression was lower than that of CtrA3.

Table 4.1

Amino acid	in CtrA3		in CtrA2	
	Total number present in the gene	Encoded by rare codons of *E. coli*	Total number present in the gene	Encoded by rare codons of *E. coli*
Arginine	21	19 (AGG, AGA)	24	23 (AGG, AGA)
Proline	20	11 (CCC)	18	5 (CCC)

4.2.3 Solubilization, purification and homogeneity:

Maltosides seem to solubilize CtrA3 and CtrA2 better than other detergents. Again, non-ionic detergents were more efficient for solubilization. DDM, having a 12-carbon length side chain has proved to be the best detergent

for these proteins. Histidine tags were used at both ends to bind the protein selectively to Ni^{2+}-NTA matrix, and bound protein was eluted by passing imidazole that displaces the His tag from Ni^{2+} co-ordination. After purification, CtrA3 purified in DDM was very homogenous showing a sharp peak when passed through Superose 6 column (Figure 3.8). When purified in OG, the protein was less stable and precipitated within a day after purification. The protein could also be purified in Cymal-6. Even though the purified protein was not as homogenous as when purified in DDM, it was stable (Figure 3.8).

In contrast, CtrA2 purified in DDM was not monodisperse, with a shoulder when passed through superdex-200 column (Figure 3.26), which might be indicative of two different oligomeric states of protein, but could also be some impurity that co-purified. In fact, a very faint band that co-purified with the protein from Ni^{2+}NTA column could be seen on SDS-PAGE (Figure 3.25). The protein was not stable for more than a week even when stored at -20°C. Glycerol had to be added in the purification protocol for increasing the stability of CtrA2. Purification of CtrA2 in Cymal-6 does not improve either purity or homogeneity (Figure 3.26).

4.2.4 ATP hydrolysis activity of CtrA3 and CtrA2:

4.2.4.1 Heavy metal ion dependency:

The heavy metal dependency of CtrA3 was similar to CopB from thermophilic archaea, *Archaeoglobus fulgidus* that is also activated by Cu^{2+} (Mana Capelli 2003). As expected, similar to CopB, CtrA3 was also activated by Ag^{+}, though to a lesser extent (Figure 4.1). It is clear that these ions are essential for ATP hydrolysis activity of CtrA3, as in the absence of Cu^{2+} or Ag^{+} the enzyme is inactive. It can be concluded that CtrA3 has a mechanism similar to that of other P-type ATPases; i.e. ion transport coupled to ATP hydrolysis. It has been

shown already for CopB from *A. fulgidus* that this enzyme transports copper across membranes. CtrA3 can be conveniently grouped as a CopB like protein.

In contrast, CtrA2 was activated by Ag^{+} more than by Cu^{2+} (Figure 4.1 and Figure 3.25) or any other metal ion, like CopA of *A. fulgidus* and other organisms, where CopA related proteins were identified (Wunderli-Ye and Solioz 2001; Mandal 2002). This explains the presence of two copper ATPases in *A. aeolicus* and many other organisms. It is possible that both these proteins have different ion selectivity: CtrA3 (CopB-like) responsible for extruding Cu^{2+} and CtrA2 (CopA-like), for extruding monovalent copper. Cu^{+} ion is highly unstable and can occur only in reduced environments. To mimic the monovalant copper, DTT was added to $CuSO_4$ solution. As shown in Figure 3.27, the activity of CtrA2 in the presence of DTT-$CuSO_4$ is higher than that in $CuSO_4$. Since there are no known Ag^{+} importers into the cells, CtrA2-like proteins probably transport Cu^{+}, but not Ag^{+}, out of the cell and the stimulation *in vitro* by Ag^{+} is most likely a non-physiological effect considering the similar charge/ volume ratio of these ions.

Based on indirect evidence (see Section 1.10.1), there have been suggestions that CtrA2 or CopA like proteins actually import Cu^{+} into the cell (Stoyanov 2003). A direct transport assay to test these results might answer questions relating to copper import mechanism in prokaryote cells, because CopA- and CopB-like proteins would then be collectively responsible for copper homeostasis in these organisms. However, since not all CopA containing prokaryotes actually live in highly reducing environments, and considering the known preference of these proteins for Cu^{+}, there must be other mechanisms to supply the reduced copper ion to these enzymes for import. Most (eukaryote) cells actually take up copper more readily when reducing agents such as DTT are added to the medium (Harris 2003; Harris et al 1998).

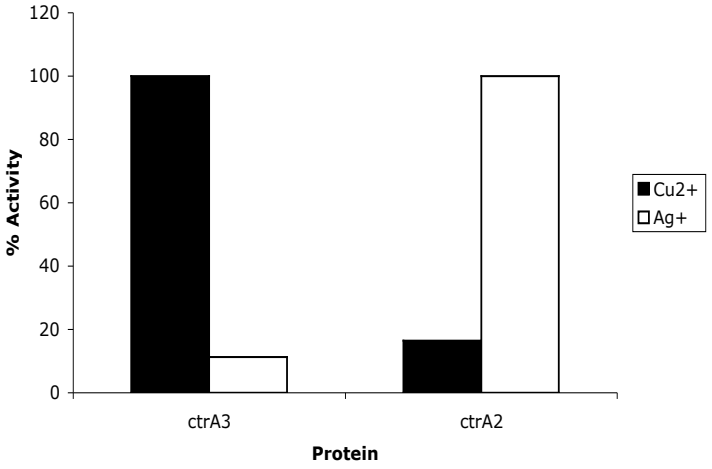

Figure 4.1 Comparison of activation of CtrA3 and CtrA2 by Cu^{2+} and Ag^{+}. The representation is merged data from Figures 3.9 and 3.27.

4.2.4.2 ATP Saturation:

Both CtrA3 and CtrA2 have different K_M and V_{max} for ATP (Figure 4.2). It is possible that different conditions stimulate these two proteins in the cell. Purified CtrA2 has an Ag-ATPase activity of 1μM/mg/min, which is higher than that reported for CopA from *A. fulgidus* (0.23μM/mg/min) (Mandal 2002) or CopA from *E. hirae* (0.15μM/mg/min) (Wunderli-Ye and Solioz, 2001).

Purified CtrA3 has a maximum activity of 2μM/mg/min in the presence of Cu^{2+} as against 0.08μM/mg/min for CopB of *A. fulgidus*. However, ZntA, another P_{IB}-ATPase from *E. coli*, was reported to have a maximum activity of 3μM/mg/min (Sharma et al. 2000). Other P-type ATPases, recombinant plant H^{+}ATPase (3μM/mg/min) (Lanfermeijer FC 1998) and native *N. crassa* proton pump (5μM/mg/min) (Mahanty SK 1994), also have similar activity maximas.

CtrA2 and CtrA3 have the highest reported activity so far for a copper transporting CPx-ATPase. It is possible that enzyme purification protocols might have had an effect on activity. The higher activity of CtrA2 and CtrA3 might also be due to the lipids associated with the protein during purification. It is also

possible that the different experimental conditions had an effect on the activity of the proteins. Alternatively, the difference in activity of CtrA2, CtrA3 and CopA, CopB might be due to natural differences between these enzymes.

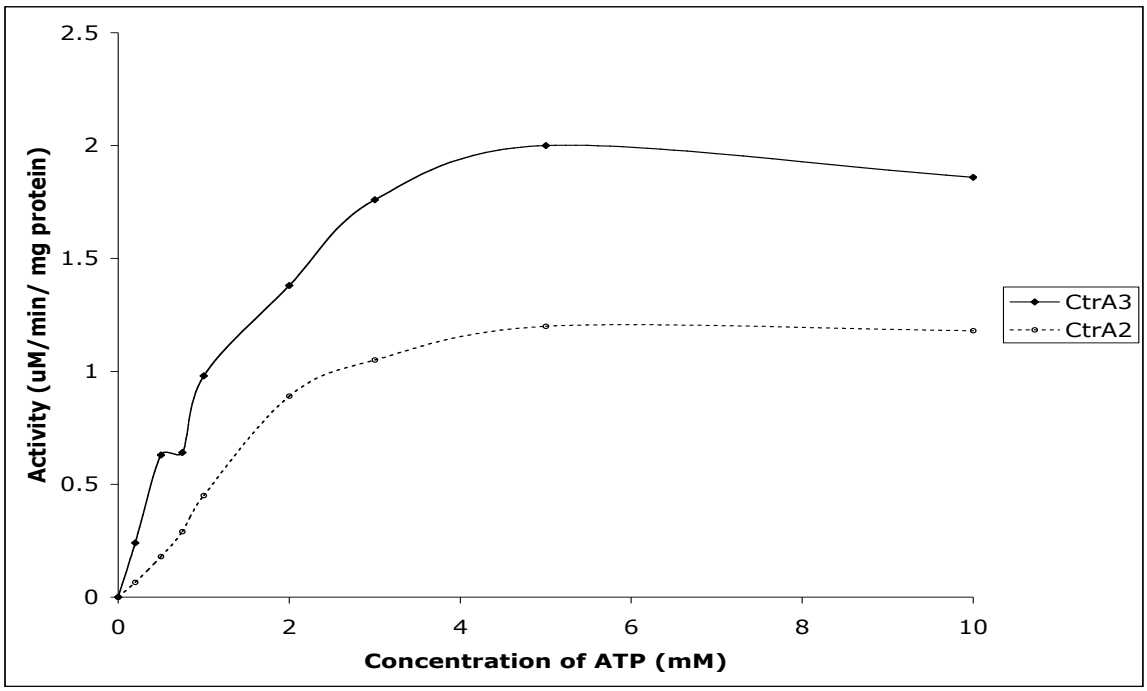

Figure 4.2 Comparative analysis of ATP hydrolysis activity of CtrA3 and CtrA2: This representation is merged data from Figures 3.14 and 3.33).

4.2.4.3 Temperature dependency:

CtrA3 was only active above 50°C (Figure 4.3). As expected for any thermophilic organism, maximal activity was observed at around 75°C. The protein was still active at 90°C. It is surprising that with approximately 45% identities with similar protein from non-thermophiles like *E. hirae*, this protein is not at all active at 37°C. Even though CtrA2 also has maximal activity at 75°C, the range of activity of CtrA2 was more; the protein was active above 30°C (Figure 4.3). Since, in addition to sequence, these proteins probably share

structural similarity to non-thermophilic P-type ATPases, it is possible that the structure is very stable and flexible. It would be very interesting to view these proteins at atomic resolution to identify the structure-stabilizing factors for comparison to the known structure of Ca^{2+}-ATPase, a mesophilic P-type ATPase.

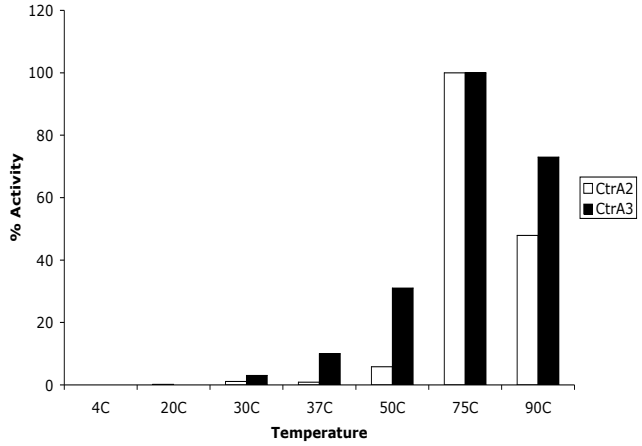

Figure 4.3 Comparison of activity of CtrA2 and CtrA3 at different temperatures. The representation is merged data from Figures 3.10 and 3.28.

4.2.4.4 Lipid dependency:

To analyze the lipid dependency of CtrA3 and CtrA2, *A. aeolicus* lipids, where the proteins naturally belong, *E. coli* lipids where the proteins were expressed and purified and soya PC, where copper pumps from other organisms were shown to be active (Mandal 2002) were tested. For CtrA3, in addition, the activity in DPPC was also tested since 2D crystals of this protein were obtained in this lipid.

CtrA3 was only active when lipids were added to the reaction mixture (Figure 3.12). It is not completely un-common that lipids are essential for the activity of membrane proteins in detergent environment (Villalba 1992; Lanfermeijer 1998). Even though all the lipids tested enhanced the activity of CtrA3 equally; the activity of the enzyme in total lipids from *Aquifex aeolicus* was only 75-80% of the maximum activity. It is an indication that CtrA3 is not optimally

active in its natural lipid environment. However, the protein was not active when purified in Cymal-6, also a maltoside detergent, even when lipids were added to the mixture One possible explanation for this behaviour might be that Cymal-6 binds the protein tightly and does not allow it to access the added lipids, that are required for activity. It is also possible that some how this detergent interacts with the protein in a way to inhibit its activity, probably by obstructing the ion-transporting path in the membrane region.

In contrast, CtrA2 showed no dependence on added lipids for activity (Figure 3.30). The protein was almost equally active in the presence of any lipid tested or in the absence of added lipid in the reaction mixture. It is likely that more lipids remain attached to this protein during purification that results in activity in the absence of additional lipids in reaction mixture. HPLC analysis of lipid extracted from purified protein samples might be helpful to identify the lipids that are bound to the protein during different stages of purification.

Most likely, both CtrA3 and CtrA2 need lipids for activity to stabilize the membrane spanning regions, especially considering the spatial distance between the predicted ion transport pathway in this region and ATP binding site.

4.2.4.5 Salt effect on ATP hydrolysis activity:

Even though CtrA3 was active in the absence of NaCl, addition of salt increased activity two fold. The enzyme saturated only at 1M NaCl (Figure 3.17). The enzyme is tolerant to high amounts of salt and this activity is probably an indicator of the extreme environments in which the bacteria thrives and the robustness of at least some of its proteins for survival in extreme conditions. However, there is no evidence that *A. aeolicus* actually lives in high NaCl conditions. Increasing the salt concentration further to 2M did not result in increased ATP hydrolysis, but also was slightly inhibitive.

CtrA2 was active in the absence of NaCl (Figure 3.31). Presence of 100-200mM NaCl in the reaction mixture increased the protein activity and further increase in salt concentration was inhibitory to the activity of protein. It is possible that CtrA2 and CtrA3 were tailored to be tolerant to different salt conditions.

4.2.4.6 Cysteine dependence:

Previous studies have indicated dependence of ATPase activity on the presence of thiolates and/ or reducing agents (Sharma et al. 2000; Mandal 2002). Both CtrA3 and CtrA2 need cysteine for activity. Both these pumps achieved maximum activity at a cysteine concentration of 20mM. However, higher amounts of cysteine had negative effect on the activity. There was some speculation about the role of cysteine in the activity of P_{IB} type ATPases (Sharma et al. 2000; Mitra et al. 2001) and it was proposed that dithiolate- or monothiolate-metal complex might be a substrate for these enzymes. However, this does not explain the requirement of cysteine in millimolar amounts (Mandal 2002). A recent report (Yang et al. 2006) shows that cysteine allosterically activates the copper pump and that the activation is independent of the metal ion. It is possible that cysteine has an effect on the rate of release of metal ion from the enzyme. Interestingly, cysteine dependence was not observed when CopB from *A. fulgidus* was activated by Cu^{2+} (Mana Capelli 2003). I do not have an immediate explanation of the differences in behaviour of CopB and CtrA3 regarding cysteine; which can be due to natural differences between these two enzymes. Since cysteine effect on P_{IB-3} type ATPases has been studied only in two cases; CtrA3 and CopB of A. fulgidus (Mana Capelli 2003), studies on more of this type of pumps might lead to some conclusion.

4.2.5 Reconstitution of lipids for crystallization:

Sucrose density gradient centrifugation (10-40%, 100,000xg) was done to check the compatibility of lipids for reconstituting proteins, after dialysis. At high

lipid-to-protein ratios (10:1 w/w), lipids always stay near the top of sucrose density (10-20%). If the protein successfully incorporates into the liposome during dialysis, it would still float on the gradient after centrifugation, because of high amount of lipid it contains. However, if the protein is not compatible to the lipid present in its environment, it aggregates during dialysis and goes down the gradient to pellet down during centrifugation. This method is easy, reliable and could be used as a first screen to select lipids for crystallization, as against freeze-fracture, that is more labor-intensive and time-consuming. It was successfully applied to select the lipid for crystallization of CtrA3 (Figure 3.20).

Of the lipids tested, CtrA3 was reconstituted best in DPPC, as observed by the sucrose-density centrifugation method. However, with other lipids, protein was detected even in the pellet of sucrose-density gradient after centrifugation, meaning that some protein still got aggregated even at high lipid-to-protein ratio. These lipids would not be very good candidates for 2D crystallization. This was actually the case, as CtrA3 reconstituted with DPPC at low LPR actually formed 2D crystals (see below).

Even though CtrA2 has 36% identity with CtrA3, it had different lipid compatibility. Reconstitution of this protein was best in DOPC. CtrA2 also had good reconstitution in *E. coli* polar lipids and DPPC, but there was some aggregation and degradation of protein in both cases (Figure 3.34).

Reconstitution of copper pumps in *A. aeolicus* lipids for crystallization was not successful. Aggregation and some degradation was observed when CtrA3 and CtrA2 were reconstituted at high LPR into these lipids. One possibility for the failure of the total lipid extract of *A. aeolicus* for crystallization might be because the lipid preparation has protein contamination. From analysis on SDS-PAGE, it was evident that most of the contaminant protein was C-ring monomer of F_0F_1ATPase.

4.2.6 2D Crystallization:

Crystals of CtrA3 were obtained only in the presence of NaCl in dialysis mixture, but the salt had to be removed prior to harvesting for well ordered crystals (Figure 3.22). Since this protein has a big cytoplasmic domain, it is possible that salt has a main role in bringing the protein molecules together. However, for close packing, the ionic interactions between the salt and cytoplasmic domain might have been detrimental. Removal of salt could effect the inter-molecular interactions and helped the crystals to re-arrange and pack together. CtrA3 was sloubilizeed in DDM and the lipid DPPC for crystallization was solubilized in OG. Since OG has a higher CMC, the rate of removal of this detergent from dialysis mixture is higher. DDM, in contrast, has very low CMC and is harder to remove from the dialysis mixture.

Crystalline order was destroyed when preservatives were tested for cryo-microscopy. It is possible that the big cytoplasmic domain plays a role here and addition of preservatives like tannin and trehalose have deleterious effect on protein arrangement and induce disruption of crystals. Trehalose was better, and in two out of 100 images taken, some spots could be seen. Glucose and non-traditional preservatives like glycerol need to be tested for better preservation of the crystal lattice.

4.2.7 Image processing:

When the images of uranyl acetate stained sample taken in FEI Technai G^2 EM, at a magnification of 42,000X captured by negative staining were processed by MRC image processing software (Crowther et al. 1996), a unit cell dimensions of *a*= 71.2, *b*=90.2, Υ=89.9 (average of three images) were obtained. However, when the images from cryo-microscopy were processed (Chintalapati et al. manuscript in preparation), the unit cell dimensions were different - *a*= 69.8,

b=80.9, ϒ=90 (average of 8 images). The larger unit cell for negatively stained images more likely reflects a variability of the unit cell in *b* direction.

4.2.8 3D Crystallization attempts:

3D crystallization of P-type ATPases has been successful only for sarcoplasmic Ca^{2+}-ATPase (Toyoshima 2000), where 3D crystals were actually stacks of 2D crystals and to some extent, *Neurospora crassa* proton pump (Scarborough 2000). Further refined screening of sarcoplasmic Ca^{2+}ATPase resulted in obtaining 3D crystals of this protein in detergent environment (Sorensen et al. 2006). 3D crystals of the *N. crassa* proton pump were reported in 2000, but the structure has not yet been solved. The 3D crystallization screens were prepared for CtrA3 using the conditions reported in (Sorensen et al. 2006) as a starting point.

Initial robotic screens using commercial crystal screens resulted in some leads; however, following these leads for setting up manual screens changing different parameters, including detergent environment of protein did not result in any crystals. One observation from the robotic screens was that CtrA3 purified in DDM was very stable and using commercial screens, the protein was still in solution in approximately 70% of the conditions. However, when the protein purified in Cymal-6 was used in these screens, a few promising conditions could be identified (Figure 3.24 and Table 3.3).

4.2.9 *A. aeolicus* lipids:

When the total lipid extract isolated from *A. aeolicus* was analyzed by TLC, at least two or three distinct lipid bands can be observed. On comparison of these lipids with standard phospholipids, it may be speculated as to what kind of phospholipids might make up the membrane of *A. aeolicus*. Most probably, PG is missing from these lipids, but the membrane environment seems to be mostly

PE and PS (Figure 3.18). However, these lipids also have some protein contamination (Figure 3.19). It is possible that the c-ring of *A. aeolicus* F_oF_1ATPase remained with the lipids after the extraction. It is known that this protein, being very hydrophobic, tolerates the lipid extraction protocol (Dr. Thomas Meier, personal communication).

4.3 Summary of characterization of copper ATPases

Both CtrA3 (CopB) and CtrA2 (CopA) are similar heavy metal transporting p-type ATPases from same organism, *A. aeolicus*. Even though there was 36% identity and approximately 57% similarity between these two proteins, they behaved completely differently in their expression levels (in *E. coli*), purification profiles, stability, activity, reconstitution into lipids and crystallization. This is a clear indication of diversity of membrane proteins and emphasizes the need to study at least one protein from each sub-group, before concluding the structure-function relationships of these proteins. The main difference between these two proteins in the transmembrane putative ion-transporting region is that CtrA3 has Cys-Pro-His (CPH) like CopB proteins, while CtrA2 has Cys-Pro-Cys (CPC) like CopA proteins.

CPH containing heavy metal transporters have been found only in prokaryotes. Activation of these enzymes by Cu^{2+} probably means that unlike in yeast and mammalian cells, where Cu^{2+} is first converted to Cu^{+} before being imported into the cells (Petris 2004), bacteria can import the divalent ion also. It has to be noted that energy dependent copper uptake by a specific copper transporter has not been directly demonstrated in prokaryotes till now and environmental copper is Cu^{2+} as Cu^{+} is not stable unless in a highly reducing environment.

It is also unlikely that CtrA2 (CopA) transports Cu^{+} into the cells. For this to happen, the mechanism of transfer of ion would be opposite to that postulated

for most copper ATPases, including human Menkes and Wilson ATPases (Voskoboinik et al. 1998; Voskoboinik et al. 2001), which also have CPC in the ion-transporting domain and transport Cu^{+}.

4.4 General remarks about membrane protein expression

It is not possible to generalize recombinant membrane protein expression. The host system reacts differently to each membrane protein, evident from differences in expression levels of two related proteins from same source (CtrA3 and CtrA2 from *A. aeolicus*, expressed in *E. coli*). Similarly the recombinant protein also reacts differently to different hosts (functional expression of AHA2 in *S. cerevisiae* and truncated expression in *P. pastoris*). Even though no expression of these two proteins was detected with out an N-terminus tag, addition of tags resulted in reasonably high amounts of expression and localization. Some parameters that might define expression of membrane proteins in a recombinant host are:

a. Codon Usage:

It is beneficial to test the codon usage of host organism to know if the cell would even attempt to produce the recombinant protein. To solve the problem of codon usage, rare-codon supplementing strains of host cells should be helpful, as has been observed in the case of CtrA2 and CtrA3. Another solution would be to modify the recombinant gene to change the rare codons to more used codons of host organism.

b. N-end rule:

Protein half-lives of only 2 minutes were reported in *E. coli* when the following amino acids were present at amino terminus Arg, Lys, Phe, Leu, Trp and Tyr (Tobias et al. 1991). It is worth attempting the expression with a tag at N-

terminus if these amino acids are present. Some times, formation of secondary structures by RNA (like hairpin loops) at translational initiation region also inhibits protein expression and targets the RNA for degradation by cell machinery. Addition of tags at N-terminus also might solve this problem. This step actually helped in increasing the expression of CtrA2 and CtrA3 many fold.

c. Toxicity:

If the expressed protein is functional at the conditions of growth of host organism and is toxic, very low or no expression can be expected. The cells might also die attempting the expression of this protein. If possible, a non-lethal mutant may be expressed; otherwise, host organism may be varied. Sometimes, complementation of host protein with recombinant protein using knockout or other means might solve the problem of toxicity. This was how AHA2 was expressed in a *S. cerevisiae* host (RS72) where the yeast proton pump was engineered to be silent when the expression of recombinant AHA2 was induced. However, in the case of copper pumps from *A. aeolicus*, the proteins were almost inactive at the growth temperature of host organism (*E. coli*) and so could be expressed to high amounts without having any effect on these cells. In fact, CtrA2 was mildly active at 37°C where *E. coli* cells were grown and hence, the expression levels were actually lower than CtrA3, which was completely inactive at this temperature.

4.5 Outlook

Cryo-electron microscopy of 2D crystals of CtrA3 would give an indication of the arrangement of transmembrane helices in this protein. This would lead to a better understanding of the differences in structural organization of heavy-metal ATPases and other P-type ATPases. Images of 2D crystals of CtrA3 can taken at tilted angles in a cryo-microscope and processed for building up a 3D model of this protein. 3 D crystallization of CtrA3 can be attempted by investigating the

purification and stability of the protein in detergents other than those carried out in this thesis. One possible way might be to delipidate the protein completely before crystallization and adding specific lipids in known quantities.

2D crystallization of CtrA2 may be attempted with a broader spectrum of lipids or mixtures of lipids. A two-dimensional projection map of CtrA2 might provide interesting details of helical arrangement of this protein for comparison with CtrA3 and other P-type ATPases. For 3D crystallization, more screening of the protein in different detergents may be attempted.

For both CtrA2 and CtrA3, high-resolution 3D structure should be the ultimate aim, as this would give much needed insight into the ion transport pathway and coupling of ion transport and ATP hydrolysis.

Since high amounts of these two proteins can be produced, more biochemical characterization would facilitate better understanding of the function of these pumps. Transport analysis of CtrA2 using radioactive Cu^{+} and Cu^{2+} should give evidence of ion transported and possibly the direction in which they are transported. Various mutants can be expressed and analyzed for their crystallization ability and activity.

ZUSAMMENFASSUNG

Membranproteine führen eine Vielfalt von Funktionen aus, zu welchen unter anderem der Transport von Molekülen über die Membran gehört, entweder zum Erhalt des Gleichgewichts von löslichen Stoffen, oder um diese gegen einen Konzentrationsgradienten als Nahrungsmittelquelle für die Zelle zu importieren. Es existieren zwei Typen von Proteinen, um Ionen über die Membran zu transportieren, Ionenkanäle und Ionenpumpen. Ionenpumpen transportieren Ionen gegen ihren elektrochemischen Gradienten entweder durch Co-Transport eines anderen Ions oder durch Prozessierung einer Energiequelle wie z.B. ATP (Adenosintriphosphat). Diejenigen, welche ATP Hydrolyse mit einem Ionentransport koppeln sind die sogenannten „Ionen bewegenden ATPasen“. Mindestens drei verschiedene Klassen von ATPasen können in verschiedenen biologischen Membranen gefunden werden, die ‚V’-Typ, die ‚F’-Typ und die ‚P’-Typ ATPasen.

Die Superfamilie der P-Typ ATPasen stellt eine grosse und ubiquitäre Gruppe von Membranproteinen dar, welche eine Rolle bei dem Transport von geladenen Substraten über biologische Membranen spielen. Alle P-Typ ATPasen teilen sich die Gemeinsamkeiten eines konservierten Aspartat-Restes, der während des Reaktionszyklus phosphoryliert wird, eines konservierten Prolin-Restes, der innerhalb des Ionentranslokationsweges in der Membran liegt und Konsensus-Domänen für die ATP Bindung und den Energie-Transfer. Die P-Typ ATPase-Superfamilie hat fünf Zweige, P_I bis P_V, die sich durch ihre Substrat-Spezifitäten unterscheiden. Innerhalb dieser Zweige können verschiedene Sub-Typen unterschieden werden.

In dieser Arbeit wurden zwei Sub-Klassen von P-Typ ATPasen untersucht, P_{IIIA} und P_{IB}. Versuche zur Überexpression und Kristallisation der Protonen Pumpe AHA2 aus Pflanzen (P_{IIIA}-ATPase) wurden durchgeführt. Zusätzlich wurden die zwei vermeintlich Kupfer-transportierenden ATPasen CtrA3 und

CtrA2 aus *Aquifex aeolicus* (beides P_{IB} Pumpen, die ähnlich zu CopA und CopB aus *Archaeoglobus fulgidus* stammen) in *Escherichia coli* überexprimiert und charakterisiert.

P_{IIIA}-Typ Pumpen wurden exklusiv in Pflanzen und Pilzen, wahrscheinlich auch in Archaea gefunden und transportieren Protonen über die Membran. Eine der biochemisch am besten charakterisierten Protonenpumpen dieses Types ist AHA2 aus *Arabidopsis thaliana*. Eine Projektionskarte bei 8 Å Auflösung dieses Enzyms zeigt bemerkenswerte Ähnlichkeit mit der Ca^{2+}-ATPase, für welche eine 3D Struktur bei 2.6 Å Auflösung bekannt ist. P_{IB}-ATPasen, auch CPX-Typ Pumpen genannt, transportieren Schwermetall-Ionen wie z.B. Cu^{+}, Cu^{2+}, Zn^{2+}, Pb^{2+}, Cd^{2+} und Co^{2+} über biologische Membranen und spielen eine wichtige Rolle bei der Homöostase und Biotoleranz dieser Ionen. Mutationen in den zwei nahe verwandten menschlichen Proteinen ATP7A und ATP7B, welche Kupferionen über die Membran transportieren, verursachen die tödlichen Menkes- und Wilson-Krankheiten. Homologe von diesen Proteinen wurden in vielen Organismen gefunden, unter anderen in Bakterien und Archaea. CopA und CopB sind zwei Proteine dieses Typs, die Kupferionen über die Zellmembran transportieren. CopB-ähnliche Proteine können fast ausschließlich in Bakterien gefunden werden, mit einem CPH-Motiv, während CopA-ähnliche Proteine ein CPC-Motiv haben und auch in eukaryontischen Kupferionen-Transportern gefunden werden, inklusive dem menschlichen ATP7A und ATP7B. Für CopB wurde vorgeschlagen, dass es Cu^{2+} über die Membran transportiert und experimentell konnte der Export von diesen Ionen gezeigt werden. CopA wird aktiviert und transportiert Cu^{+}, aber der Export dieses Ions konnte bisher noch nicht direkt gezeigt werden. Trotzdem deutet indirekte Evidenz darauf hin, dass dieses Protein beim Import von Cu^{+} in prokaryontische Zellen involviert sein könnte.

1. AHA2:

Es wurden Versuche zur Überexpression der pflanzlichen Protonenpumpe AHA2 in der Hefe *Pichia pastoris* unternommen. Nur eine abgeschnittene Version von AHA2 wurde in diesem Wirt exprimiert und konnte deshalb nicht für weitere Studien gebraucht werden. *P. pastoris* Stämme scheinen kein geeigneter Wirt für die Expression von AHA2 zu sein.

Der Fokus dieser Arbeit wurde dann auf AHA2 verschoben, welches im *Saccharomyces cerevisiae* Stamm RS72 exprimiert und gereinigt wurde. Die Expression der Protonenpumpe PMA1 im Wirt wurde unter die Regulation eines Galaktose-Promotors gesetzt und die pflanzliche Protonenpumpe AHA2 wurde via eines *pma1*-Promotor enthaltenden Plasmids eingeführt. Die Wachstums- und Reinigungsprotokolle mussten aufgrund von Laborbeschränkungen von der publizierten Methode abgwandelt werden, was vermutlich einen Effekt auf das produzierte Protein hat. Das gereinigte Protein aus *S. cerevisiae* konnte nicht für strukturelle Untersuchungen mit Elektronenmikroskopie reproduzierbar in 2D kristallisiert werden.

2. CtrA3:

Das Gen, welches für die Expression von ctrA3 aus *A. aeolicus* zuständig ist, wurde aus genomischer DNA mit Hilfe von PCR amplifiziert und in verschiedene Expressionsvektoren zur Expression in *E. coli* kloniert. Es konnte keine Expression in den Klonen untersucht werden, bei denen kein tag am N-terminus vorhanden war. Die beste Expression konnte im *E. coli* Stamm RP-Codon Plus erreicht werden, im Plasmid pET28A, mit His- und T7 tags am N-terminus von CtrA3. Die transformierten Zellen brauchten keine Induktion; Wachstum der Zellen über Nacht bei 37°C war ausreichend für die Proteinexpression. Ungefähr 1.2 bis 1.5 mg/ml reines Protein konnten aus 1 L einer über Nacht angewachsenen Kultur gewonnen werden.

Das exprimierte Protein wurde anhand einer Ni^{2+}-NTA Matrix gereinigt, unter Ausnutzung des His-tags, welcher auf dem rekombinanten Protein präsent war. CtrA3 wurde in n-Dodecyl-β-D-maltosid solubilisiert und gereinigt. Das Protein konnte auch in Gegenwart von anderen Detergenzien gereinigt werden, wie z.B. Cymal-6 und n-Octyl-β-D-glucopyranosid. Das in Octyl-β-D-glucopyranosid gereinigte CtrA3 war dennoch keine 24 Stunden stabil. Das in Cymal-6 gereinigte Protein war zwar stabil, mit Hilfe von Gelfiltration konnte aber festgestellt werden, dass es nicht so monodispers ist, wie das in n-Dodecyl- β-D-maltosid gereinigte CtrA3.

CtrA3 wurde auf seine Hydrolyse-Aktivität hin getestet. Ähnlich wie CopB war es nur in der Gegenwart von Cu^{2+} aktiv und zu einem Teil auch in der Gegenwart von Ag^{+}. Nur oberhalb einer Temperatur von 50°C war CtrA3 aktiv. Die maximale Aktivität von CtrA3 konnte bei 75°C, bei pH 7.0 und mit Cystein gemessen werden. Für die Aktivität von CtrA3 waren Lipide entscheidend; es konnte keine ATP Hydrolyse ohne diese detektiert werden. Das Protein war vollständig aktiv, als L-α-Phosphatidyl-cholin aus Sojabohnen zur Reaktion zugegeben wurde. Trotzdem konnte CtrA3 kein ATP hydrolysieren nachdem das Protein in Cymal-6 gereinigt wurde, nicht einmal bei Zugabe von Lipiden zur Reaktionslösung. Obwohl CtrA3 in Abwesenheit von Salz aktiv war, konnte die maximale Aktivierung des Enzyms bei 400 mM NaCl erreicht werden.

Mehrere Lipide wurde zur Rekonstitution von CtrA3 in Liposomen für die 2D Kristallisation getestet. Um die Lipid-Kompatibilität bezüglich der Protein Inkorporation zu überprüfen, wurde CtrA3 mit verschiedenen Lipiden mit einem hohen Lipid-zu-Protein Verhältnis von 10:1 und mit anschliessender Zentrifugation auf einem Zucker-Dichtegradienten dialysiert. Im Gradienten konnten die in die Lipide inkorporierten Proteine in der Liposomenfraktion gefunden werden. Ein Grossteil von CtrA3 wurde in 1,2-Dipalmitoyl-sn-glycero-3-phosphocholine ohne irgendwelche Aggregation inkorporiert. Dieses Lipid wurde dann auch für die Rekonstitution von CtrA3 bei einem tiefen Lipid-Protein

Verhältnis gebraucht, und bei einem Lipid-Protein Verhältnis von 0.3 bis 0.5 konnte ein 2D-kristallines Gitter untersucht werden. Zur Ausbildung von Kristallen war NaCl unerlässlich, aber die am besten geordneten Kristalle konnten gefunden werden, als das Salz vor dem Sammeln durch Dialyse entfernt wurde.

Die Zugabe von Schutzmitteln wie Trehalose und Tannin, oder das direkte Eintauchen der Kristalle in flüssiges Ethan war nachteilig für das Kristallgitter. Nicht-herkömmliche Schutzmittel wie Glycerin könnten deshalb zu einem besseren Gefrierschutz getestet werden.

Das in Cymal-6 gereinigte CtrA3 wurde für das 3D Kristallisations-screening verwendet. Dennoch konnten bisher keine 3D Kristalle gefunden werden, einige vielversprechende Bedingungen, bei denen Mikro-Nadeln und Spherulite gesichtet wurden, konnten allerdings identifiziert werden. Versuche zur Optimierung dieser Screens resultierten in keiner Verbesserung der 3D Kristalle. Das in n-Dodecyl-β-D-maltosid gereinigte CtrA3 war nicht optimal für 3D Kristallisation, da ein grosser Anteil des Proteins auch bei einer hohen Konzentration von 15 mg/ml in den kommerziellen 3D Kristallisations-screens immer noch komplett gelöst war.

3. CtrA2:

Ähnlich wie bei ctrA3 wurde das Gen ctrA2 aus der genomischen DNA von *A. aeolicus* amplifiziert und in *E. coli* exprimiert. CtrA2 wurde ebenfalls nicht exprimiert ohne einen zusätzlichen N-terminalen tag. Die beste Expression konnte mit T7- und His-tags am N-Terminus, im *E. coli* Stamm RP-Codon Plus mit dem Plasmid pET28A erhalten werden. Das exprimierte Protein wurde in Anwesenheit von n-Dodecyl-β-D-maltosid solubilisiert und gereinigt. Es war nur zusammen mit Glycerin in der Detergens-Lösung stabil. Das Protein war nicht sehr homogen als es durch eine Superdex-200 Gelfiltrationssäule gereinigt

wurde. Weder die Reinheit noch die Homogenität konnte verbessert werden, als CtrA2 mit Cymal-6 gereinigt wurde.

Die funktionelle Charakterisierung von CtrA2 wurde anhand der ATP Hydrolyse Aktivität untersucht. Ähnlich wie bei dem *A. fulgidus*-homologen CopA wurde CtrA2 durch Ag^{+} aktiviert. Es konnte nur eine minimale ATP Hydrolyse Aktivität in der Anwesenheit von Cu^{2+} festgestellt werden. Cystein war unbedingt notwendig für die Aktivität von CtrA2. Die maximale Aktivierung dieses Enzyms konnte bei pH 7.5 gemessen werden. Maximale Aktivität von CtrA2 wurde bei einer NaCl Konzentration von 400 mM gefunden, ähnlich wie bei CtrA3.

Es ist möglich, dass beide Kupfer-ATPasen von *A. aeolicus* eine unterschiedliche Ionenspezifität haben, CtrA3 spezifisch für Cu^{2+} und CtrA2 spezifisch für Cu^{+}. Die maximale Aktivierung von CtrA2 wurde auch bei 75°C untersucht, aber dieses Enzym zeigte einen breiteren Temperaturbereich für die Aktivität als CtrA3; im Unterschied zu CtrA3, bei welchem erst bei über 50°C Aktivität gemessen werden konnte, war CtrA2 schon oberhalb von 30°C aktiv. Dieses Protein zeigte weder eine Abhängigkeit der Aktivität durch die Zugabe von Lipid zur Probe. Noch hatte die Zugabe von verschiedenen Lipiden irgendeinen Effekt auf die Aktivität.

Die Rekonstitution von CtrA2 wurde ähnlich wie bei CtrA3 durch das Testen verschiedener Lipide für die 2D Kristallisation durchgeführt. Bei einem hohen Lipid-Protein Verhältnis rekonstituierte CtrA2 am besten in 1,2-Dioleoyl-sn-Glycero-3-Phosphocholin. Das Testen eines tiefen Lipid-Protein Verhältnisses und das Wechseln der Bedingungen wie die Temperatur, der pH und die Pufferkomponenten ergaben keine Kristalle.

Obwohl beide, CtrA3 und CtrA2, ähnliche Schwermetall-transportierende P-Typ ATPasen vom gleichen Organismus sind und 36% Identität teilen, verhalten sie sich komplett unterschiedlich bezüglich ihres Expressions-Grades

in *E. coli*, ihres Reinigungsprofils, ihrer Aktivität und bezüglich ihrer Rekonstitution in Lipiden. Es konnten 2D Kristalle von CtrA3 erzielt werden.

In der Zukunft sollte die Elektron Kryo-Mikroskopie von CtrA3 weitere Einsichten in die Anordnung der Helices dieses Proteins geben; bisher gibt es keine einzige Schwermetall-transportierende P-Typ ATPase, bei der es Belege über die helikale Anordnung der Helices gibt. Zur Konstruktion eines 3-dimensionalen Modells dieses Proteins müssen mit Kippwinkel-Bilder erstellt und prozessiert werden. Nach der Untersuchung der Reinigung und Stabilität des Proteins in anderen Detergenzien kann 3D-Kristallisation versucht werden. Bei CtrA2 könnte die Analyse einer breiteren Anzahl von Lipiden oder Mixturen von Lipiden helfen, das Protein in 2D zu kristallisieren.

APPENDIX

A.1 Protein Sequences of ctrA3 and ctrA2

A.1.1CtrA3:

MHEHHDKHKHELKRKSEKHEHAHHAEIIKRKALITTILTVPVVVLSPSIQELIGIKV
SFPYSNWVILLLSTAVFIYGGTFFLKGMLEELKKKNPGMMTLVGLAISVAYIYSVY
TFFFGGKEFFWELTTLIVVMLWGHYVEMKSVLGAGRALEELVKLIPSKAHLVTQ
KGLIDVPVEKLKKGDLVLVRPGEKIPTDGTVVEGNTHVDESMLTGESRPVPKKP
GDKVIGGSVNLEGSIKVRVEKTGEETYLKQVIKLVKEAQESKTKLQSLADRAAFY
LTVIAVSLGSISLLFWWYYLGDLNFAVERAVTVMVTACPHALGLAIPLVVSISTSY
SARNGILVRNRLALEKAKDIDVVVFDKTGTLTEGKLGVTEVITKDIEEGEFLKFVA
SVENHSEHVIARAIVSYAKEKEEVKNFKAFPGKGVCGEVSGRNVCVGTLEFLKE
INVKLDEELVERARSLQSEGKTVVFASMDGKLAGIIALADRIKEESYEAVRSLKEL
GKKVVMITGDSEEVAKYVAKELEMDEYFARVLPHEKAQKIKELQDRGYSVAMV
GDGVNDAPALIQADVGIAIGSGTDIAIESADVILVKSDPRDVVKVIKLSQVTVSKM
LQNLFWAVGYNVITLPLATGLGYPWGFVLKPAVGAIFMSASTVIVALNSMLMKK
ELR

A.1.2 CtrA2:

MRKAFKVYGMSCVNCARAIEITLKRTEGVKNVNVSFELGRVEVEFDEDLISEEEI
VKKIEELGYSVERKKDYDKLFLGLGVLSSLFFLVGMFFTFPLKYELQFLLSSIVQF
TAGWKFYRGAYSSLKKGIGSMDTLVALGTTGAYVYSVLSYFNLINSTPFFETNV
FLITFVRLGKFIEEKAKERAVKGLKELVNLSFRKVKVLEGEKEVEKNVREVFKGE
KVVYRSGEQILLDGVIIKGEGLVNEAVITGEPVPILKKEGDEVYSGSVLEKGYIITK
VTKTFESSFINTMKKLVEESLKEKPKIQRISDKVSHYFVLFVVILSVITFLTWFIKT
GEINRAVQFSLAVLVVSCPCAFGIAVPLAVSVGIYKAVKRGILPKKGTIFEVAPKV
DTVIFDKTGTLTEGKLKVKEINVPEKYFDVLYSMENYSNHPVAKAVREYLKPYVK
REAKLEGCEEILGVGVRCGEFIAGKAELWGKNSQNGVIRVGFGTKDKLIGEIILE
DSVRKEAKEVVEFLKGKGINVILLTGDTKENAQRIAKELGIKEVIANVKPEEKLKV
VKELQEKGRKVCMVGDGVNDAPALAQSDLGIAVAEGTDLAKLSGDVVIHKLSSL
PQVFTLSERVYRKIKENFFWAFAYNVTFIPIAAGVLWSKGIYLKPEFAGLLMALS
SVSVVLNTLRLLKD

A.2 Vector Maps

A.2.1 pET28A (from Novagen manual):

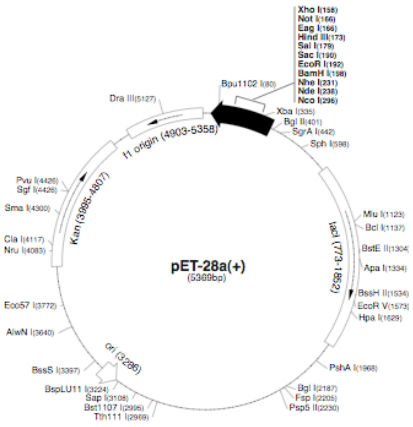

A.2.2 pASK-IBA (from IBA vector manual):

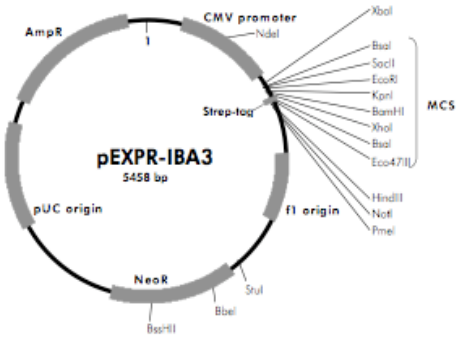

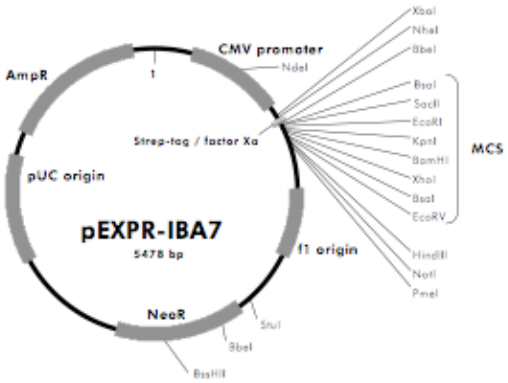

A.2.3 pPIC3.5K (from Invitrogen manual):

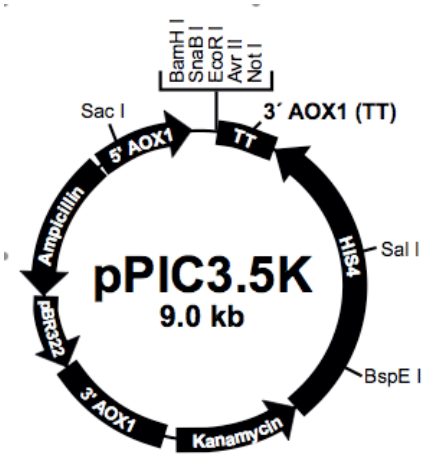

A.2.4 pMP649 (from Department of Plant Biology, Royal Veterinary and Agricultural University, Copenhagen, Denmark):

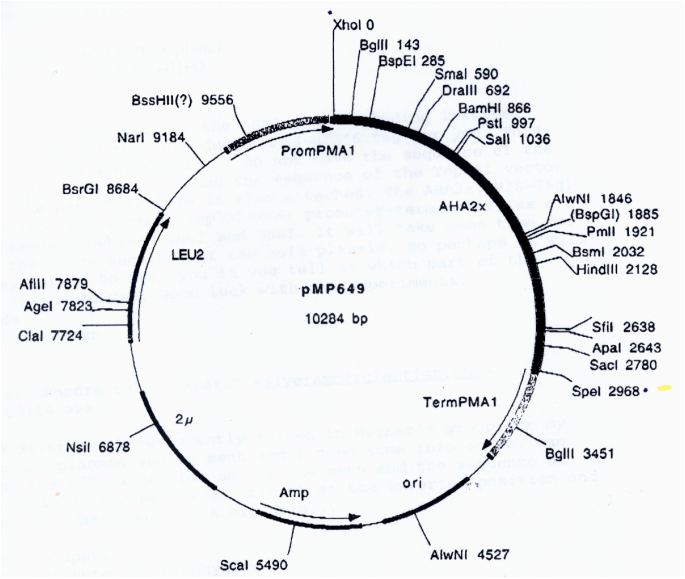

A.3 Recipes of growth media

A.3.1 LB:

1% Tryptone

0.5% Yeast Extract

1% NaCl

1.5% Agar for plates

A.3.2 SGAH Plates:

50mM Succinic acid pH5.5

0.003% Histidine

0.003% Adenine

0.7% YNB without amino acids

2% Galactose

A.3.3 YPD:

1% Yeast Extract

2% Peptone

2% Dextrose

2% Agar for plates

G418 (for selection: 0.25- 1mg/ml)

A.3.4 RDB:

1M Sorbitol

2% Dextrose

1.34% YNB without amino acids

4 X 10^{-5}% Biotin

0.005% amino acids (L-glutamic acid, L-methionine, L-lysine, L-leucine, L-isoleucine)

2% Agar for plates

A.3.5 SOC:

2% Tryptone

0.5% Yeast Extract

10mM NaCl

2.5mM KCl

20mM Mg^{2+} (10mM $MgCl_2.6H_20$, 10mM $MgSO_4.7H_20$)

20mM Glucose

pH 7.0

A.3.6 YPAG:

1% Yeast Extract

2% Peptone

0.003% Adenine

2% Galactose

A.3.7 MGY/MM:

1.34% YNB

1% Glycerol (for MGY) OR 0.5% Methanol (MM)

4 X 10^{-5}% Biotin

A.4 Abbreviations

Abs_{600nm}	Absorbance at 600nm in spectrophotometer
AHT	Anhydrotetracycline
APS	Ammonium persulfate
ATP	Adenosine triphosphate
BN	Blue Native
BPB	Bromophenolblue
BSA	Bovine Serum Albumin
$C_{12}E_8$	Polyoxyethylene (8) dodecyl ether
CBB	Coomassie Brilliant Blue
CCD	Charged Couple Device
CD	Circular dichroism
CMC	Critical Micelle Concentration
Cryo-EM	Cryo Electron microscopy
Cymal 6	n-Cyclohexyl-1-hexyl-b-D-maltoside
DDM	n-Dodecyl-b-D-maltoside
DM	n-Decyl-b-D-maltoside
DMPC	1,2-Dimyristoyl-sn-Glycero-3-Phosphocholine
DMSO	Dimethyl Sulfoxide
DNA	Deoxy Ribo Nucleic Acid
dNTPs	deoxy ribo nucleic acid triPhosphates
DOPC	1,2-Dioleoyl-sn-Glycero-3-Phosphocholine
DPPC	1,2-Dipalmitoyl-sn-glycero-3-phosphocholine
DPPE	1,2-Dipalmitoyl-sn-glycero-3-phosphoethanolamine
DPPG	1,2-Dipalmitoyl-sn-glycero-3-phosphoglycerol
DPPS	1,2-Dipalmitoyl-sn-glycero-3-phosphoserine
DTT	Dithiothreitol
EDTA	Ethylenedinitrilotetraacetic acid
EM	Electron microscopy
ER	Endoplasmic reticulum

GPCR	G-protein coupled receptor
GTED20	Glycerol 20%-Tris-EDTA-DTT buffer
HIC	Hydrophobic interaction chromatography
IPTG	Isopropyl-b-D-thiogalactopyranoside
IRES	Internal ribosomal entry site
LB	Luria-Bertani medium
LDAO	n-Dodecyl-N,N-dimethylamine-N-oxide
LPR	Lipid to protein ratio
MBD	Metal binding domain
Mega 8	Octanoyl-N-methylglucamide
Mes	4-Morpholineethanesulfonic acid
MGY	Minimal glycerol medium
MM	Minimal methanol medium
$MRGSH_6$ tag	Methionine-Arginine-glycine-Serine-Histidine (6 times)
Ni^{2+}NTA	Nickel chelated NitriloTriAcetic acid
NMR	Nulear magnetic resonance
OG	n-Octyl-b-D-glucopyranoside
PC	Phosphatidyl choline
PCR	Polymerase Chain Reaction
PDB	Protein Data Bank
PE	Phosphatidylethanolamine
PEG	Polyethylene glycol
PG	Phosphatidylglycerol
PLPC	1-Palmitoyl-2-linoleyl phosphatidylcholine
PM	Plasma membrane
PMSF	Phenylmethanesulfonyl fluoride
PVDF	Polyvinylidene fluoride
RDB	Regeneration dextrose base medium
RNA	Ribonucleic acid
SDS	Sodium dodecyl sulfate
SDS-PAGE	Sodium dodecyl sulfate-Polyacrylamide gel electrophoesis

SFV	Semiliki forest virus
SGAH	Succinate-galactose-adenine-histidine medium
SOC	Super optimal broth with catabolite repressor (glucose) medium
Soya PC	L-α-Phosphotidyl-choline from Soybean
TAE	Tris-Acetate-Ethylene Diamino Tetra Acetic Acid
TBS	Tris Buffered Saline
TBS-T	Tris buffered saline with Tween20
TEMED	N,N,N',N'-Tetramethylethyenediamine
TLC	Thin Layer Chromatography
TM	Transmembrane
Tris	Tris -(hydroxymethyl-aminomethan)
UV	Ultraviolet
w/w	weight/weight
YNB*	Yeast nitrogen Base with Ammonium sulfate and without amino acids
YPAG	Yeast extract-Peptone-Adenine-Galactose medium
YPD	Yeast extract-Peptone-Dextrose medium

BIBLIOGRAPHY

Albers, R. (1967) Biochemical aspects of active transport. *Annu Rev Biochem*, **36**, 727-756.

Alberts B, A.J., Julian Lewis, Martin Raff, Kleith Roberts, Peter Walter. (2002) Membrane Transport of Small Molecules and the Electrical Properties of Membranes. *The Molecular Biology of Cell*.

Altendorf, K., Gassel, M., Puppe, W., Mollenkamp, T., Zeeck, A., Boddien, C., Fendler, K., Bamberg, E. and Drose, S. (1998) Structure and function of the Kdp-ATPase of Escherichia coli. *Acta Physiol Scand Suppl*, **643**, 137-146.

Anderson, J.A., Nakamura, R.L. and Gaber, R.F. (1994) Heterologous expression of K+ channels in Saccharomyces cerevisiae: strategies for molecular analysis of structure and function. *Symp Soc Exp Biol*, **48**, 85-97.

Arguello, J.M. (2003) Identification of Ion-Selectivity Determinants in Heavy-Metal Transport P1B-type ATPases. *Journal of Membrane Biology*, **195**, 93-108.

Arguello, J.M., Mandal, A.K. and Mana-Capelli, S. (2003) Heavy metal transport CPx-ATPases from the thermophile Archaeoglobus fulgidus. *Ann N Y Acad Sci*, **986**, 212-218.

Auer M, S.G., Kuhlbrandt W. (1998) Three dimensional map of the plasma membrane H+ATPase in the open conformation. *Nature*, **392**, 840-843.

Axelsen, K.B. and Palmgren, M.G. (1998) Evolution of substrate specificities in the P-type ATPase superfamily. *J Mol Evol*, **46**, 84-101.

Balamurugan, K. and Schaffner, W. (2006) Copper homeostasis in eukaryotes: Teetering on a tightrope. *Biochim Biophys Acta*.

Bannwarth, M. and Schulz, G.E. (2003) The expression of outer membrane proteins for crystallization. *Biochim Biophys Acta*, **1610**, 37-45.

Begenisich, T. (1994) Permeation properties of cloned K+ channels. In Peracchia, C. (ed.), *Hand Book of Membrane Channels: Molecular and cellular physiology*. Academic Press, pp. 17-28.

Bill, R.M. (2001) Yeast--a panacea for the structure-function analysis of membrane proteins? *Curr Genet*, **40**, 157-171.

Bin Fan, B.P.R. (2002) Biochemical characterization of copA, the E. coli Cu(I) translocating P-type ATPase. *Journal of Biological Chemistry*, **277**, 46987-46992.

Bissig, K.D., Wunderli-Ye, H., Duda, P.W. and Solioz, M. (2001) Structure-function analysis of purified Enterococcus hirae CopB copper ATPase: effect of Menkes/Wilson disease mutation homologues. *Biochem J*, **357**, 217-223.

Blaauw, M., Dekker, N., Verheij, H.M., Kalk, K.H. and Dijkstra, B.W. (1995) Crystallization and preliminary X-ray analysis of outer membrane phospholipase A from Escherichia coli. *FEBS Lett*, **373**, 10-12.

Brierley, R.A. (1998) Secretion of recombinant human insulin-like growth factor I (IGF-I). *Methods Mol Biol*, **103**, 149-177.

Buch-Pederson M, P.M. (2003) Conserved Asp684 in transmembrane segment M6 of plant plasma membrane p-type proton pump AHA2 is a molecular determinant of proton translocation. *Journal of Biological Chemistry*, **278**, 17845-17851.

Bull, P.C. and Cox, D.W. (1994) Wilson disease and Menkes disease: new handles on heavy-metal transport. *Trends Genet*, **10**, 246-252.

Caffrey, M. (2003) Membrane protein crystallization. *J Struct Biol*, **142**, 108-132.

Cai, J. and Gros, P. (2003) Overexpression, purification, and functional characterization of ATP-binding cassette transporters in the yeast, Pichia pastoris. *Biochim Biophys Acta*, **1610**, 63-76.

Cereghino, J.L. and Cregg, J.M. (2000) Heterologous protein expression in the methylotrophic yeast Pichia pastoris. *FEMS Microbiol Rev*, **24**, 45-66.

Christodoulou, J., Danks, D.M., Sarkar, B., Baerlocher, K.E., Casey, R., Horn, N., Tumer, Z. and Clarke, J.T. (1998) Early treatment of Menkes disease with parenteral copper-histidine: long-term follow-up of four treated patients. *Am J Med Genet*, **76**, 154-164.

Cid, A., Perona, R. and Serrano, R. (1987) Replacement of the promoter of the yeast plasma membrane ATPase gene by a galactose-dependent promoter and its physiological consequences. *Curr Genet*, **12**, 105-110.

Cobine, P., Wickramasinghe, W.A., Harrison, M.D., Weber, T., Solioz, M. and Dameron, C.T. (1999) The Enterococcus hirae copper chaperone CopZ delivers copper(I) to the CopY repressor. *FEBS Lett*, **445**, 27-30.

Collinson, I., Breyton, C., Duong, F., Tziatzios, C., Schubert, D., Or, E., Rapoport, T. and Kuhlbrandt, W. (2001) Projection structure and oligomeric properties of a bacterial core protein translocase. *Embo J*, **20**, 2462-2471.

Crowther, R.A., Henderson, R. and Smith, J.M. (1996) MRC image processing programs. *J Struct Biol*, **116**, 9-16.

Daleke, D.L. (2003) Regulation of transbilayer plasma membrane phospholipid asymmetry. *J Lipid Res*, **44**, 233-242.

Dekker, N., Merck, K., Tommassen, J. and Verheij, H.M. (1995) In vitro folding of Escherichia coli outer-membrane phospholipase A. *Eur J Biochem*, **232**, 214-219.

Depalo, N., Catucci, L., Mallardi, A., Corcelli, A. and Agostiano, A. (2004) Enrichment of cardiolipin content throughout the purification procedure of photosystem II. *Bioelectrochemistry*, **63**, 103-106.

DiDonato, M. and Sarkar, B. (1997) Copper transport and its alterations in Menkes and Wilson diseases. *Biochim Biophys Acta*, **1360**, 3-16.

Dubendorff, J.W. and Studier, F.W. (1991) Controlling basal expression in an inducible T7 expression system by blocking the target T7 promoter with lac repressor. *J Mol Biol*, **219**, 45-59.

Dufour, J.P., Boutry, M. and Goffeau, A. (1980) Plasma membrane ATPase of yeast. Comparative inhibition studies of the purified and membrane-bound enzymes. *J Biol Chem*, **255**, 5735-5741.

Dutzler, R., Campbell, E.B. and MacKinnon, R. (2003) Gating the selectivity filter in ClC chloride channels. *Science*, **300**, 108-112.

Eraso, P., Cid, A. and Serrano, R. (1987) Tight control of the amount of yeast plasma membrane ATPase during changes in growth conditions and gene dosage. *FEBS Lett*, **224**, 193-197.

Etana Padan, C.H., Hellut Reilander. (2003) Production and purification of recombinant membrane proteins. In Carola Hunte, G.v.J., Hermann Schaegger (ed.), *Membrane Protein purification and crystallization: A practical guide*. Academic Press, pp. 55-83.

Flachmann, R. (1999) Overexpression of eukaryotic membrane proteins in transgenic tobacco: pioneering the 'green expression system' with the purification and crystallization of recombinant light-harvesting complex II. *Biochem Soc Trans*, **27**, 923-927.

Francis, M.S. and Thomas, C.J. (1997) The Listeria monocytogenes gene ctpA encodes a putative P-type ATPase involved in copper transport. *Mol Gen Genet*, **253**, 484-491.

Francis, M.S. and Thomas, C.J. (1997) Mutants in the CtpA copper transporting P-type ATPase reduce virulence of Listeria monocytogenes. *Microb Pathog*, **22**, 67-78.

Frank, J. (2002) Single particle imaging of macromolecules by cryo-electron microscopy. *Annual Review of Biophysics and Biomolecular Structure*, **31**, 303-319.

Fraser, M.J. (1992) The baculovirus-infected insect cell as a eukaryotic gene expression system. *Curr Top Microbiol Immunol*, **158**, 131-172.

Gerard Deckert, P.V.W., Terry Gaasterland, william G. Young, Anna L. Lenox, David E. Graham, Ross Overbeek, Majory A. Snead, Martin Keller, Monette Aujay, Robert Huber, Robert A. Feldman, Jay M. Short, Gary J. Olsen, Ronald V. Swanson. (1998) The Complete genome of the hyperthermophilic bacterium Aquifex aeolicus. *Nature*, **392**, 353-358.

Goffeau, A., Barrell, B.G., Bussey, H., Davis, R.W., Dujon, B., Feldmann, H., Galibert, F., Hoheisel, J.D., Jacq, C., Johnston, M., Louis, E.J., Mewes, H.W., Murakami, Y., Philippsen, P., Tettelin, H. and Oliver, S.G. (1996) Life with 6000 genes. *Science*, **274**, 546, 563-547.

Gonen, T., Cheng, Y., Sliz, P., Hiroaki, Y., Fujiyoshi, Y., Harrison, S.C. and Walz, T. (2005) Lipid-protein interactions in double-layered two-dimensional AQP0 crystals. *Nature*, **438**, 633-638.

Gouaux, E. and Mackinnon, R. (2005) Principles of selective ion transport in channels and pumps. *Science*, **310**, 1461-1465.

Grisshammer, R. and Tate, C.G. (1995) Overexpression of integral membrane proteins for structural studies. *Q Rev Biophys*, **28**, 315-422.

Grossman, T.H., Kawasaki, E.S., Punreddy, S.R. and Osburne, M.S. (1998) Spontaneous cAMP-dependent derepression of gene expression in stationary phase plays a role in recombinant expression instability. *Gene*, **209**, 95-103.

Hanai, T., Haydon, D.A. and Taylor, J. (1965) Some Further Experiments on Bimolecular Lipid Membranes. *J Gen Physiol*, **48**, SUPPL:59-63.

Harris, E.D. (2003) Basic and Clinical Aspects of Copper. *Critical Reviews in Clinical Laboratory Sciences*, **40**, 547-586.

Harris, E.D., Qian, Y., Tiffany-Castiglioni, E., Lacy, A.R. and Reddy, M.C. (1998) Functional analysis of copper homeostasis in cell culture models: a new perspective on internal copper transport. *Am J Clin Nutr*, **67**, 988S-995S.

Hatefi, Y. (1985) The mitochondrial electron transport and oxidative phosphorylation system. *Annu Rev Biochem*, **54**, 1015-1069.

Hebert, H., Purhonen, P., Vorum, H., Thomsen, K. and Maunsbach, A.B. (2001) Three-dimensional structure of renal Na,K-ATPase from cryo-electron microscopy of two-dimensional crystals. *J Mol Biol*, **314**, 479-494.

Hebert H, R.X., K. Thomsen, A.B. Maunsbach. (2000) In K. Taniguchi, S.K. (ed.), *Na/K-ATPase and Related ATPases*. Elsevier, Amsterdam, pp. 43-48.

Hennessey, J.P., Jr. and Scarborough, G.A. (1988) Secondary structure of the Neurospora crassa plasma membrane H+-ATPase as estimated by circular dichroism. *J Biol Chem*, **263**, 3123-3130.

Hunte, C. and Michel, H. (2002) Crystallisation of membrane proteins mediated by antibody fragments. *Curr Opin Struct Biol*, **12**, 503-508.

Hunte C, K.A. (2003) Antibody Fragment mediated crystallization of membrane proteins. In Carola Hunte, G.v.J., Hermann Schaegger (ed.), *Membrane Protein Purification and Crystallization: A Practical Guide*. Academic Press, pp. 205-218.

Hunte C, M.H. (2003) Membrane Protein Crystallization. In Carola Hunte, G.v.J., Hermann Schaegger (ed.), *Membrane Protein Purification and Crystallization: A Practical Guide*. Academic Press, pp. 143-160.

Inesi, G. and Kirtley, M.R. (1992) Structural features of cation transport ATPases. *J Bioenerg Biomembr*, **24**, 271-283.

Jahn T, J.D., Birgitte Andersen, Brith Leidvik, Charlotta Otter, Carin Briving, werner Keuhlbrandt, Michael G Palmgren. (2001) Large scale expression, purification and 2D crystallization of recombinant plant plasma membrane H+ATPase. *journal of Molecular biology*, **309**, 465-476.

Jorgensen, P.L. (1975) Purification and characterization of (Na+, K+)-ATPase. V. Conformational changes in the enzyme Transitions between the Na-form and the K-form studied with tryptic digestion as a tool. *Biochim Biophys Acta*, **401**, 399-415.

Jorgensen, P.L. and Andersen, J.P. (1988) Structural basis for E1-E2 conformational transitions in Na,K-pump and Ca-pump proteins. *J Membr Biol*, **103**, 95-120.

Kelley, K.C., Huestis, K.J., Austen, D.A., Sanderson, C.T., Donoghue, M.A., Stickel, S.K., Kawasaki, E.S. and Osburne, M.S. (1995) Regulation of sCD4-183 gene expression from phage-T7-based vectors in Escherichia coli. *Gene*, **156**, 33-36.

Klammt, C., Lohr, F., Schafer, B., Haase, W., Dotsch, V., Ruterjans, H., Glaubitz, C. and Bernhard, F. (2004) High level cell-free expression and specific labeling of integral membrane proteins. *Eur J Biochem*, **271**, 568-580.

Koglin, A., Klammt, C., Trbovic, N., Schwarz, D., Schneider, B., Schafer, B., Lohr, F., Bernhard, F. and Dotsch, V. (2006) Combination of cell-free expression and NMR spectroscopy as a new approach for structural investigation of membrane proteins. *Magn Reson Chem*, **44**, 17-23.

Kuehlbrandt, W. (2003) Two-dimensional crystallization of membrane proteins: A practical guide. In Carola Hunte, G.v.J., Hermann Schaegger (ed.), *Membrane Protein Purification and crystallization: A Practical Guide*. Academic Press, pp. 253-284.

Kuehlbrandt, W. (2004) Biology, Structure and Mechanism of p-type ATPases. *Nature Reviews Molecular and Cell Biology*, **5**, 282-295.

Kuehlbrandt W, Z.J., Dietrich J. (2002) Structure mechanism and regulation of neurospora plasma membrane H+ATPase. *Science*, **297**, 1692-1696.

Kunji, E.R., Chan, K.W., Slotboom, D.J., Floyd, S., O'Connor, R. and Monne, M. (2005) Eukaryotic membrane protein overproduction in Lactococcus lactis. *Curr Opin Biotechnol*, **16**, 546-551.

Kuo, A., Bowler, M.W., Zimmer, J., Antcliff, J.F. and Doyle, D.A. (2003) Increasing the diffraction limit and internal order of a membrane protein crystal by dehydration. *J Struct Biol*, **141**, 97-102.

Labarre, C., van Tilbeurgh, H. and Blondeau, K. (2006) Pichia pastoris is a valuable host for the expression of genes encoding membrane proteins from the hyperthermophilic Archeon Pyrococcus abyssi. *Extremophiles*.

Laeuger, P. (1984) Thermodynamic and Kinetic Properties of Electrogenic Ion Pumps. *Biochemica et Biophysica Acta*, **779**, 307-341.

Lanfermeijer, F.C., Venema, K. and Palmgren, M.G. (1998) Purification of a histidine-tagged plant plasma membrane H+-ATPase expressed in yeast. *Protein Expr Purif*, **12**, 29-37.

Licata, L., Haase, W., Eckhardt-Strelau, L. and Parcej, D.N. (2006) Over-expression of a mammalian small conductance calcium-activated K+ channel in Pichia pastoris: effects of trafficking signals and subunit fusions. *Protein Expr Purif*, **47**, 171-178.

Lloyd, D.R. and Phillips, D.H. (1999) Oxidative DNA damage mediated by copper(II), iron(II) and nickel(II) fenton reactions: evidence for site-specific mechanisms in the formation of double-strand breaks, 8-hydroxydeoxyguanosine and putative intrastrand cross-links. *Mutat Res*, **424**, 23-36.

Lodish H, B.A., Lawrence Zipursky S, Matsudaira P, Baltimore D, Darnell J. (2003) Biomembranes: Structural Organization and Basic Functions. *Molecular Cell Biology*, **Fourth Edition**.

Lundstrom, K., Wagner, R., Reinhart, C., Desmyter, A., Cherouati, N., Magnin, T., Zeder-Lutz, G., Courtot, M., Prual, C., Andre, N., Hassaine, G., Michel, H., Cambillau, C. and Pattus, F. (2006) Structural genomics on membrane proteins: comparison of more than 100 GPCRs in 3 expression systems. *J Struct Funct Genomics*.

Ma, C. and Chang, G. (2004) Structure of the multidrug resistance efflux transporter EmrE from Escherichia coli. *Proc Natl Acad Sci U S A*, **101**, 2852-2857.

Macauley-Patrick, S., Fazenda, M.L., McNeil, B. and Harvey, L.M. (2005) Heterologous protein production using the Pichia pastoris expression system. *Yeast*, **22**, 249-270.

Mahanty, S.K., Rao, U.S., Nicholas, R.A. and Scarborough, G.A. (1994) High yield expression of the Neurospora crassa plasma membrane H(+)-ATPase in Saccharomyces cerevisiae. *J Biol Chem*, **269**, 17705-17712.

Mana Capelli S, A.K.M., Jose M. Arguello. (2003) Archaeoglobus fulgidus copB is a thermophilic Cu2+ ATPase. *Journal of Biological Chemistry*, **278**, 40534-40541.

Mandal A. K, W.D.C., Jose M. Arguello. (2002) Characterization of thermophilic P type Ag+/Cu+ ATPase from extremophile Archaeoglobus fulgidus. *Journal of Biological Chemistry*, **277**, 7201-7208.

Matadeen, R., Patwardhan, A., Gowen, B., Orlova, E.V., Pape, T., Cuff, M., Mueller, F., Brimacombe, R. and van Heel, M. (1999) The Escherichia coli large ribosomal subunit at 7.5 A resolution. *Structure*, **7**, 1575-1583.

Mellano, M.A. and Cooksey, D.A. (1988) Nucleotide sequence and organization of copper resistance genes from Pseudomonas syringae pv. tomato. *J Bacteriol*, **170**, 2879-2883.

Miroux, B. and Walker, J.E. (1996) Over-production of proteins in Escherichia coli: mutant hosts that allow synthesis of some membrane proteins and globular proteins at high levels. *J Mol Biol*, **260**, 289-298.

Mitra, B. and Sharma, R. (2001) The cysteine-rich amino-terminal domain of ZntA, a Pb(II)/Zn(II)/Cd(II)-translocating ATPase from Escherichia coli, is not essential for its function. *Biochemistry*, **40**, 7694-7699.

Morsomme, P., Chami, M., Marco, S., Nader, J., Ketchum, K.A., Goffeau, A. and Rigaud, J.L. (2002) Characterization of a hyperthermophilic P-type ATPase from Methanococcus jannaschii expressed in yeast. *J Biol Chem*, **277**, 29608-29616.

Morsomme P, B.M. (2000) The plant plasma membrane H+ATPase: structure, function and regulation. *Biochemica et Biophysica Acta*, **1465**, 1-16.

Mosser, G. (2001) Two-dimensional crystallogenesis of transmembrane proteins. *Micron*, **32**, 517-540.

Niimi, M., Wada, S., Tanabe, K., Kaneko, A., Takano, Y., Umeyama, T., Hanaoka, N., Uehara, Y., Lamping, E., Niimi, K., Tsao, S., Holmes, A.R., Monk, B.C. and Cannon, R.D. (2005) Functional analysis of fungal drug efflux transporters by heterologous expression in Saccharomyces cerevisiae. *Jpn J Infect Dis*, **58**, 1-7.

Odermatt, A., Krapf, R. and Solioz, M. (1994) Induction of the putative copper ATPases, CopA and CopB, of Enterococcus hirae by Ag+ and Cu2+, and Ag+ extrusion by CopB. *Biochem Biophys Res Commun*, **202**, 44-48.

Odermatt, A., Suter, H., Krapf, R. and Solioz, M. (1993) Primary structure of two P-type ATPases involved in copper homeostasis in Enterococcus hirae. *J Biol Chem*, **268**, 12775-12779.

Okamura, H., Denawa, M., Ohniwa, R. and Takeyasu, K. (2003) P-type ATPase superfamily: evidence for critical roles for kingdom evolution. *Ann N Y Acad Sci*, **986**, 219-223.

Oki, S. (1968) Dielectric constant and refractive index of lipid bilayers. *J Theor Biol*, **19**, 97-115.

Palmgren, M. (2001) Plant Plasma Membrane H+ATPases: Powerhouses for Nutrient Uptake. *Annual Review of Plant Physiology and Plant Molecular Biology*, **52**, 817-845.

Palmgren, M.G. and Axelsen, K.B. (1998) Evolution of P-type ATPases. *Biochim Biophys Acta*, **1365**, 37-45.

Palmgren, M.G., Sommarin, M., Serrano, R. and Larsson, C. (1991) Identification of an autoinhibitory domain in the C-terminal region of the plant plasma membrane H(+)-ATPase. *J Biol Chem*, **266**, 20470-20475.

Parcej, D.N. and Eckhardt-Strelau, L. (2003) Structural characterisation of neuronal voltage-sensitive K+ channels heterologously expressed in Pichia pastoris. *J Mol Biol*, **333**, 103-116.

Parsegian, A. (1969) Energy of an ion crossing a low dielectric membrane: Solutions to four relevant electrostatic problems. *Nature*, **221**, 844-846.

Pearson, R.G. (1963) Hard and Soft Acids and Bases. *Journal of the American Chemical Society*, **85**, 3533-3539.

Pedersen P.L, E.C. (1987) Ion motive ATPases. I. Ubiquity, properties and significance to cell function. *Trends in Biochemical Sciences*, **12**, 146-150.

Petris, M.J. (2004) The SLC31 (Ctr) copper transporter family. *Pflugers Arch*, **447**, 752-755.

Pomorski, T., Lombardi, R., Riezman, H., Devaux, P.F., van Meer, G. and Holthuis, J.C. (2003) Drs2p-related P-type ATPases Dnf1p and Dnf2p are required for phospholipid translocation across the yeast plasma membrane and serve a role in endocytosis. *Mol Biol Cell*, **14**, 1240-1254.

Portillo, F., de Larrinoa, I.F. and Serrano, R. (1989) Deletion analysis of yeast plasma membrane H+-ATPase and identification of a regulatory domain at the carboxyl-terminus. *FEBS Lett*, **247**, 381-385.

Post, R.L., Hegyvary, C. and Kume, S. (1972) Activation by adenosine triphosphate in the phosphorylation kinetics of sodium and potassium ion transport adenosine triphosphatase. *J Biol Chem*, **247**, 6530-6540.

Pufahl, R.A., Singer, C.P., Peariso, K.L., Lin, S.J., Schmidt, P.J., Fahrni, C.J., Culotta, V.C., Penner-Hahn, J.E. and O'Halloran, T.V. (1997) Metal ion chaperone function of the soluble Cu(I) receptor Atx1. *Science*, **278**, 853-856.

Reilander, H. and Weiss, H.M. (1998) Production of G-protein-coupled receptors in yeast. *Curr Opin Biotechnol*, **9**, 510-517.

Rensing, C., Fan, B., Sharma, R., Mitra, B. and Rosen, B.P. (2000) CopA: An Escherichia coli Cu(I)-translocating P-type ATPase. *Proc Natl Acad Sci U S A*, **97**, 652-656.

Rensing, C., Ghosh, M. and Rosen, B.P. (1999) Families of soft-metal-ion-transporting ATPases. *J Bacteriol*, **181**, 5891-5897.

Rhodes, A.D., Bevan, N., Patel, K., Lee, M. and Rees, S. (1998) Mammalian expression of transmembrane receptors for pharmaceutical applications. *Biochem Soc Trans*, **26**, 699-704.

Rosen, B.P. (2002) Transport and detoxification systems for transition metals, heavy metals and metalloids in eukaryotic and prokaryotic microbes. *Comp Biochem Physiol A Mol Integr Physiol*, **133**, 689-693.

Rudnick, G. (1986) ATP-driven H+ pumping into intracellular organelles. *Annu Rev Physiol*, **48**, 403-413.

Sarramegna, V., Talmont, F., Demange, P. and Milon, A. (2003) Heterologous expression of G-protein-coupled receptors: comparison of expression systems fron the standpoint of large-scale production and purification. *Cell Mol Life Sci*, **60**, 1529-1546.

Scarborough, G.A. (2000) Crystallization, structure and dynamics of the proton-translocating P-type ATPase. *J Exp Biol*, **203**, 147-154.

Schertler, G.F.X. (1992) overproduction of membrane proteins. *Current Opinions in Structural Biology*, **2**, 534-544.

Schulz, G.E. (2000) beta-Barrel membrane proteins. *Curr Opin Struct Biol*, **10**, 443-447.

Sedmak, J.J. and Grossberg, S.E. (1977) A rapid, sensitive, and versatile assay for protein using Coomassie brilliant blue G250. *Anal Biochem*, **79**, 544-552.

Sharma, R., Rensing, C., Rosen, B.P. and Mitra, B. (2000) The ATP hydrolytic activity of purified ZntA, a Pb(II)/Cd(II)/Zn(II)-translocating ATPase from Escherichia coli. *J Biol Chem*, **275**, 3873-3878.

Solioz, M., Mathews, S. and Furst, P. (1987) Cloning of the K+-ATPase of Streptococcus faecalis. Structural and evolutionary implications of its homology to the KdpB-protein of Escherichia coli. *J Biol Chem*, **262**, 7358-7362.

Solioz, M. and Odermatt, A. (1995) Copper and silver transport by CopB-ATPase in membrane vesicles of Enterococcus hirae. *J Biol Chem*, **270**, 9217-9221.

Solioz, M. and Vulpe, C. (1996) CPx-type ATPases: a class of P-type ATPases that pump heavy metals. *Trends Biochem Sci*, **21**, 237-241.

Sorensen, T.L., Olesen, C., Jensen, A.M., Moller, J.V. and Nissen, P. (2006) Crystals of sarcoplasmic reticulum Ca(2+)-ATPase. *J Biotechnol*.

Stanton, M.G. (1968) Colorimetric determination of inorganic phosphate in the presence of biological material and adenosine triphosphate. *Anal Biochem*, **22**, 27-34.

Stoyanov, M.S.J.V. (2003) Copper homeostasis in Enterococcus hirae. *FEMS Microbiology Reviews*, **27**, 183-195.

Sudbery, P.E. (1996) The expression of recombinant proteins in yeasts. *Curr Opin Biotechnol*, **7**, 517-524.

Suzuki, M. and Gitlin, J.D. (1999) Intracellular localization of the Menkes and Wilson's disease proteins and their role in intracellular copper transport. *Pediatr Int*, **41**, 436-442.

Tamm, L.K., Arora, A. and Kleinschmidt, J.H. (2001) Structure and assembly of beta-barrel membrane proteins. *J Biol Chem*, **276**, 32399-32402.

Tobias, J.W., Shrader, T.E., Rocap, G. and Varshavsky, A. (1991) The N-end rule in bacteria. *Science*, **254**, 1374-1377.

Ton, V.K. and Rao, R. (2004) Functional expression of heterologous proteins in yeast: insights into Ca2+ signaling and Ca2+-transporting ATPases. *Am J Physiol Cell Physiol*, **287**, C580-589.

Tottey, S., Rich, P.R., Rondet, S.A. and Robinson, N.J. (2001) Two Menkes-type atpases supply copper for photosynthesis in Synechocystis PCC 6803. *J Biol Chem*, **276**, 19999-20004.

Toyoshima, C., Nomura, H. and Tsuda, T. (2004) Lumenal gating mechanism revealed in calcium pump crystal structures with phosphate analogues. *Nature*, **432**, 361-368.

Toyoshima C, N.M., Nomura H, Ogawa H. (2000) Crystal Structure of calcium pump of sarcoplasmic reticulum at 2.6A resolution. *Nature*, **405**, 647-655.

Tumer, Z., Lund, C., Tolshave, J., Vural, B., Tonnesen, T. and Horn, N. (1997) Identification of point mutations in 41 unrelated patients affected with Menkes disease. *Am J Hum Genet*, **60**, 63-71.

Ubarretxena-Belandia, I., Baldwin, J.M., Schuldiner, S. and Tate, C.G. (2003) Three-dimensional structure of the bacterial multidrug transporter EmrE shows it is an asymmetric homodimer. *Embo J*, **22**, 6175-6181.

Unger, V.M. (2000) Assessment of electron crystallographic data obtained from two-dimensional crystals of biological specimens. *Acta Crystallogr D Biol Crystallogr*, **56**, 1259-1269.

Unger, V.M. (2001) Electron cryomicroscopy methods. *Curr Opin Struct Biol*, **11**, 548-554.

Uozumi, N. (2001) Escherichia coli as an expression system for K(+) transport systems from plants. *Am J Physiol Cell Physiol*, **281**, C733-739.

Urbanski, N.K. and Beresewicz, A. (2000) Generation of *OH initiated by interaction of Fe2+ and Cu+ with dioxygen; comparison with the Fenton chemistry. *Acta Biochim Pol*, **47**, 951-962.

Valentine, J.S. and Gralla, E.B. (1997) Delivering copper inside yeast and human cells. *Science*, **278**, 817-818.

Valko, M., Morris, H. and Cronin, M.T. (2005) Metals, toxicity and oxidative stress. *Curr Med Chem*, **12**, 1161-1208.

Vallejo, C.G. and Serrano, R. (1989) Physiology of mutants with reduced expression of plasma membrane H+-ATPase. *Yeast*, **5**, 307-319.

Valpuesta, J.M., Carrascosa, J.L. and Henderson, R. (1994) Analysis of electron microscope images and electron diffraction patterns of thin crystals of phi 29 connectors in ice. *J Mol Biol*, **240**, 281-287.

Villalba JM, P.M., Berberian GE, Ferguson C, Serrano R. (1992) Functional expression of plant plasma membrane H+ATPase in yeast endoplasmic reticulum. *Journal of Biological Chemistry*, **267**, 12341-12349.

Vinothkumar, K.R., Smits, S.H. and Kuhlbrandt, W. (2005) pH-induced structural change in a sodium/proton antiporter from Methanococcus jannaschii. *Embo J*, **24**, 2720-2729.

Voskoboinik, I., Brooks, H., Smith, S., Shen, P. and Camakaris, J. (1998) ATP-dependent copper transport by the Menkes protein in membrane vesicles isolated from cultured Chinese hamster ovary cells. *FEBS Lett*, **435**, 178-182.

Voskoboinik, I. and Camakaris, J. (2002) Menkes copper-translocating P-type ATPase (ATP7A): biochemical and cell biology properties, and role in Menkes disease. *J Bioenerg Biomembr*, **34**, 363-371.

Voskoboinik, I., Greenough, M., La Fontaine, S., Mercer, J.F. and Camakaris, J. (2001) Functional studies on the Wilson copper P-type ATPase and toxic milk mouse mutant. *Biochem Biophys Res Commun*, **281**, 966-970.

Voskoboinik, I., Strausak, D., Greenough, M., Brooks, H., Petris, M., Smith, S., Mercer, J.F. and Camakaris, J. (1999) Functional analysis of the N-terminal CXXC metal-binding motifs in the human menkes copper-transporting P-type ATPase expressed in cultured mammalian cells. *J Biol Chem*, **274**, 22008-22012.

Vulpe, C.D. and Packman, S. (1995) Cellular copper transport. *Annu Rev Nutr*, **15**, 293-322.

White, C.E., Hunter, M.J., Meininger, D.P., White, L.R. and Komives, E.A. (1995) Large-scale expression, purification and characterization of small fragments of thrombomodulin: the roles of the sixth domain and of methionine 388. *Protein Eng*, **8**, 1177-1187.

Williams, L.E., Pittman, J.K. and Hall, J.L. (2000) Emerging mechanisms for heavy metal transport in plants. *Biochim Biophys Acta*, **1465**, 104-126.

Wunderli-Ye, H. and Solioz, M. (2001) Purification and functional analysis of the copper ATPase CopA of Enterococcus hirae. *Biochem Biophys Res Commun*, **280**, 713-719.

Yang, G.X., Liu, T.L., Zhang, H., Wu, C.Q. and Shen, D.L. (2006) Expression and localization of recombinant human B2 receptors in the methylotrophic yeast Pichia pastoris. *Genetika*, **42**, 893-897.

Yang, Y., Mandal, A.K., Bredeston, L.M., Luis Gonzalez-Flecha, F. and Arguello, J.M. (2006) Activation of Archaeoglobus fulgidus Cu(+)-ATPase CopA by cysteine. *Biochim Biophys Acta*.

Yildiz, O., Vinothkumar, K.R., Goswami, P. and Kuhlbrandt, W. (2006) Structure of the monomeric outer-membrane porin OmpG in the open and closed conformation. *Embo J*, **25**, 3702-3713.

Yoshimizu, T., Omote, H., Wakabayashi, T., Sambongi, Y. and Futai, M. (1998) Essential Cys-Pro-Cys motif of Caenorhabditis elegans copper transport ATPase. *Biosci Biotechnol Biochem*, **62**, 1258-1260.

Zhang, H. and Cramer, W.A. (2004) Purification and crystallization of the cytochrome b6f complex in oxygenic photosynthesis. *Methods Mol Biol*, **274**, 67-78.

CURRICULUM VITAE

Name	Sivaram Chandra Chintalapati
Date of Birth	26th June 1974
Place of Birth	Tenali, India

EDUCATION:

1993-1996	Bachelor of Sciences in Microbiology, Biochemistry, Applied Nutrition and Public Health, Nagarjuna University, Nagarjuna Nagar, India
1996-1998	Master of Science in Biotechnology, Nagarjuna University, Nagarjuna Nagar, India
1998-1999	Employee at Dr. Reddy's Laboratories- Diagnostics Division, Hyderabad, India
2000-2003	Research Trainee at Central Drug Research Institute, Lucknow, India
2003-2007	PhD student in the Department of Structural biology, Max Planck Institute of Biophysics and Johann Wolfgang Goethe-Universität

PUBLICATIONS:

Sivaram Chintalapati, Rana Al-Kurdi, Werner Kuehlbrandt: Characterization of CtrA2 and CtrA3, two Putative Copper Transporting P-type-ATPases, from *Aquifex aeolicus*; manuscript in preparation

ACKNOWLEDGEMENTS

I wish to thank Prof. Dr. Werner Kuehlbrandt for giving me the opportunity to work in his group, for the independence he gave me in the laboratory, for patiently teaching me the art of writing a scientific publication and for his support and encouragement when the going was tough.

I wish to thank Prof. Bernd Ludwig for accepting me as his student for Johann Wolfgang Goethe Universität, here in Frankfurt.

I do not have words to express my gratitude to Ms. Luise Eckhardt-Strelau, without whom my life in the laboratory and in Germany might have been impossible. In addition to maintaining the laboratory and translating most of the German mail I received, she had time to discuss the world affairs in general. I spent a wonderful time in L2.120 where I shared the laboratory with Dr. David Parcej and his group for the first three years of my stay. I thank him for all the scientific discussions that we had and for his brilliant insight into almost every thing, from *Pichia* expression to cricket.

I would like to thank Dr. Thomas Meier not just for the discussions, support and encouragement, but also for kindly translating my thesis summary to German. I wish I could spend more time in the laboratory with him, I could have learnt much more.

I wish to thank Dr. Winfred Hasse, for his kind words and help with freeze fracture images and analysis and Dr. Goetz Hofhaus for reading trough the Introduction and Materials and Methods of this thesis and for his valuable advise in improvements. Thanks to Mr. Deryck Mills for helping me a lot with the electron microscopes and giving me tips to improve my bowling scores.

I would like to thank Prof. Dr. Michael Palmgren, Dr. Morten Buch-Pedersen and the Department of Plant Biology at Plant Physiology and Anatomy Laboratory in The Royal Veterinary and Agricultural University, Copenhagen, where I spent some time understanding the *S. cerevisiae* expression system for plant proton pump.

My sincere thanks to Dr. Janet Vonk for organizing IMPReS in the best possible way. I also wish to express my sincere gratitude to my thesis committee (Prof. Dr. Clemens Glaubitz and Prof. Dr. Ernst Bamberg, in addition to Prof. Dr. Werner Kuehlbrandt and Prof. Dr. Bernd Ludwig) who had been following my work annually.

I wish to thank Ms. Franziska Langerheinrich for her help when I landed here initially and Ms. Monika Hobrack for her help in paper work and personally for helping me a lot in searching a new apartment.

I wish to thank Dr. Rana Al-Kurdi for the scientific collaboration we had and Dr. Anke Terwisscha-van-Scheltinga for discussions in 3D crystallography. I also wish to thank Mirko Lotz for being a very good friend and for looking through all the crap with me in the EM during my initial crystallization trials. Even though I would not mention any more names, I wish to thank each and every member of our department for the support, encouragement and the excellent scientific environment they created.

I wish to thank the Max Planck society and International Max Planck Research School for the financial assistance and to the 'Verwaltung' department of our institute for the excellent administration.

I also wish to thank Peter Romeis and all the staff of Prolytic GmbH for being excellent friends and an extended family in Frankfurt. I also thank all my Indian friends here in our institute and in the university for letting me share my joy and sorrow. I just cannot imagine my life here without them, especially the care they showered upon me when I was in the hospital.

Any words of gratitude would not be sufficient for my wife Archana who has been with me all through my ups and downs and for the sacrifices she made to make my PhD a reality. I also have no words to express my feelings towards my mother who has sacrificed everything in her life just for my future and she, along with my sister and brother-in-law gave the essential and constant support I needed for surviving here. I really miss my father; had he been alive, he would have been proud of this achievement.